The University Of Sheffield.

Analysis of *Enterococcus faecalis* mutants affected in septum cleavage during cell division

by

Fathe Mohamed Elsarmane

A thesis submitted in partial fulfilment of the requirements for the degree of Doctor of Philosophy

The University of Sheffield, UK
Faculty of Science
Department of Molecular Biology and Biotechnology
Firth Court, Western Bank, Sheffield S10 2TN

Submission date
September/2016

Abstract

Enterococcus faecalis is a Gram-positive commensal bacterium forming diplococci/short chains that can also be an opportunistic pathogen. Some infections caused by *E. faecalis* such as endocarditis and bacteraemia can be life-threatening and difficult to treat due the resistance of this organism to several classes of antibiotics. Recent data revealed that the morphology of *E. faecalis* is an important factor for pathogenesis. Whilst strains forming diplococci or short chains can evade phagocytes and cause lethality in the zebrafish model of infection, isogenic derivatives forming long cell chains are more susceptible to phagocyte uptake and become avirulent. The enzyme dedicated to septum cleavage in *E. faecalis*, *N*-acetylglucosaminidase AtlA therefore has a key role during pathogenesis. The aim of this project was to identify genes involved in the control of AtlA activity during cell division. We used two distinct phenotypic screens to isolate spontaneous and transposon mutants impaired in septum cleavage. Our results indicate that several mechanisms ensure spatial and temporal control of AtlA enzymatic activity during growth.

Dedication

I would like to thank Allah for giving me the ability to achieve all uncountable previous goals. I dedicate this thesis to my family who supported me during my life. In addition, I dedicate to all my respected teachers; my friends particularly. In addition, I dedicate Dr Fathalla Ben Omran; Dr Adham El-Shawaidhe; Dr Raju; Dr Mohamed Rasheed and Dr Mwafak El Azuzi.

Acknowledgements

This project would not be completed without the support and the assistance of several people.

I am deeply grateful to Dr Pascale Serror and Prof David Hornby for agreeing to examine this work.

I express my gratitude to my supervisor, Dr Stéphane Mesnage for his valuable guidance, encouragement, support; most significantly for his remarkable patience and the guidance to avoid getting lost in my exploration.

I wish to express my gratitude to my advisors Prof David Kelly and Dr Robert Fagan for their valuable and suggestions and advice during the annual meetings.

I would like to thank Prof Simon Foster for giving me the opportunity to carry out some of my experiments in his laboratory.

A special thanks to Dr Qaiser I Sheikh, Mrs Linda Harris and Dr Sameer Qureshi for their assistance.

I also wish to express my thanks to the cultural attaché of Libyan embassy at London.

Finally, I acknowledge the Faculty of Medical Technology for awarding me a PhD study scholarship.

Abbreviations

Amp	Ampicillin
AdmA	AtlA display mutant A
AtlA	*N*-acetylglucosaminidase
AtlB	*N*-acetylmuramidase
AtlC	*N*-acetylmuramidase
cfu	Colony forming unit
Chl	Chloramphenicol
m-DAP	*meso*-diaminopimelic acid
D-Glu	D-glutamic acid
dH2O	Distilled water
DMSO	Dimethyl sulphoxide
DNA	Deoxyribonucleic acid
EDTA	Ethylene diamine tetra-acetic acid
Glc*N*Ac	*N*-acetylglucosamine
HPLC	High performance liquid chromatography
IPTG	Isopropyl beta-D-thiogalactopyranoside
Kan	Kanamycin
kDa	Kilodaltons
L-Ala	L-alanine
LB	Luria-Bertani medium
mg	Milligram
mL	Millilitres
mM	Millimolar
Mur*N*Ac	*N*-acetylmuramic acid
Ni-NTA	Nitrilotriacetic acid
PBP	Penicillin-binding protein
PBS	Phosphate buffered saline
PCR	Polymerase chain reaction
psi	Pounds per square inch
rp-HPLC	Reverse-phase high performance liquid chromatography
rpm	Revolutions per min

SDS	Sodium dodecyl sulphate
SDS-PAGE	Sodium dodecyl sulphate polyacrylamide gel electrophoresis
Spp.	Species
TA	Teichoic acids
TAE	Tris-acetate EDTA
Taq	Thermostable DNA polymerase derived from *Thermus aquaticus*
TBS	Tris buffered saline
TEMED	*N,N,N'N'*-tetramethyl-ethylenediamine
THY	Todd Hewitt yeast
Tris	Tris (hydroxyl methyl) aminomethane
µg	Microgram
µl	Microlitre
µm	Micrometre
µM	Mircomolar
UV	Ultra violet
v/v	Volume for volume
WT	Wild type
WTA	Wall teichoic acids
w/v	Weight for volume
x	Times
σ	Sigma
ϕ	Phage
~	Approximately

Table of contents

Chapter 1 Introduction

Chapter 2 Material and Methods

List of figures

Chapter 1

Chapter 3

List of Tables

Chapter 1

Chapter 2

Chapter 3

Chapter 1

Introduction

1.1. *Enterococcus faecalis*

1.1.1. Discovery of enterococci as a novel bacterial genus

The first description of "*Enterococcus*" was reported by Thiercelin in a French publication in 1899 (Thiercelin, 1899). He isolated a bacterium found in large numbers from human faeces and named it as "Enterocoque". In this publication, Thiercelin described a gram-positive organism with an ovoid shape forming diplococci or short chains.

Virulence tests revealed that mice were very susceptible to infections by this germ whereas guinea pigs were resistant to infections. Rabbits were only killed when injected in high doses.

Interestingly, Thiercelin mentions that the "Enterocoque" he described was similar to others isolated from patients with enteritis, appendicitis, and meningitis. It is therefore tempting to assume that the article published by Thiercelin is the first description of the opportunistic pathogen that we know now as *Enterococcus faecalis*.

At the beginning of the 19th century, numerous publications described Gram-positive organisms forming diplococci or short chains isolated from infected patients or from various biological samples (pus, saliva, faeces, etc.). Some of these organisms were referred to as *Streptococcus faecalis* and it is difficult to know whether or not they corresponded to what was later defined as *Enterococcus faecalis*. In 1905, it was proposed that antistreptococcic sera might help to discriminate between Streptococci and apply a suitable treatment (Gordon, 1905).

This work highlighted the diversity of the streptococcus group and the need to better classify them, thus defining ''Strepto-biology'' (Gordon, 1905). Nine distinct properties were defined to differentiate streptococci (Gordon, 1905) based on (i) the clotting of litmus milk; (ii) the reduction of neutral red broth during anaerobic incubation; (iii-ix) the production of an acid reaction aerobically when bacteria are cultivated in slightly alkaline broth containing 1%(w/v) of saccharose, lactose, raffinose, inulin, salicin, coniferin or mannite (Gordon, 1905).

Despite data from the literature indicating that organisms closely related to *S. faecalis* have unique properties amongst streptococci, the genus *Enterococcus* was only formally identified in 1984 by Schleifer and Kilpper-Balz using DNA hybridization methods (Schleifer and Kilpper-Bälz, 1984).

1.1.2. Morphology

Enterococci cells are ovoid and mostly arranged in pairs (diplococci) or short chains typically containing 4 to 6 cells (Murray, 1990; Hardie and Whiley, 1997). Enterococci are non-sporulating bacteria and the vast majority of species are non-motile with a few exceptions (e.g., *E. gallinarum* and *E. casseliflavus*) (Byappanahalli et al., 2012) (**Fig. 1A** and **B**).

Most enterococci form white/cream colonies on agar plates except *E. sulfureus*, *E. casseliflavus*, and *E. mundtii* which produce yellow pigments (Witte, 2003). *E. faecalis* colonies appear dome-shaped with entire edges, getting flatter after prolonged incubations (**Fig. 1C**).

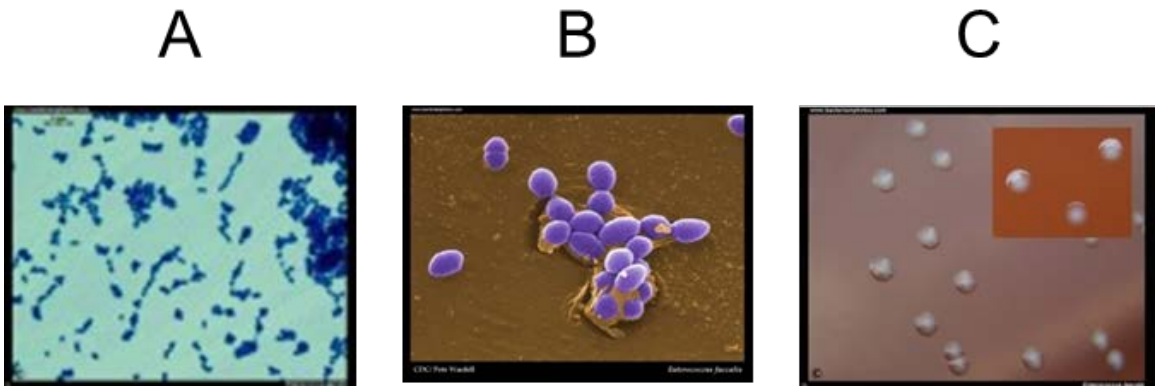

Figure 1. Phenotype of *E. faecalis* cells and colonies (**A**), optical light microscopy of *E. faecalis* cells after Gram-staining. (**B**), scanning electron micrograph (SEM) of enterococci grown in liquid media showing the oval cell shape and the formation of diplococci. (**C**), colonies of *E. faecalis* grown on blood agar plate after cultivation for 24 hours under aerobic conditions at 37°C (colonies are non-haemolytic). [Reference: http://www.bacteriainphotos.com/bacteria-photo-gallery.html].

1.1.3. Distinctive metabolic and phenotypic properties

Like streptococci, enterococci are aerotolerant anaerobes. They do not use oxygen as an electron acceptor. They are homofermentative, predominantly producing lactic acid from glucose. Their growth is generally increased in a CO_2-enriched environment. Enterococci most often appear non-haemolytic (gamma-haemolytic type) but some strains are alpha- or more rarely beta-haemolytic, displaying differential activities towards different types of erythrocytes. For example, it was reported that in the case of *E. faecalis* horse red blood cells are the most sensitive, sheep and bovine blood cells are resistant (Izumi et al., 2005).

Virulent V583 *E. faecalis* strain produces a cytolysin with beta-haemolytic activity encoded by a plasmid that found on a pathogenicity island (Shankar et al., 2002). Like streptococci and unlike micrococci (such as *Staphylococcus aureus*), enterococci are catalase-negative but may appear weakly positive for this activity in the presence of heme. This cofactor is required for the expression of the gene *katA* encoding this enzyme, which has been considered as a pseudogene for this reason (Frankenberg et al., 2002) . Enterococci can be distinguished from streptococci based on their antigenic properties. The extraction of cell wall antigens allows the definition of several agglutination groups (Lancefield groups A-V) in the presence of specific antibodies (Lancefield, 1933)..

Group D contains enterococci and a limited number of streptococci including *Streptococcus bovis* and *Streptococcus gallolyticus.* The distinction between enterococci and streptococci belonging to the Lancefield group D requires other specific tests. These include the colurimetric detection of L-pyrrolidonyl-beta-naphthylamide hydrolysis by an aminopeptidase enzyme (Bosley et al., 1983) or the hydrolysis of aesculine in the presence of bile salts or growth in the presence of 0.05% potassium tellurite. Growth on media containing tellurite leads to the formation of black colonies. This test is particularly suitable to identify *E. faecalis* as other enterococci are generally inhibited by tellurite (Facklam and Collins, 1989).

Other metabolic properties can be used to identify enterococci. They essentially rely on sugar fermentation profiles (mannitol, sorbitol, L-arabinose, D-raffinose, sucrose, lactose), enzymatic activities (such as arginine hydrolysis), growth at defined temperatures or in the presence of bile salts (Fertally and Facklam, 1987; Klein, 2003). Identification galleries are commercially available. One example is shown in (**Fig. 2**). Some compounds allow the discrimination between enterococci. For example, *E. faecalis* strongly reduces triphenyltetrazolium-chloride (TTC) and produces bright red colony on a medium with TTC, whereas *E. faecium* weakly reduce TTC, forming pale pink colonies (Reuter, 1992).

Pre-formulated media are now available to specifically allow the growth of enterococci. Aesculin-bile-azide medium (ABA, in its commercial formulation called Enterococcosel ECS), Citrate azide tween carbonate agar (CATC), Crystal violet azide agar (KA), Kanamycin aesculin azide agar (KAA), Slanetz and Bartley medium (ME), Streptococcus selective agar (ScS) and Thallous acetate tetrazolium glucose agar (TITG) (Reuter, 1992).

Enterococci do not require adenosine, guanosine, uracil, or thymine and can be grown in a synthetic medium as long as it is supplemented with several amino acids and vitamins. It has been known for a long time that enterococci require multiple vitamins (Niven and Sherman, 1944).

Specific requirements are not known and synthetic media described usually contain nicotinic acid, pantothenic acid, biotin, pyridoxine, riboflavin, and sometimes folic acid (Murray et al., 1993). Four amino acids (histidine, isoleucine, methionine, and tryptophan) are essential for several *E. faecalis* strains whilst other amino acids are often required to promote growth or to increase growth rate. Amino-acid requirements are variable depending on the strain considered. For example *E. faecalis* strains ATCC 29212 and JH2-2 are auxotroph for arginine, glutamate, glycine, leucine and valine whereas OG1 strain grows poorly without these amino acids (Murray et al., 1993); depletion of cysteine, serine, or threonine has no effect on JH2-2 and OG1RF strains whereas it affects growth of *E. faecalis* ATCC 29212 (Murray et al., 1993).

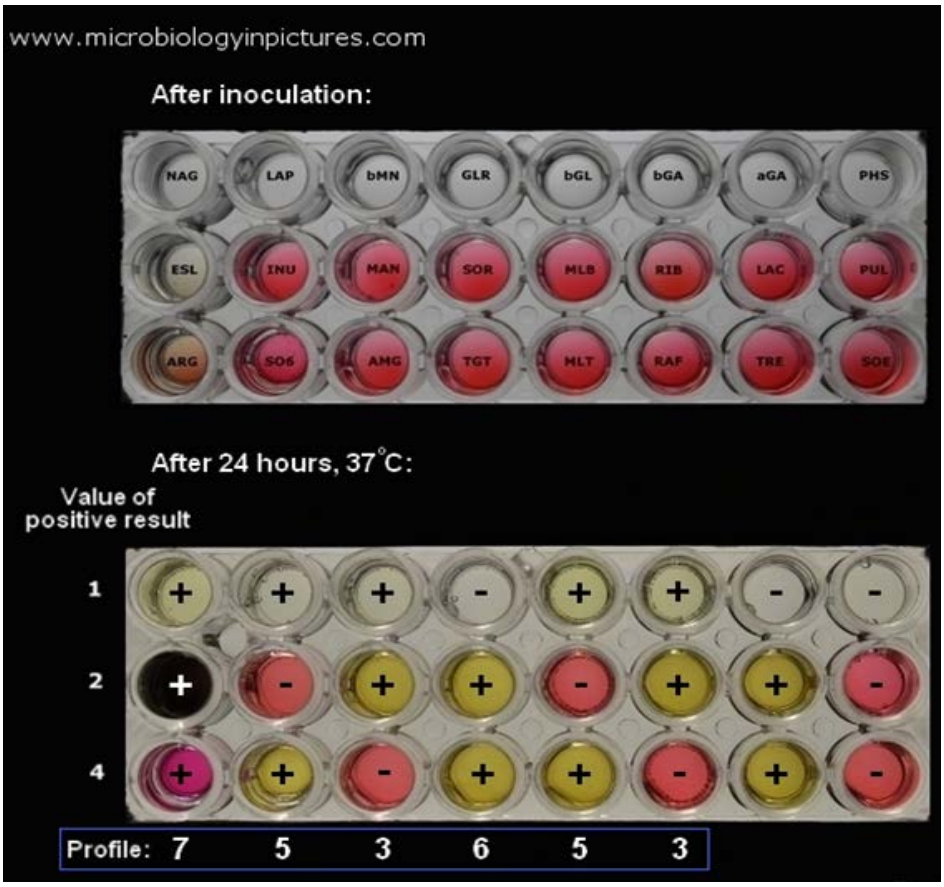

Figure 2. *E. faecalis* identification using a commercially available gallery based on colorimetric tests (STREPTOtest 24, ErbaLachema). The metabolic assays are as follows: line 1, detection of *N*-acetyl-*N*-glucosaminidase, L-leucin-aminopeptidase, β-mannosidase, β-glucuronidase, β-glucosidase, β-galactosidase, α-galactosidase and phosphatase activities; lane 2, detection of esculin hydrolysis, inulin, mannitol, sorbitol, melibiose, ribose, lactose and pullulan fermentation; Line 3, arginine dihydrolase activity, Growth in 6.5% NaCl, α-methylglucosidase activity, tagatose, maltose, raffinose, trehalose, sorbose fermentation.

A typical strategy used to identify enterococci is described in (**Fig. 3**). It combines several identification criteria (antigenic properties, growth conditions, and fermentation profile).

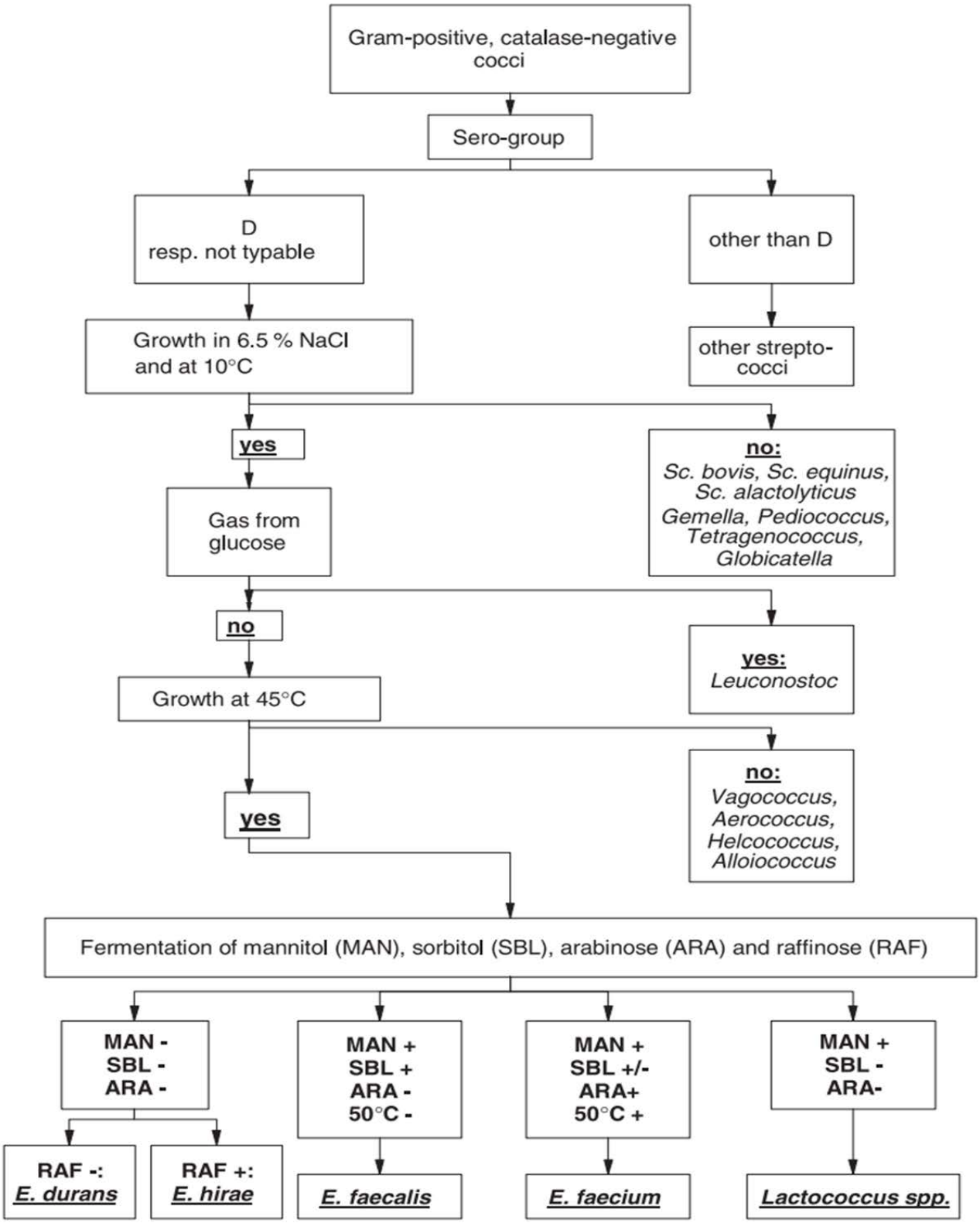

Figure 3. Differentiation of enterococci from other Gram-positive catalase-negative cocci (Klein, 2003).

1.1.4. Molecular Identification

DNA-DNA and DNA-rRNA hybridization methods have been used to group several species from the Lancefield group D in a novel genus called "Enterococcus" (Schleifer and Kilpper-Bälz, 1984). Schleifer and Kilpper-Bälz's results clearly revealed that within the Enterococcus group, two species (formerly *Streptococcus faecalis* and *Streptococcus faecium*, renamed *E. faecalis* and *E. faecium*) showed only limited DNA homology. As pointed out by the authors, this distinction was supported by distinct peptidoglycan composition (*E. faecalis* containing L-Ala instead of D-Asp in PG crossbridges) see chapter 1.2.

As an alternative to 16S rDNA sequencing, Enterococcal strains can be identified by sequencing a 438-bp-long PCR fragment internal to the *sodA* gene encoding the manganese-dependent superoxide dismutase amplified with degenerate primers (Poyart et al., 2002). The *sodA* gene represents a more discriminative target sequence than 16S rRNA gene to differentiate enterococci.

Epidemiologic studies are particularly important to identify clinical isolates responsible for hospital-acquired infections. Identification of *E. faecalis* is possible using multilocus sequence typing (MLST) to define related strains forming clonal complexes (Ruiz-Garbajosa et al., 2006), some of which defining High Risk Enterococcal Clonal Complexes (HiRECC (Leavis et al., 2006).

1.1.5. Habitat

Most enterococci are commensal bacteria frequently found in the gastro-intestinal tract (GIT) of human, mammals, insects or birds (**Fig. 4**) and are frequently isolated from faeces. Due to their capacity to grow and resist in a wide range of conditions, they are frequently isolated from plants, soil, wastewater or fermented food or dairy products that they can contaminated (Murray, 1990). Two major species, *E. faecalis,* and *E. faecium* are isolated from human faeces. *E. faecalis* is one of the first organisms to colonize newborns (Adlerberth and Wold, 2009) but although this organism can reach concentrations as high as 10^7colony-forming units (CFU) per gram of faeces, however, is not amongst the most abundant in adult microbiota (Murray, 1990).

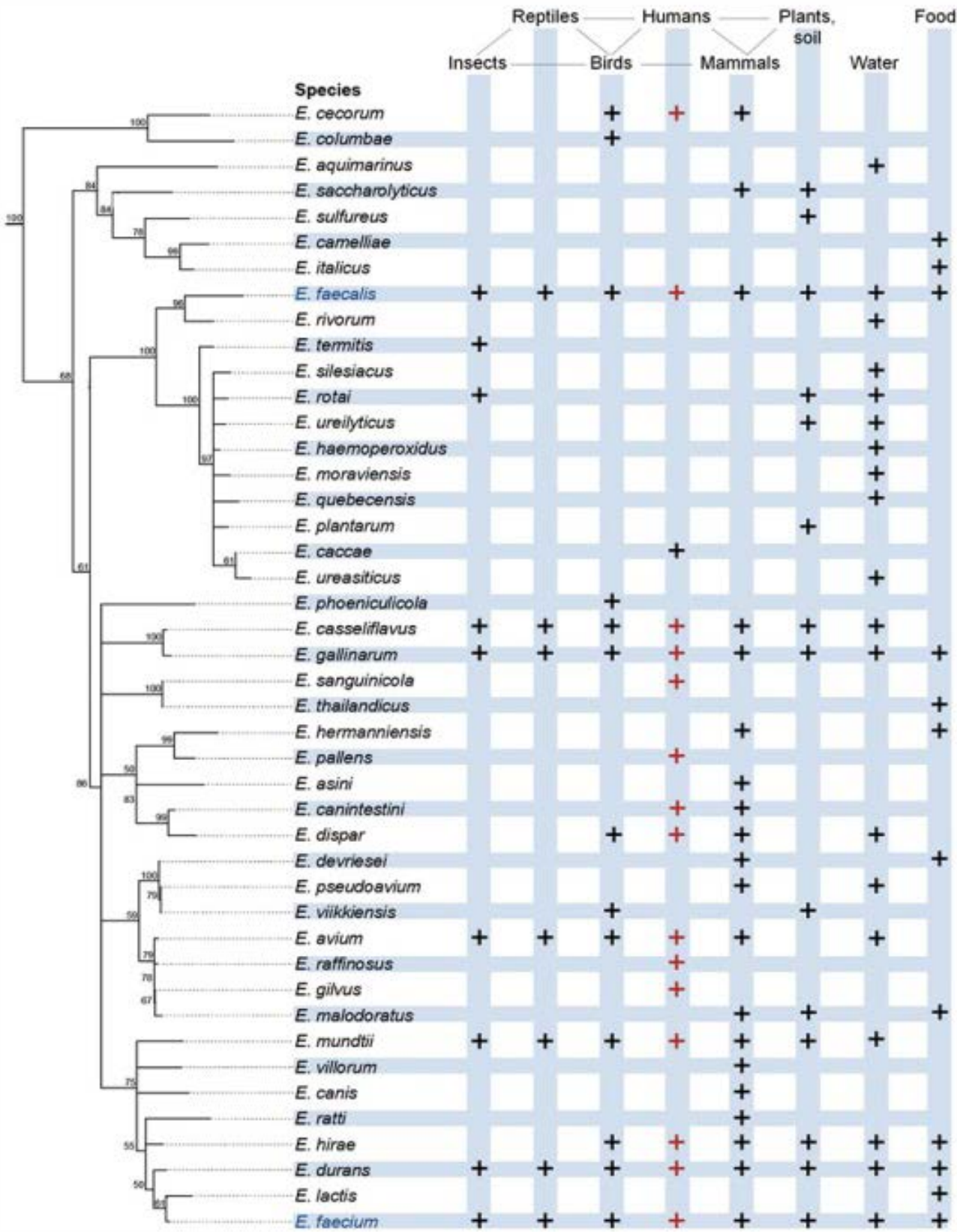

Figure 4. **Distribution of enterococci in different hosts.** The dendrogram shows phylogenic relationships. The sources of isolation are indicated for each species. A simplified food chain is shown. Red symbols indicate species that have been described in human infections (Lebreton et al., 2014).

1.1.6. Genomic data

The genome of *E. faecalis* V583 was the first genome sequence published (Paulsen et al., 2003). This strain is the first clinical isolate resistant to vancomycin isolated in the United States. The *E. faecalis* V583 genome contains one chromosome (3.2Mbp) encoding 3337 predicted proteins, and three plasmids pTEF1, pTEF2 and pTEF3 of 66.3kbp, 57.7 kbp and 18.0 kbp, respectively (Paulsen et al., 2003).

The genome of *E. faecalis* V583 is characterised by the presence of mobile DNA (38 insertion sequences), seven prophages, integrated plasmid genes, and a large pathogenicity island corresponding to an integrative transposon. V583 genome also encodes a vancomycin-resistance mechanism. Altogether, mobile and foreign DNA represents approximately a quarter of the genome (Paulsen et al., 2003). The description of *E. faecalis* V583 genome revealed the genomic fluidity in this bacterium and explained the capacity of this particular strain to cause hospital-acquired infections. It is interesting to note that *E. faecalis* V583 genome encodes 134 putative surface-exposed proteins that may be associated with colonization or virulence.

The availability of the V583 genome has allowed performing comparative genomic hybridization experiments to define the minimal core genome of *E. faecalis*. Two independent studies reported that the core genome of *E. faecalis* contains 2057 genes (McBride et al., 2007) and 2092 genes (Lepage et al., 2006).

Recent studies revealed that unlike in *E. faecium*, a limited genetic diversity is observed amongst *E. faecalis* strains (Palmer et al., 2012). Although the shared gene content varies between species (from 70.9 to 96.5%), the average nucleotide identity (ANI) is extremely high (99.5%) amongst shared genes (Palmer et al., 2012). More pronounced differences were reported between *E. faecium* genomes, reflecting the existence of two distant clades with 93.9 to 95.6% ANI. These values overlap an ANI species line of 94 to 95%.

1.1.7. Resistance to stress

Enterococci can survive in a wide range of harsh conditions. *E. faecalis* has an optimum growth temperature of 35°C, but it can grow from 10 to 45°C (Sherman, 1937) and between pH 4.0-10.0. *E. faecalis* is resistant to high salt concentrations. Growth in the presence of 6.5% (m/v) NaCl is sometimes used as a discriminant growth condition (Facklam, 1973).

The resistance to various stresses has been reported (Rince et al., 2000). These include high osmolarity, heat, ethanol treatment; exposure to heavy metals, sodium hypochloride; hydrogen peroxide, sodium dodecyl sulfate (SDS; 0.01%) and detergents as well as pH 4.8 or 10.5. The ability to resist such harsh conditions is associated with a complex network of two-component systems (Hancock and Perego, 2002) and transcriptional regulators which allow the expression of several proteins called Gsp (General stress proteins) (Rince et al., 2000). An extra cytoplasmic sigma factor called sigma V belonging to the LysR family has been identified in *E. faecalis* and shown to coordinate resistance to acid stress, ethanol treatments and heat shock (Benachour et al., 2005).

1.1.8. Pathogenesis of *E. faecalis*

1.1.8.1. Infections caused by *E. faecalis*

Enterococci are one of most common organisms causing hospital-acquired infections (HAI). A recent survey of HAI from the CDC's National Healthcare Safety Network identified enterococcal species as the second cause of infections after *S. aureus* (Sievert et al., 2013). *E. faecalis* and *E. faecium* accounted for 51% and 21% of these strains. Towards the end of the 1980s, enterococcal infections were essentially caused by *E. faecalis* (Murray, 1990), but it appears that *E. faecium* is now more prevalent. Enterococcal infection occurs mostly in elderly, in immunocompromised patients or following an antibiotic treatment causing an imbalance of the normal microbiota.

1.1.8.2 *E. faecalis* virulence factors

Some pathogens like *S. aureus* produce a multitude of potent virulence factors and rely on several mechanisms to escape host defences. Instead, *E. faecalis* produces several "opportunism factors" which altogether enable this bacterium to cause infections. These factors are described below:

(i) Secreted factors: Two proteases, the gelatinase GelE and the serine protease SprE are secreted by several *E. faecalis* strains. GelE has been shown to contribute to tissue damage by degrading proteins from the extracellular matrix such as fibrin (Waters et al., 2003; Thurlow et al., 2010). Some *E. faecalis* strains also produce a cytolysin encoded on a plasmid that can integrate on the chromosome in a pathogenicity island (Coburn and Gilmore, 2003; Shankar et al., 2002).

(ii) Cell wall polymers: Three polymers covalently bound to peptidoglycan have been reported in *E. faecalis* (see paragraph 1.2.2.). The capsule has been shown to prevent complement-mediated opsonophagocytosis (Thurlow et al., 2009). The enterococcal polysaccharide antigen (Epa) is also contributing to *E. faecalis* resistance to innate immunity (Prajsnar et al., 2013; Teng et al., 2002). The third type of wall-associated polymers corresponds to teichoic acids. They have also been shown to confer resistance to complement-mediated opsonophagocytosis (Geiss-Liebisch et al., 2012).

(iii) Pili: All *E. faecalis* strains have a chromosomal locus called *ebp* (endocarditis and biofilm associated pili) encoding pili. These structures were shown to contribute to virulence in several infection models including the rat endocarditis model (Nallapareddy et al., 2006) and the mice urinary tract infection model (Kemp et al., 2007). Another locus named *bee* (biofilm enhancer in *Enterococcus*) has been proposed to encode pili but it is only present in a very limited number of clinical isolates (approximately 1%) (Schluter et al., 2009)

(iv) Adhesins: *E. faecalis* produces several proteins which contribute to the interaction with the host. The aggregation substance (AS), encoded by the plasmidic *pgrB* gene, is covalently bound to peptidoglycan. It contains a tripeptide arg-gly-asp (RGD) that has been proposed to contribute to the binding to host integrins (Chuang et al., 2009). The aggregation substance also binds to lipoteichoic acids of recipient cells to promote conjugation (Waters et al., 2004). The V583 genome encodes seventeen Microbial Surface Component Recognition Adhesins for the Microbial Matrix (MSCRAMMs) potentially involved in the binding to host molecules. These adhesins include Ace (Rich et al., 1999) that binds to collagen and Esp, which is also involved in the formation of biofilms (Shankar et al., 2001; Tendolkar et al., 2005).

1.1.8.3. Experimental infection models

To study the wide range of infections caused by *E. faecalis*, several infection models have been described. Invertebrate models of infection include the wax moth *Galleria mellonella* and the bacteriovorous nematode *Caenorhabditis elegans*. *G. mellonella* has an innate immune system producing phagocytes and effectors such as lysozyme and antimicrobial peptides, similar to those produced by humans (Yuen and Ausubel, 2014).

Vertebrate models of infections have been described in mice, rats, rabbits and more recently zebrafish. Depending on the type of infection studied, one model is preferred over the others. For example, rabbits and rats are used to study endocarditis (Dube et al., 2012; Haller et al., 2014) whereas mice are preferred to study urinary tract infections or bacteraemia (Singh et al., 2009; Teng et al., 2009). Recently, a zebrafish model of infection has been described (Prajsnar et al., 2013). Thanks to the transparency of zebrafish larvae, this model allows to follow the infection process using fluorescent bacteria.

1.1.9. Resistance to antibiotics

E. faecalis is intrinsically resistant to several antimicrobial agents and can also acquire resistance to a wide range of other antibiotics. As a consequence, infections caused by this nosocomial pathogen can be difficult to treat.

1.1.9.1. Resistance to β-lactams

β-lactams inhibit the enzymes called D,D-transpeptidases or penicillin-binding proteins (PBPs) that polymerise peptidoglycan, the essential component of the cell envelope (see paragraph 1.2.). *E. faecalis* produces PBP5, an enzyme with low affinity for cephalosporins. As a result, this bacterium is intrinsically resistant to these antibiotics and can grow in the presence of high concentrations (up to 1000µg/mL; (Arbeloa et al., 2004). *E. faecalis* can also acquire high resistance to penicillin by overexpression of PBP5 (Duez et al., 2001) or acquisition of β-lactamase genes that inactivate β-lactams (Murray and Mederski-Samaroj, 1983). Although this is a rare mechanism of resistance, it has been suggested that enterococcal beta-lactamase genes can be transferred from staphylococci to enterococci (Bonafede et al., 1997).

1.1.9.2. Resistance to glycopeptides

The first vancomycin-resistant clinically enterococcal isolate was reported in Europe in 1988. Similar strain was later identified in United States. Subsequently, vancomycin-resistant enterococci became abundant in hospitals in several countries (Courvalin, 2006). This mechanism of resistance has been extensively studied in *E. faecalis*. Vancomycin-Resistant Enterococci (VRE) is one of the leading causes of nosocomial infections in the US (http://www.cdc.gov/HAI/organisms/vre/vre.html).

Vancomycin binds non-covalently to the D-Ala-D-Ala extremity of the peptidoglycan precursors and inhibits the activity of PBPs by steric hindrance (Courvalin, 2006). Several types of resistance have been described (VanA to VanG) based on the levels of resistance to vancomycin and teicoplanin. The *van* genes are often carried on a mobile element such as the vancomycin-resistance *vanB locus* on the conjugative transposon Tn*1549* (Garnier et al., 2000). Collectively, *van* genes contribute to modify the peptidoglycan peptide stem so that glycopeptide affinity is reduced. The substitution of the C-terminal D-Ala residue by D-lactate (D-Lac) reduces the affinity of vancomycin for the peptide stems by a factor 1000 (**Fig. 5**).

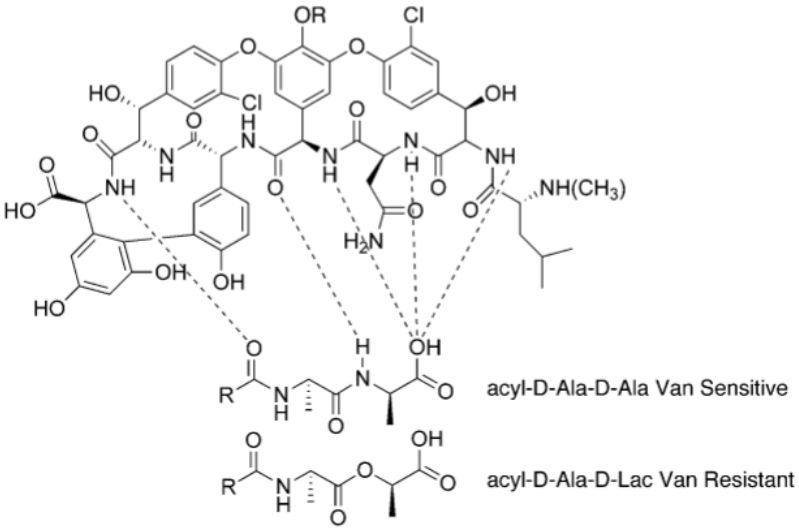

Figure 5. Interaction of vancomycin with peptidoglycan peptide stems. Vancomycin establishes five hydrogen bonds with the acyl-D-Ala-D-Ala terminus of peptidoglycan chains and their precursors. Resistance results from the loss of the amide group in acyl-D-Ala-D-Lactate resulting in loss of one hydrogen bond (Wright, 2011).

1.1.9.3. Resistance to antibiotics targeting protein synthesis

Enterococci are intrinsically resistant to aminoglycosides, macrolides, lincosamides and streptogramins. These antibiotics all bind to the 30S or the 50S subunits of the bacterial ribosome, thereby inhibiting protein synthesis. This leads to cell growth arrest and then cell death.

Resistance to antibiotics inhibiting protein synthesis involves a wide range of mechanisms, some of which occur synergistically to confer very high levels of resistance. Aminoglycosides resistance is primarily due to the fact that enterococci are impermeable to these antibiotics so that they cannot reach their cytoplasmic targets (Zimmermann et al., 1971).

Efflux mechanisms have been reported for streptogramins, lincosamides and tetracyclines (Singh et al., 2002).

In addition to these mechanisms conferring intrinsic resistance, *E. faecalis* can also acquire genes that modifying antibiotics such as (phosphotransferases, nucleotidyltransferases or acetyltransferases; (Ramirez and Tolmasky, 2010) that inactivate the drugs as well as enzymes able to modify the ribosomes. This is the case of the *erm* genes products dimethylate an adenine in the 23S rRNA (Weisblum, 1995) giving cross-resistance to macrolides, lincosamides and group B streptogramins having overlapping binding sites on the ribosome (MLS_B phenotype).

1.1.9.4. Resistance to antibiotics targeting DNA metabolism

Quinolones are rarely used to treat enterococcal infections as enterococci show low levels of intrinsic resistance. They can also acquire higher levels of resistance. A study of 322 clinical enterococcal isolates revealed that none were susceptible to the frequently-used quinolone, ciprofloxacin (Hallgren et al., 2001). Mechanisms of resistance are not fully characterised in enterococci but the *E. faecalis qnr* gene was proposed to confer moderate resistance (Arsene and Leclercq, 2007).

1.2. The cell wall of Gram-positive bacteria

In gram-positive bacteria, the cell envelope is composed of the cell wall and the cytoplasmic membrane. It also contains a space between the cytoplasmic membrane and peptidoglycan defined as ‘‘periplasm’’, by analogy with Gram-negative bacteria, which possess an outer membrane. The bacterial cell wall is mainly composed of a giant molecule called peptidoglycan (PG) or murein. In Gram-positive bacteria, the PG is the major component of their cell wall which is responsible for the mechanical resistance to osmotic stresses and maintenance the shape of the bacterium (Vollmer and Bertsche, 2008). PG is also used as scaffold to display protein such as S-layer protein and polymers such as teichoic acid or capsules (**Fig. 6**) (Silhavy et al., 2010). Lipoteichoic acids covalently attached to the cytoplasmic membrane are also embedded in the cell wall; these polymers will not be described in this introduction.

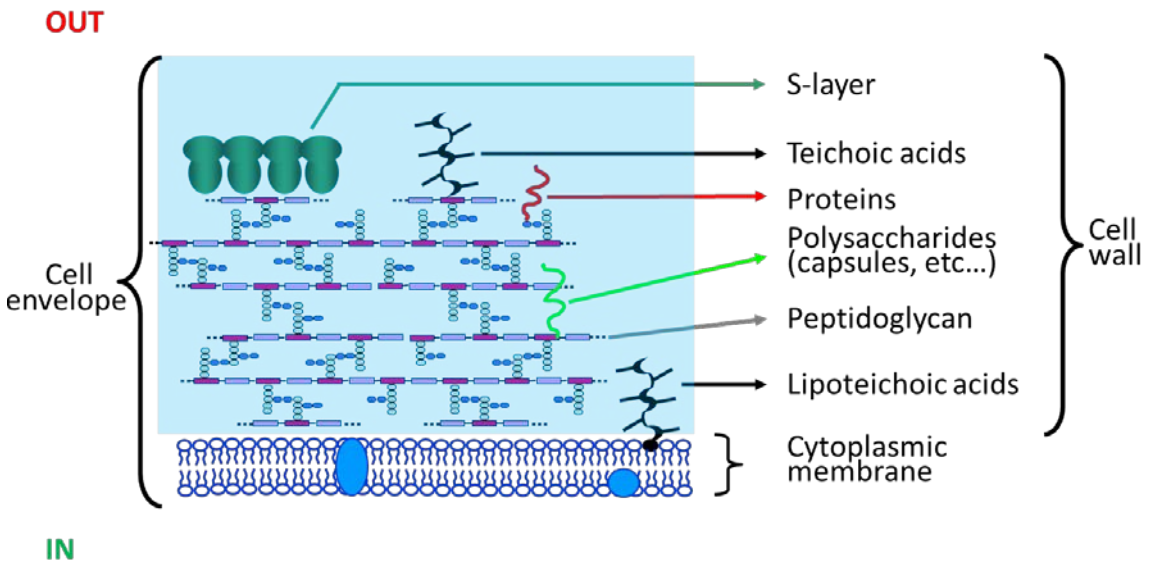

Figure 6. Schematic organisation of the bacterial cell envelope in Gram-positive bacteria. The cell envelope is composed of the cell wall and the cytoplasmic membrane. The cell wall contains S-layer proteins, teichoic acids, proteins, polysaccharides, and peptidoglycan. Lipoteichoic acids are embedded in the cell wall but attached to the cytoplasmic membrane.

1.2.1. Peptidoglycan (PG)

Peptidoglycan is a heteropolymer made of glycan strands that are cross-linked by short peptides. It has properties unique to the bacterial kingdom and represents therefore an ideal target for antibiotics. Several antibiotics widely used to treat infection including β-lactams (penicillin) and glycopeptides (vancomycin) inhibit the synthesis of PG (Bugg and Walsh, 1992).

1.2.1.1. Structure and composition of peptidoglycan

PG consists of two parts: (i) glycan strands, composed of alternating *N*-acetylglucosamine (Glc*N*Ac) and *N*-acetylmuramic Acid (Mur*N*Ac) residues, which are, linked together by β-(1,4) glycosidic bonds and (ii) peptide stems, composed of L- and D-amino acids. In most Gram-positive bacteria the peptide stem is [L-Ala-γ-D-Gln-DAA-D-Ala-D-Ala], where DAA is a diamino acid, usually L-Lysine or *meso*-diaminopimelic acid (*m*-DAP). The peptide stem is attached to the lactoyl group of the Mur*N*Ac residues (van Heijenoort, 2001; Vollmer and Bertsche, 2008) (**Fig. 7**).

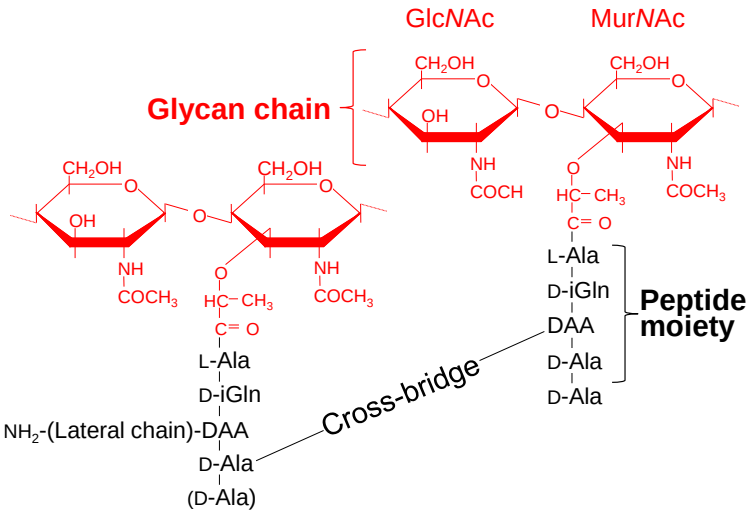

Figure 7. Structure of the Gram-positive peptidoglycan (PG). PG consists of glycan chains, cell wall peptides, and cross-bridges. Glycan chains are composed of the repeating disaccharide Glc*N*Ac-Mur*N*Ac. The composition of the pentapeptide stem linked to the lactyl group of the Mur*N*Ac is most often L-Ala-D-iGln-DAA-D-Ala-D-Ala, where DAA represents a diamino acid such as L-Lysine or *meso*-diaminopimelic acid. The peptide chains can be substituted by lateral chains of variable length and composition that constitute cross-bridges after incorporation of the precursors into the existing network.

1.2.1.1.1. Glycan strands

The composition of the glycan strands is extremely conserved in bacteria (always made of Glc*N*Ac and Mur*N*Ac) (Beeby et al., 2013) but their length differs between species and several modifications have been described (Vollmer, 2008).

1.2.1.1.1.1. Glycan chain length

The length of the glycan strands is heterogeneous within a given bacterial species and the average length varies from one bacterium to another. For example, *S. aureus* has short chains (5-20 disaccharides) (Wheeler et al., 2011) whereas *Bacillus subtilis* has long glycan chains (>100 disaccharides) (Hayhurst et al., 2008). The average length of the glycan strands is not related to the thickness of the peptidoglycan layers (Vollmer and Bertsche, 2008).

The average length of the glycan strands can be determined by different methods:

1- Gel filtration after labelling of the glycan stands with radioactive Glc*N*Ac.

2- Chemical reduction which specifically labels the residues at the end of the chain.

Via method is based on the quantification of the ratio between reduced and non-reduced hexosamine residues (Harz et al., 1990).

3- Via the enzymatic addition of radiolabeled galactosamine residues. This method is based on the quantification of the galactosamine residues at the end of the glycan chain (Schindler et al., 1976). Individual glycan strands of specific lengths can be seprated analysed by HPLC. This method involves three steps: the release of the glycan strands using an amidase (an enzyme cleaving between glycan chains and peptide stems); purification of the glycan strands by ion exchange chromatography; and finally separation of the glycan strands via reverse phase HPLC (Harz et al., 1990).

1.2.1.1.1.2. Glycan chain modifications

Several modifications of the glycan strands have been described (**Fig. 8**): (i) the addition of polymers such as teichoic acids to the hydroxyl group on C6 of Mur*N*Ac; (ii) *O*-acetylation of Glc*N*Ac or Mur*N*Ac residues on the C6 position, a modification that prevents hydrolysis by some autolysins such as lysozyme. The enzymes involved in PG *O*-acetylation (*O*-acetyltransferases) have been identified in several bacteria (Bera et al., 2005; Hebert et al., 2007); (iii) de-*N*-acetylation the Mur-*N*AC or Glc*N*Ac residues. The enzymes involved in PG de-*N*-acetylation are *O*-acetyl peptidoglycan esterases (APEs) (Vollmer, 2008) and have been described in several bacteria (Benachour et al., 2012; Boneca et al., 2007; Vollmer and Tomasz, 2000); (iv) *N*-glycolylation in some mycobacteria (Raymond et al., 2005) or the formation of δ-lactam groups in spores (Atrih et al., 1996).

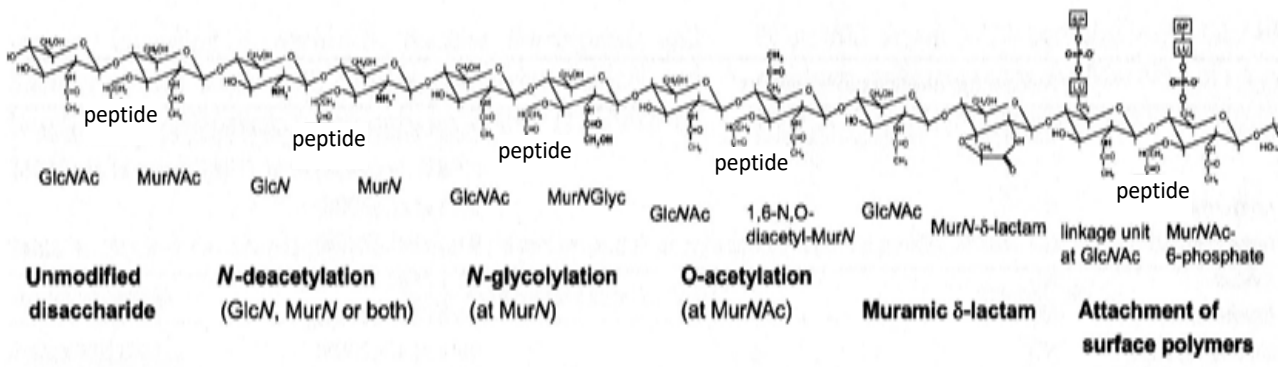

Figure 8. Modifications of PG glycan strands; adapted from (Vollmer, 2008).

1.2.1.1.2. Peptide stems

In PG precursors, the lactoyl group of each Mur*N*Ac is substituted by the pentapeptide stem. Unlike proteins, made exclusively of L-amino acids, PG peptide stems contain D-amino acids. In the majority of Gram-positive bacteria, these amino acids are: L-Alanine, **γ**-D-Glutamic acid, L-Lysine or *meso*-diaminopimelic acid, D-Alanine and D-Alanine. Several modifications of these amino acids have been reported (Vollmer and Bertsche, 2008) and are summarised (**table 1**). In Gram-positive cocci, the peptide stem contains lateral chains on the residue at position 3. Another source of variation is related to the bond between peptide stems (van Heijenoort, 2001).

1.2.1.1.2.1. Variation in peptide stem composition

The amino acid in position 1 is extremely conserved, and is L-Ala in the vast majority of Gram-positive bacteria. In position 2, a γ-D-Glu residue is always present on the PG precursors, but can be amidated (Gln) (Vollmer and Bertsche, 2008). A diamino acid is found in position 3; it can be *m*-DAP or L-Lysine in most gram positive bacteria, but it can be L-Homoserine in *Corynebacterium poinsettiae* (**table 1**). In position 4, a D-Ala is always present. Finally, the residue in position 5 (C-terminal of the peptide stem) varies. In most cases, D-Ala residue, but this residue can be replaced by other residues such as Ser, Gly or D-Lac, a modification associated with vancomycin resistance (Vollmer and Bertsche, 2008).

Position	Residue encountered	Examples
1	L-Ala	Most species
	Gly	*Mycobacterium leprae, Brevibacterium imperiale*
	L-Ser	*Butyribacterium rettgeri*
2	D-Isoglutamate	Most Gram-negative species
	D-Isoglutamine*	Most Gram-positive species, Mycobacteria
	threo-3-Hydroxyglutamate*	*Microbacterium lacticum*
3	*meso*-A_2pm	Most Gram-negative species, Bacilli, Mycobacteria
	L-Lys	Most Gram-positive species
	L-Orn	Spirochetes, *Thermus thermophilus*
	L-Lys/L-Orn	*Bifidobacterium globosum*
	L-Lys/D-Lys	*Thermotoga maritima*
	LL-A_2pm	*Streptomyces albus, Propionibacterium petersonii*
	meso-Lanthionine	*Fusobacterium nucleatum*
	L-2,4-Diaminobutyrate	*Corynebacterium aquaticum*
	L-Homoserine	*Corynebacterium poinsettiae*
	L-Glu	*Arthrobacter* J. 39
	Amidated *meso*-A_2pm*	*Bacillus subtilis*
	2,6-Diamino-3-hydroxypimelate†	*Ampuraliella regularis*
	L-5-Hydroxylysine†	*Streptococcus pyogenes*‡
	N^{γ}-Acetyl-L-2,4-diaminobutyrate*	*Corynebacterium insidiosum*
4	D-Ala	All bacteria
5	D-Ala	Most bacteria
	D-Ser	*Enterococcus gallinarum*
	D-Lac	*Lactobacillus casei*, Enterococci with acquired resistance to vancomycin

Table 1. Amino acid variations in the peptide stem. *These residues result from reactions occurring after the formation of cytoplasmic precursors. †The process of formation of these residues is unclear. ‡ In this organism, a 10: 1 ratio of lysine to hydroxylysine was foun, adapted from (Vollmer et al., 2008).

1.2.1.1.2.2. Variation in the lateral chain

For a given bacterium, the composition of the lateral chain is invariable, but its composition and length (one to five residues) varies between bacteria. It can contain D- or L-amino acids, for example, two L-Ala in *E. faecalis*, D-Asp or D-Asn in *E. faecium*, or five Gly in *S. aureus.* After polymerisation of peptide stems, the lateral chains form cross bridges (Vollmer and Bertsche, 2008; van Heijenoort, 2001).

1.2.1.1.3. PG crosslinks

Three modes of cross-linking exist (**Fig. 9**):

1- 3-4 Cross-links, these types of crosslinks are the most common, they are made by D,D-transpeptidases. This type of cross-link results from the transpeptidation between the amino group of the side chain of the residue at the position 3 (acceptor peptide subunit) and the D-Ala at position 4 (donor peptide subunit). The linkage can be direct or not depending on the presence of a lateral chain (van Heijenoort, 2001).

2- 3-3 Cross-links; this type can be found in certain Corynebacteria and mycobacteria and is made by L, D-transpeptidases. This type of cross-link results from the transpeptidation between the amino group of the side chain of the residue at the position 3 and the diamino acid in the position 3 (Vollmer et al., 2008).

3- 2-4 Cross-links, this kind of crosslink is rare and found in certain species of bacteria (Coryneform) particularly in phytopathogenic Corynebacteria. This type of cross-link involves the α-carboxy group of the D-Glu at the position 2 and the carboxy group of the D-Ala of the acyl donor at the position 4 (Schleifer and Kandler, 1972). The enzymes responsible for this type of crosslinks have not been described

The degree of cross-linking ("crosslink index") can vary from one species to another. For example, it is 20% for *Escherichia coli* and >90% for *S. aureus* (Vollmer et al., 2008).

1.2.1.1.4. Classification of peptidoglycan composition

The classification of PG structures ''Chemotypes'' can be achieved by a tridigital system (**table 2**) (Schleifer and Kandler, 1972).

1- The first letter (Roman capital letter) refers to the mode of cross-linking: **A**: 3-4 Cross-Linking or **B**: 2-4 Cross-Linking.

2- The second digit (Number) indicates the type of interpeptide bridge involved in cross-linking. (For example direct cross-linked is 1)

3- The third letter (Greek) depends on the amino acids found in position 3 of the peptide stem.

Several examples of peptidoglycan chemotypes are described in (**Fig. 9**).

This system does not include a specific group corresponding to PG with 3-3 bounds.

Group A – cross-linkage between position 3 (diamino acid) and 4 (D-alanine)			
Subgroup	Type of cross-linkage	Variation(s)	Amino acid in position 3
A1	Direct (no interpeptide bridge)	α	L-lysine
		β	L-ornithine
		γ	*meso*-diaminopimelic acid
A2	Polymerized peptide subunits	None	L-lysine
A3	Monocarboxylic L-amino acids	α	L-lysine
	or glycine, or both	β	L-ornithine
		γ	*meso*-diaminopimelic acid
A4	Contains a dicarboxylic amino acid	α	L-lysine
		β	L-ornithine
		γ	*meso*-diaminopimelic acid
Group B – cross-linkage between position 2 (D-glutamic acid) and 4 (D-alanine)			
Subgroup	Type of cross-linkage	Variation(s)	Amino acid in position 3
B1	Contains an L-diamino acid	α	L-lysine
		β	L-homoserine
		γ	L-glutamic acid
		δ	L-alanine
B2	Contains a D-diamino acid	α	L-ornithine
		β	L-homoserine

Table 2. Summary of the peptidoglycan classification scheme. The classification of PG structures ''chemotypes'' involves a tri-digital system describing the type of crosslink, the presence of cross-bridges and the type of amino-acid in position 3.

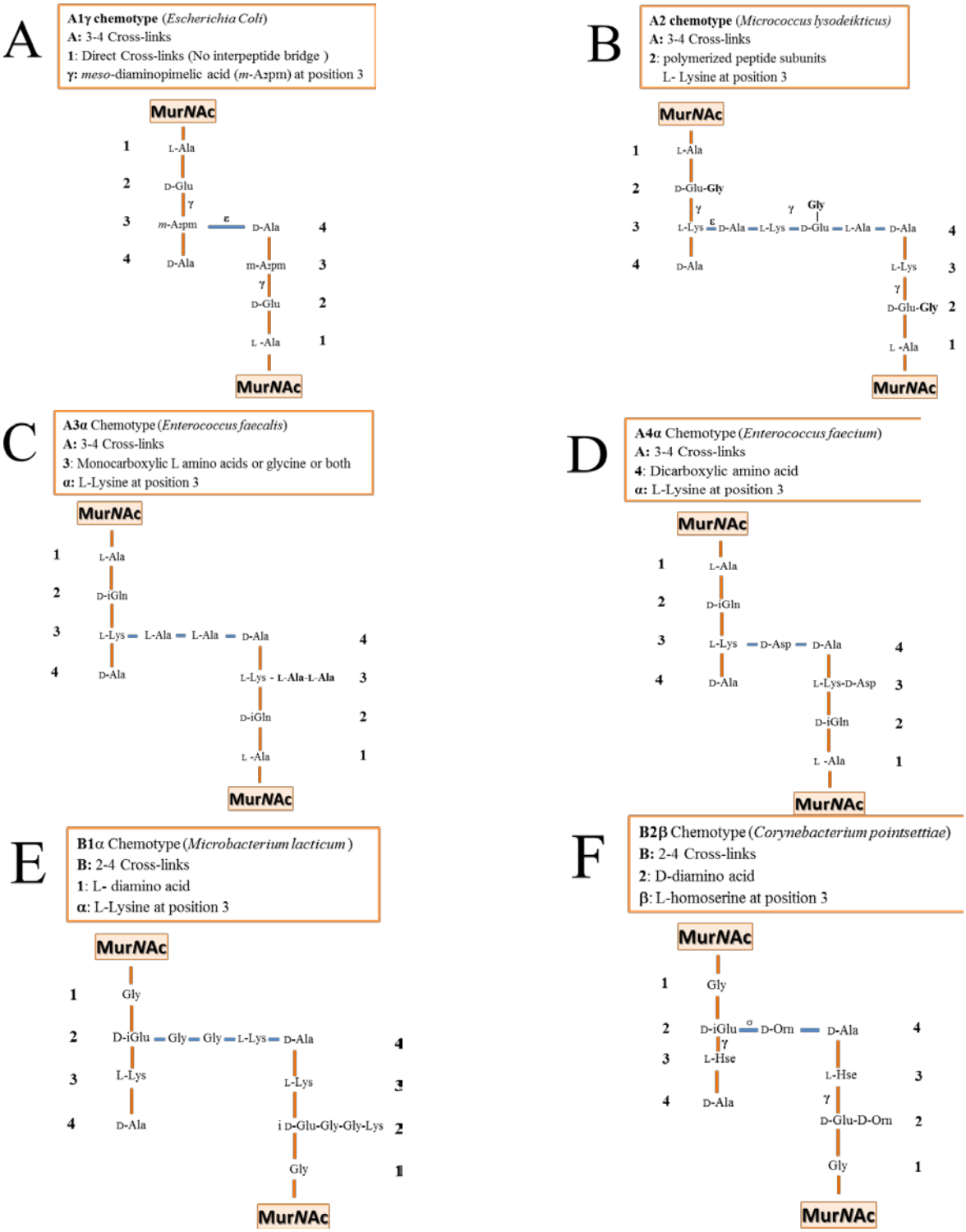

Figure 9. Examples of peptidoglycan chemotypes of different bacteria. (**A**), A1γ chemotype (*Escherichia coli*). A: 3-4 Cross-links, 1: direct cross-links (No interpeptide bridge), γ: m-A2pm in position 3. (**B**), A2 chemotype (*Micrococcus lysodeikticus*), A: 3-4 cross-links, 2: crossbridge made of a polymerized peptide subunits with L- Lysine in position 3. (**C**) A3α chemotype (*Enterococcus faecalis*), A: 3-4 cross-links, 3: crossbridge made of monocarboxylic L-amino acid, α: L-Lysine at position 3. (**D**), A4α chemotype (*Enterococcus faecium*), A: 3-4 Cross-links, 4: crossbridge made of a dicarboxylic amino acid, α: L-Lysine in position 3. (**E**) B1α chemotype (*Microbacterium lacticum*), B: 2-4 cross-links, 1: crossbridge made of L- diamino acids and glycine, α: L-Lysine in position 3. (**F**), B2β chemotype (*Corynebacterium pointsettiae*), B: 2-4 Cross-links, 2: crossbridge made of a D-diamino acid, β: L-homoserine in position 3.

1.2.1.2. PG synthesis

Peptidoglycan synthesis occurs in three stages summarised in (**Fig. 10**) (van Heijenoort, 2001). **The first cytoplasmic stage** results in the formation of the soluble precursors (UDP-Mur*N*Ac-pentapeptides) (Barreteau et al., 2008). **The second stage is membrane-associated;** soluble precursors are transferred on a lipid transporter at the inner face of the cytoplasmic membrane then Glc*N*Ac and the lateral chains are added before translocation at the cell surface. **During the last extracytoplasmic stage,** PG precursors are incorporated into the existing network by the action of transpeptidases and glycosyltransferases (Scheffers and Pinho, 2005; van Heijenoort, 2001).

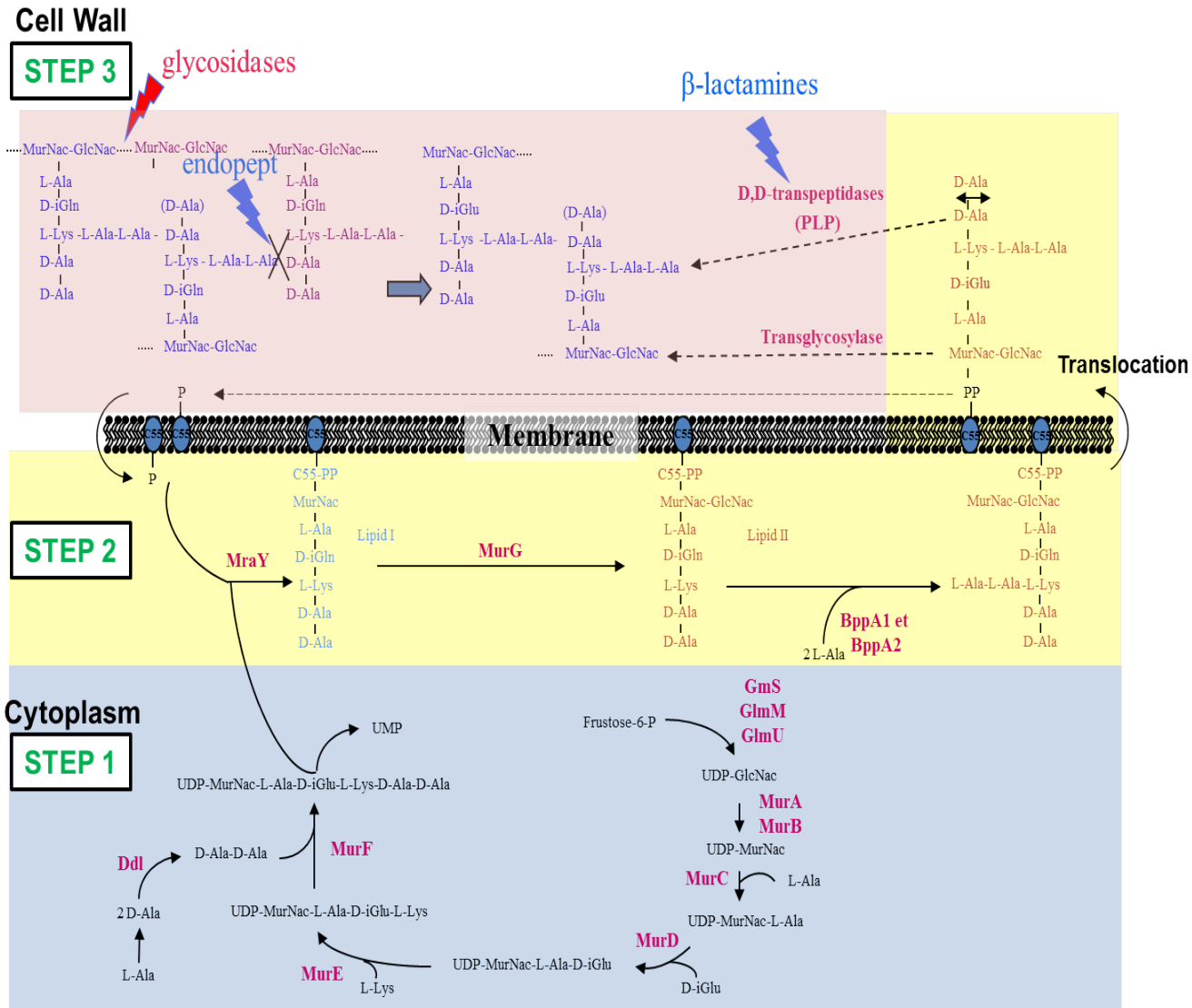

Figure 10. Major steps of PG synthesis. Step 1 occurs in the cytoplasm and leads to the production of soluble precursors (UDP-Mur*N*Ac-pentapeptides) by action of several enzymes. Step 2 is a membrane-associated step which starts at the inner side of the cytoplasmic membrane. It is responsible for synthesis of lipid-linked precursors and their translocation on the outer face of the cytoplasmic membrane. Step 3 of PG synthesis is the polymerization of PG precursors by enzymes called D,D-transpeptidases or Penicillin Binding Protein (PBP).

1.2.1.2.1. Cytoplasmic step (synthesis of soluble precursors)

The cytoplasmic steps can be divided into three series of reactions described below.

1.2.1.2.1.1. Biosynthesis of UDP-Glc*N*Ac

Fructose-6-Phosphate (F-6-P) is first converted to Glucosamine-6-Phosphate: (GlcN-6-P) by the action of the glucosamine-6-phosphate synthase (GlmS). GlcN-6-P is then converted to Glucosamine-1-Phosphate (GlcN-1-P) by the action of the phospho-glucosamine mutase GlmM. Finally, GlcN-1-P is transformed to UDP-Glc*N*Ac by the action of the bifunctional: (GlmU) enzyme, which has both GlcN-1-P acetyl transferase and *N*-acetylglucosamine-1-phosphate uridyl transferase activities. The overall reactions are summarised in **Fig. 11A**.

1.2.1.2.1.2. Biosynthesis of UDP- Mur*N*Ac

This step requires two enzymes: MurA transfers enolpyruvate from PEP to position 3 of the Glc*N*Ac residue to yield UDP-Glc*N*Ac enolpyruvate. The enolpyruvate moiety is then reduced to D-lactoyl by MurB to produce UDP-MurNAc. These two reactions are summarized in **Fig. 11B**.

1.2.1.2.1.3. Biosynthesis of UDP-Mur*N*Ac-pentapeptide

This step requires several enzymes that sequentially add amino acids onto the lactoyl group of UDP-Mur*N*Ac and form amide or peptide bonds. Each amino acid is added following activation with ATP. These enzymes are called Mur Ligases (MurC, MurD, MurE and MurF). MurC incorporates L-Ala; MurD incorporates D-Glutamic Acid; MurE incorporates the diamino acid (usually L-Lys or *meso*-DAP) and MurF incorporates the dipeptide D-Ala-D-Ala. The reactions are described in **Fig. 11C** using *E. coli* peptidoglycan composition as an example.

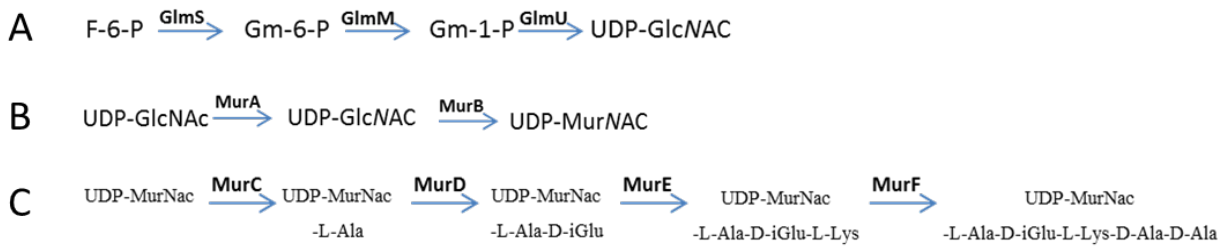

Figure 11. Cytoplasmic reactions leading to the synthesis of soluble precursors. (**A**), formation of the soluble precursor UDP-Glc*N*Ac from F-6-P. Three enzymes (GlmS, GlmM and GlmU) are involved. (**B**), formation of UDP-Mur*N*Ac from UDP-Glc*N*Ac by the combined activity of MurA and MurB. (**C**), formation of the soluble UDP-MurNAc-pentapeptide precursors. Sequential additions of amino acids are mediated by MurC, MurD, MurE, and MurF.

1.2.1.2.2. Membrane associated step (synthesis of lipid-linked intermediates)

1.2.1.2.2.1. Formation of lipid I

The soluble precursor UDP-Mur*N*Ac-pentapeptide is transferred to a lipid transporter called bactoprenol. The bactoprenol is a hydrophobic transporter that helps to transfer the soluble (hydrophilic) PG precursors from the aqueous environment of the cytoplasm through the hydrophobic cytoplasmic membrane. This first step is catalysed by the enzyme MraY that adds the UDP-Mur*N*Ac onto bactoprenol.

1.2.1.2.2.2. Formation of lipid II

The enzyme MurG then adds a Glc*N*Ac residue to lipid I to form lipid II. At this stage, the lateral chain is added to the disaccharide-pentapeptide by aminoacyl transferases. L-amino acids are added by enzymes using aminoacyl-tRNAs as substrates. In *E. faecalis*, the enzymes BppA1 and BppA2 add two L-Ala residues as a lateral chain. D-amino acids are added by enzymes carrying out ATP-dependent carboxylate-amine ligations (Bellais et al., 2006).

1.2.1.2.2.3. Translocation of lipid II

Lipid II is translocated across the cytoplasmic membrane to the extra-cytoplasmic space by a ‘‘flippase’’. Using different experimental strategies, three enzymes have been proposed to play this role: FtsW (Mohammadi et al., 2011), MurJ & (Sham et al., 2014) or AmJ (Meeske et al., 2015).

1.2.1.2.3. Extra-cytoplasmic step (polymerization reactions)

During this stage, the PG precursors attached to the lipid transporter are incorporated into the existing PG (**Fig. 10**). Polymerisation reactions are catalysed by bifunctional enzymes that are known as penicillin binding proteins (PBPs). PBPs can have two different enzymatic activities: they act as glycosyltransferases to extend the glycan chains and transpeptidases to form the peptide crosslinks. Bifunctional PBPs with both glycosyltransferase and transpeptidases activities are called ‘‘class A’’ PBPs. PBPs with only transpeptidase activity called ‘‘class B’’ PBPs. Finally low molecular weight PBPs with carboxypeptidase activity called ‘‘class C’’ PBPs. During the polymerisation reaction, one D-Ala-D-Ala extremity of a precursor used as a ‘‘donor’’ is cleaved to form a covalent bond with the PBP. The cleavage reaction provides energy necessary for the transpeptidation reaction which occurs outside the cytoplasmic membrane in the absence of energy donors such as ATP (van Heijenoort, 2007; van Heijenoort, 2001; Johnson et al., 2013).

1.2.2. Polymers covalently associated to PG

Gram-positive bacteria produce various polymers that are covalently anchored to the PG molecule. The following section will describe the composition of major types of polymers found in *E. faecalis* and briefly describe some of their roles during growth and interaction with the host during pathogenesis.

1.2.2.1. Teichoic acids

In Gram-positive bacteria, teichoic acids (TAs) are envelope components that can represent more than 50% of the cell wall. TAs are covalently bound to the C6-OH group of Mur*N*Ac residues. TAs are attached to peptidoglycan via a linkage unit composed of two sugars (Glc*N*Ac and Man*N*Ac) and contain a variable number of phosphate repeats (**Fig. 12**) (Neuhaus and Baddiley, 2003). The phosphate groups of TAs are negatively charged and represent a polyanionic matrix. The negative charge conferred by TAs can be modulated via the esterification of TAs with D-alanyl esters and glycosyl residues (Neuhaus and Baddiley, 2003). Most TA are glycerol-phosphate or ribitol-phosphate polymers as shown in **Fig. 12A** In rare cases, TAs can have an unusual composition. In *E. faecium*, The composition of TAs and their structure were analyzed by GC-MS and NMR. A mixture of glucose, glycerol, and phosphate was found in an approximate ratio of 2:1:2. The structure of the repeating unit of TAs was solved by NMR and shown to correspond to contain a kojibiosyl [α-D-glucopyranosyl-(1.2)-D-glucose] (**Fig. 12B**). In *E. faecalis*, the composition of TAs remains unclear, but it was proposed that two TAs are produced in equal amounts with repeating units of →6)[α-L-Rhap-(1→3)]β-D-Gal*p*NAc-(1→5)-Rbo-1-P→ and →6)β-D-Glc*p*-(1→3)[α-D-Glc*p*-(1→4)]-β-D-GalpNAc- (1→5)-Rbo-1-P→ (**Fig. 12C**).

For a long time, it has been proposed that the presence of TAs was essential because repeated attempts to build null mutants affected in various steps of the biosynthetic pathway had remained unsuccessful. Work on *S. aureus* showed that it is possible to abolish the production of TAs by inactivating *tagO*, the gene involved in the first step of the TA synthesis (the formation of undecaprenylPP-Glc*N*Ac, required to generate the linkage unit) (Weidenmaier et al., 2004). Based on this result, it was proposed that previous unsuccessful attempts to build other mutants could be explained by the toxic accumulation of incomplete TA products in the cell, depleting the availability of lipid transporter.

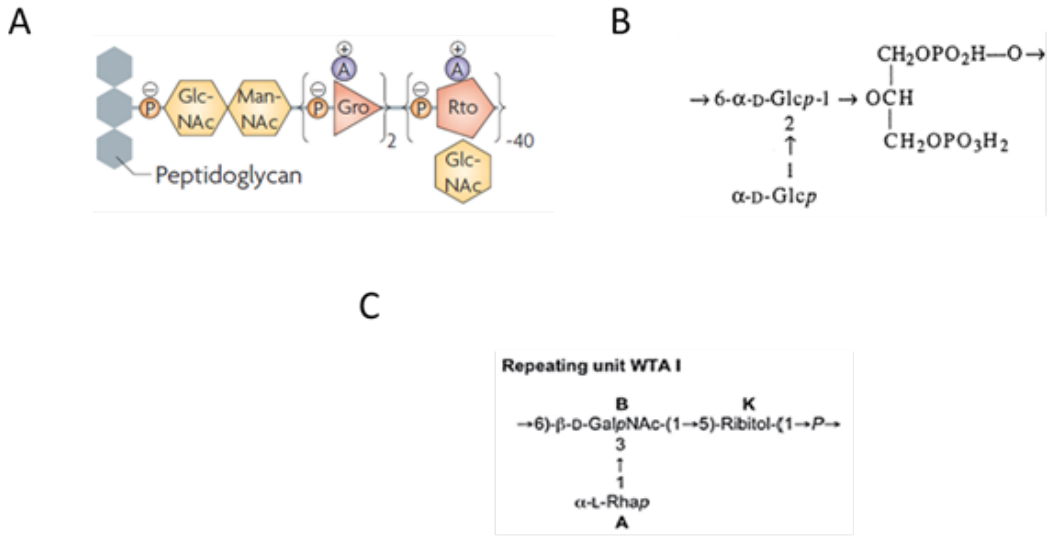

Figure 12. Schematic representation of TA from Gram-positive bacteria. (**A**), TA structure of *S. aureus*, P, phosphate; Glc*N*Ac, *N*-acetylglucosamine; Man*N*Ac, *N*-acetylmannosamine; Gro, glycerol; A, D-alanine and Rto, ribitol (Weidenmaier and Peschel, 2008) (**B**), TA structure of *E. faecalis* 12030 (Wang et al., 1999). (**C**), Structure of *E. faecalis* TA repeating units of *E. faecalis* V583 (Geiss-Liebisch et al., 2012).

Several roles have been proposed for teichoic acids. They are used as receptors for phages adsorption and can also modulate the resistance of bacteria to antimicrobial peptides (**Fig. 13**).

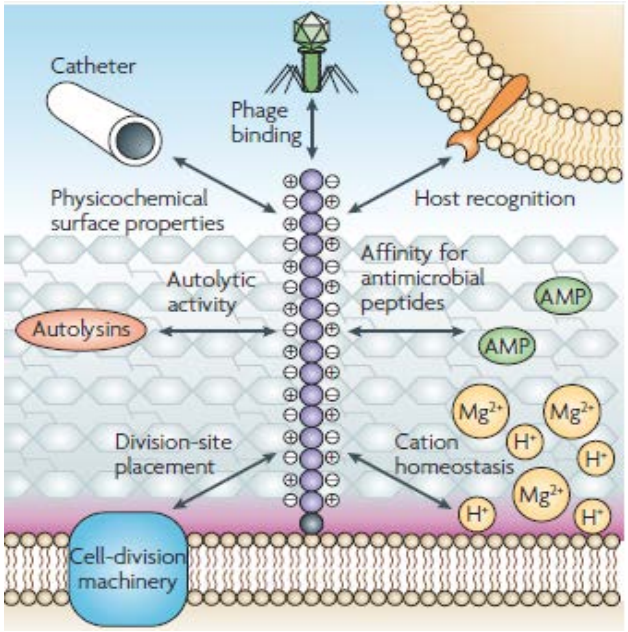

Figure 13. Roles of teichoic acid (TAs) in the cell wall of *S. aureus*. TAs are involved in localization of cell-division machinery, control of autolysin activity, modulation of biofilm formation the adsorption of phages, interactions with host cells, susceptibility and/or resistance to antimicrobial peptides (AMPs) and the maintenance of ion homeostasis (Weidenmaier and Peschel, 2008).

1.2.2.2. Capsules

In addition to TAs, the cell wall of gram-positive bacteria can also contain capsules (CPSs) that form a "shield" around the bacterium (Chapot-Chartier and Kulakauskas, 2014). The vast majority of CPSs are made of carbohydrates covalently bound to PG. Only few capsules are made of polypeptides, the most studied example being the poly-γ-D-glutamic acid of *Bacillus anthracis* (Candela and Fouet, 2005).

Capsules made of carbohydrates are covalently anchored onto the C6-OH groups of Mur*N*Ac (Coley et al., 1978) or Glc*N*Ac residues in the case of group B streptococci (Deng et al., 2000). In the case of *Bacillus anthracis*, which contains a peptidic caspule made of poly-γ-D-glutamic acid, it is anchored onto the peptide stems of PG (Candela and Fouet, 2005).

The composition of CPSs is variable between strains of the same species. Different CPS compositions and structures underpin the capacity of pathogenic strains to interact with their host. One of the best studied example is the CPS of *S. pneumoniae* which is a major virulence factor (Garcia et al., 2000).

E. faecalis produces a capsule composed of glucose, galactose residues and glycerol phosphate encoded by a genetic locus named *cps* containing 11 ORFs (Hancock and Gilmore, 2002). The capsule has been shown to contribute to define four of the 21 serotypes proposed by Maekawa (Maekawa et al., 1992; Hancock et al., 2003). The four capsule serotypes (A, B, C, or D) have been analysed (Thurlow et al., 2009). It was shown that seven of the nine genes in the *cps* operon are crucial for capsule production. Serotypes A and B do not make a capsular polysaccharide, and the fact that they define distinct serotypes indicate that this typing method also recognize other surface components. Biochemical analyses suggested that one cps gene (*cpsF*) is responsible for glucosylation of serotype C capsular polysaccharide (Thurlow et al., 2009).

1.2.2.3. Secondary cell wall polymers: the Enterococcal polysaccharide antigen (Epa)

Several Gram-positive pathogens produce, in addition or in place of caspules and teichoic acids another type of polymer called "secondary cell wall polymer" (SCWP). Unike capsules, which are commonly considered as the outermost structures, such polymers are buried in the cell wall. They can play an important role in during growth and pathogenesis.

For example, *B. anthracis* produces a pyruvylated polysaccharide essential for the non-covalent anchoring of surface proteins containing a surface-layer homology (SLH) domain. (Mesnage et al., 2000).

It has been reported that in some cases, SCWP represent a large proportion of the cell wall, up to 50% (Doran and Mattingly, 1982). An example of a widespread SCWP is the rhamnose-containing surface polysaccharide found in group A and group B streptococci as well as enterococci and lactococci (Mistou et al., 2016).

This type of polymer contains rhamnose as a major component and a variable combination and linkages of Glc, Glc*N*Ac, Gal, GalNAc and phosphate (**Fig. 14**) that define several Lancefield groups.

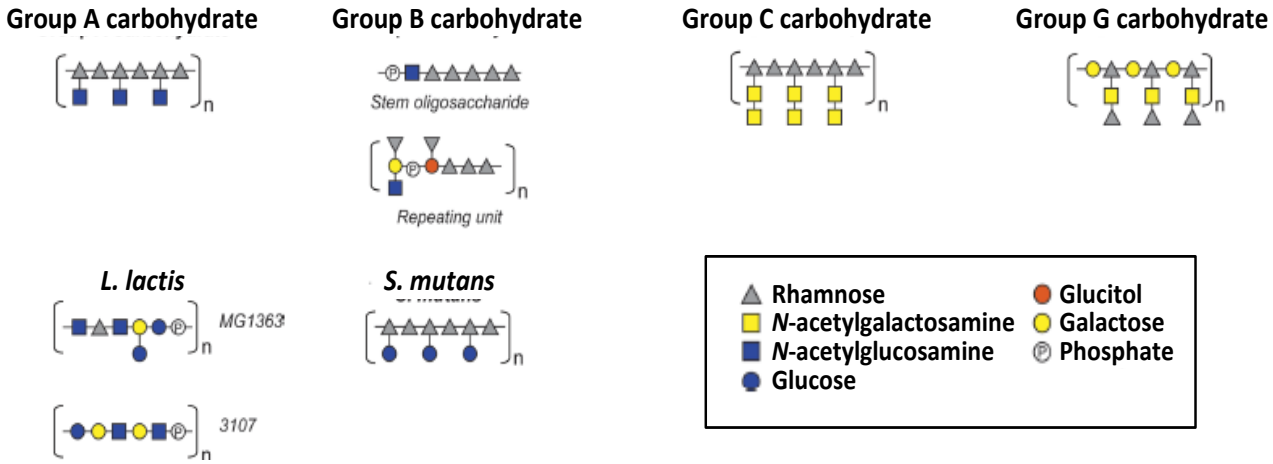

Figure 14. Composition of rhamnose-containing SCWP in Gram-positive bacteria (adapted from (Mistou et al., 2016)**.**

The rhamnopolysaccharides biosynthesis pathway follows 5 successive steps similar to most if not all surface polymers (**Fig. 15**). The synthesis starts by the addition of a UDP-Glc*N*Ac residue on a lipid transporter (initiation); glycosyltransferases add monosaccharides to polymerise the glycan chain (elongation). At this stage, the polysaccharide chain is transferred at the cell surface via a membrane transporter (translocation) where it will be covalently linked to the Mur*N*Ac residue of PG (linkage). The last step corresponds to additional modifications that are currently not formally identified, but are likely to be mediated at least in part by glycosyl transferases.

The role of the rhamnopolysaccharide has been studied in various Gram-positive organisms and it has been shown that it plays a major role in various steps of the infectious proccess. Mutants lacking the rhamnopolysacccharide have severe growth and cell division abnormalities (Caliot et al., 2012) suggesting that this polymer is important for the positioning or regulation of the activity of enzyme proteins involved in cell wall metabolism. Interestingly, modifications of the rhamnopolysaccharide that do not lead to growth defect are associated with a significant attenuation in virulence in a mouse peritonitis model (Xu et al., 2000; Teng et al., 2009).

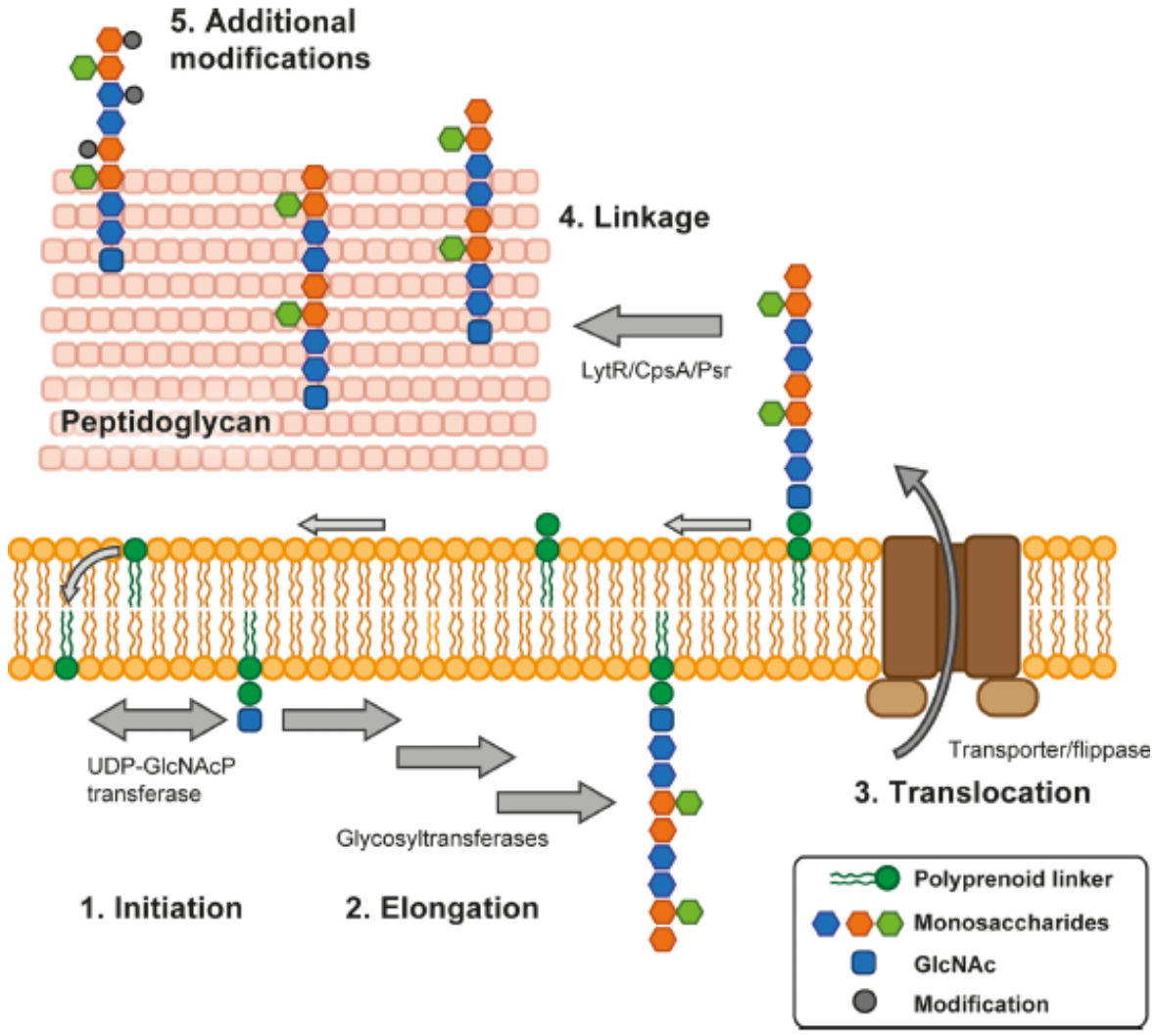

Figure 15. Major steps of the rhamnopolysaccharide biosynthesis pathway. (Adapted from (Mistou et al., 2016).

E. faecalis epa mutants also show an increased phagocyte uptake both *in vitro* (Teng et al., 2002) and *in vivo* (Prajsnar et al., 2013), indicating that the rhamnopolysaccharide has antiphagocytic properties.

1.2.3. PG Associated Proteins

Bacterial surface proteins contribute in the host-pathogen and host-symbiont interactions. In Gram-positive bacteria, surface proteins can be covalently or non-covalently bound to PG.

1.2.3.1. Covalent binding

1.2.3.1.1. LPXTG

The covalent binding of proteins is extremely conserved in Gram-positive bacteria and was first studied using protein A as a model protein (Schneewind et al., 1992). Proteins covalently bound to the PG are secreted proteins containing a signal peptide and a C-terminal sorting signal that consists of an LPXTG-like motif, a hydrophobic domain, and a positively charged tail (Schneewind et al., 1992; Ton-That et al., 2004). After secretion, the protein is retained in the cytoplasmic membrane; the LPXTG-like consensus sequence is then recognized and cleaved by a transpeptidase called sortase which links it to the PG cross-bridge of precursor. This mechanism is summarized in (**Fig. 16**). Most genomes encode several sortases that recognise LPXTG-like sequences and anchor proteins on the PG by the same mechanism.

E. faecalis and *E. faecium* produce LPxTG surface proteins considered to be important virulence determinants (Hendrickx et al., 2009). In *E. faecalis*, LPXTG proteins include the collagen-binding protein Ace and the pilin required for the assembly of type 4 pili (Hendrickx et al., 2009).

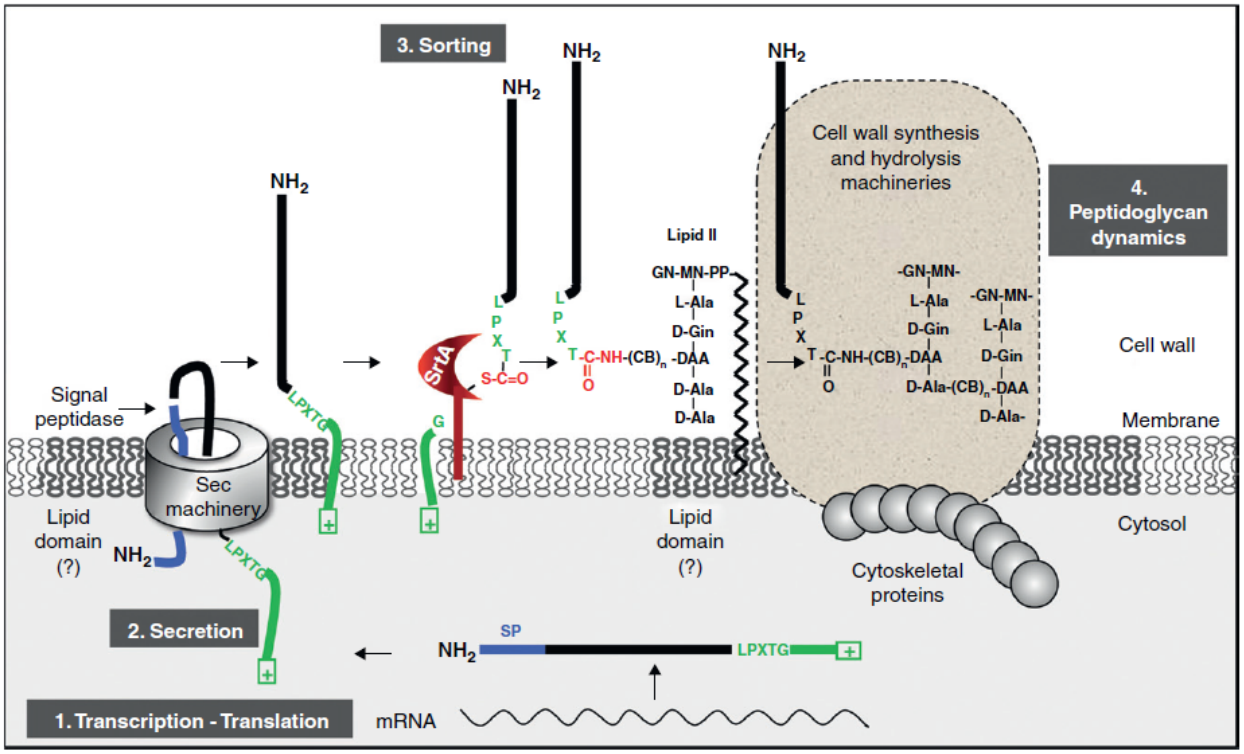

Figure 16. The SrtA-mediated sorting pathway in Gram-positive bacteria. Following transcription and translation, polypeptide precursors with an N-terminal signal peptide (SP, in blue) and a C-terminal sorting signal (in green: LPXTG motif, hydrophobic domain and positively charged tail (boxed +)) are secreted across the membrane through the Sec pathway. Following cleavage of the signal peptide, the exported protein is transiently retained in the membrane and then processed by the membrane-bound transpeptidase sortase SrtA, which recognizes the LPXTG sequence and cleaves its substrate between the threonine and glycine residues of the motif. An acyl-enzyme intermediate is formed between the active site cysteine of SrtA and the carboxyl-group of threonine. The enzyme then recognizes lipid II as the second substrate. Subsequent formation of a peptide bond between the carbonyl of the threonine and the free amino group of the cross-bridge peptide (CB) results in covalent attachment of the protein to lipid II. The surface protein is next incorporated into the mature PG via the cell wall synthesis machinery. It then follows expansion and reshaping of the PG during cell growth and division, upon the action of hydrolytic enzymes (autolysins) (Bierne and Dramsi, 2012).

1.2.3.2. Non-covalent binding

1.2.3.2.1. LysM

LysM (Lysin Motif) is a ubiquitous domain that binds to PG in a non-covalent manner (Buist et al., 2008). LysM motifs are found in surface proteins from both Gram-negative and Gram-positive proteins. They consist of imperfect repeats of 44 to 50 amino acid residues separated by linkers of low sequence complexity (Buist et al., 2008). LysM binding modules form a very conserved structure consisting of two beta strands flanked by two alpha helices (Bateman and Bycroft, 2000).

LysM domains are found at the N- or C-terminal of proteins and are often present in multiple copies to form multimodular domain (between 1 and 12 repeats). It has been proposed that LysM repeats are like "beads on a string" that confer additive binding (Mesnage et al., 2014). Recent work revealed that the structural organisation of LysM domains is very diverse and our beads on a string model is not universal. For example some eukaryotic LysM domains form trimeric structures via disulphide bounds (Ohnuma et al., 2008). In other cases, the binding can be mediated by more than one LysM module (Sánchez-Vallet et al., 2013) or at the interface between LysM and another domains (Schanda et al., 2014). LysM domains bind to Glc*N*Ac-X-Glc*N*Ac motifs in the glycan chains of PG. The acetyl groups of the Glc*N*Ac residues are recognized by two hydrophobic pockets whilst several residues make stacking and hydrophobic interactions with the sugar backbone that fits in a well defined cleft (**Fig. 17**).

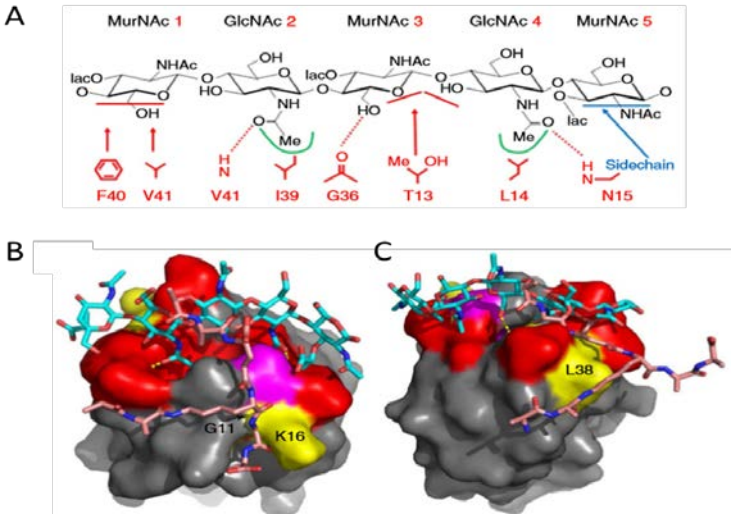

Figure 17. Structural model of a complex of an *E. faecalis* LysM module bound to a PG fragment. (**A**), key interactions between Mur*N*Ac-(Glc*N*Ac-Mur*N*Ac) 2 and LysM residues are described. Hydrogen bonds are shown by dashed lines. The horizontal bars indicate that the hydrophobic interaction is to the face of a sugar ring. The two pockets interacting with *N*-acetyl groups are indicated by green lines. Also shown in blue is the binding location involving N15 which may be important for distinguishing between chitin and peptidoglycan (**B**) and (**C**), Model of a LysM module in complex with a peptidoglycan fragment. The peptide stem is shown in two possible orientations, either side of the glycan backbone, interacting either with G11/K16 or with L38 (Mesnage et al., 2014).

The subcellular localization of some LysM proteins has been studied (e.g., AcmA in *L. lactis*, LytN in *S. aureus* or Cse in *Streptococcus thermophilus*). These proteins were found to be localized at the septum, but it remains unknown if all LysM proteins are targeted to this region of the cell. This septal localization was proposed to be due to the presence of secondary cell wall polymers preventing the binding of LysM proteins on the cell surface (Steen et al., 2003).

Interestingly, LysM binding modules can have distinct charges (basic or acidic). In *L. lactis*, it has been shown that the basic LysM domain of AcmA can bind peptidoglycan at pH 4–10, whereas the LysM domain of AcmD only bound at a ~pH 4 (Steen et al., 2003).
E. faecalis V583 encodes 12 proteins with LysM modules at their C-terminal. The glucosaminidase AtlA contains six C-terminal LysM modules (Eckert et al., 2006).

1.2.3.2.2. Pbp and Ser/Thr kinase attached (PASTA) domains

PASTA domains are made of imperfect repeats of approximately 70 residues found in proteins from Gram-positive bacteria. The crystal structure of *S. pneumoniae* Pbp2x in complex with cefuroxime, revealed that PASTA repeats could bind β-lactams (Gordon et al., 2000). A couple of years later, it was proposed that PASTA domains could bind PG (Yeats et al., 2002).
PASTA domains contain 2 (*S. pneumoniae* Pbp2x) to 5 repeats (*Enterococcus faecalis* PknB) of conserved structure. Apart from Pbp2x, where the two PASTA modules interact through a hydrophobic surface, other PASTA domains studied by X-ray crystallography present an extended conformation and form a linear structure (Ruggiero et al., 2011a; Paracuellos et al., 2010; Barthe et al., 2010) (**Fig. 18**).

In silico experiments have proposed binding sites for PG fragments (Paracuellos et al., 2010), and it was suggested that binding to PG fragments could induce dimerization of PASTA-containing proteins (Barthe et al., 2010; Paracuellos et al., 2010).
Surprisingly, only two studies have shown a direct binding of PASTA motifs to PG fragments using surface plasmon resonance (Mir et al., 2011) or NMR (Squeglia et al., 2011). Muramyl tetrapeptides represent the minimal PG motif recognised by *Mycobacterium tuberculosis* PknB PASTA domains. Using several synthetic PG fragments, Mir et al. showed that mDAP, the presence of amidated Glu in position 2 and the Mur*N*Ac residue are important determinants for binding (Mir et al., 2011). In another study, *B. subtilis* PrkC was shown to bind mDAP residues (Squeglia et al., 2011).

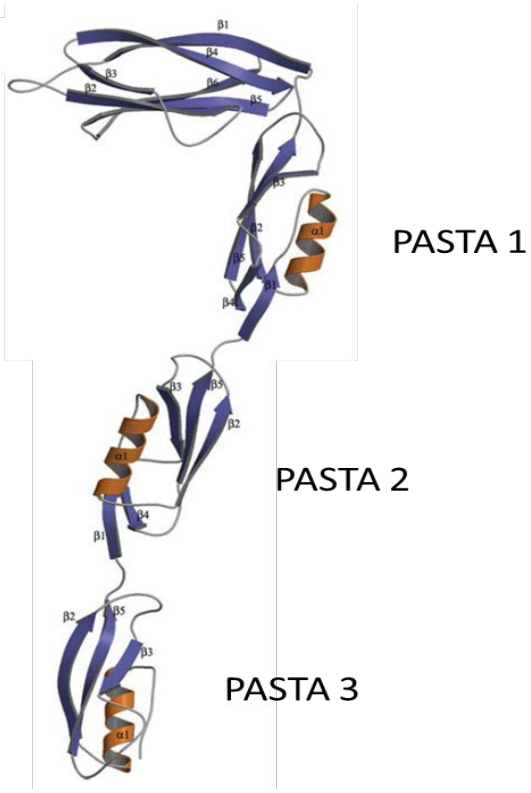

Figure 18. Crystal structure of the PASTA domain from *S. aureus* serine/threonine kinase PrkC. Helices and *β*-strands are shown in orange and blue respectively (Ruggiero et al., 2011b).

1.2.3.2.3. SH3b

The SH3b domain was first described in the lysostaphin enzyme (Baba and Schneewind, 1996). Lysostaphin is produced by *Staphylococcus simulans* biovar *staphylolyticus* and specifically digests *S. aureus* PG (Thumm and Gotz, 1997). The PG binding activity of the SH3b domain has been studied in a lysostaphin close homolog, *S. capitis* ALE-1, also targeting *S. aureus*. The structure of this domain is very similar to the SH3 (**S**rc **H**omology **3**) domains from eukaryotes that recognises short proline-rich peptide segments in proteins (Pawson, 1995). The SH3b domain of ALE-1 (92 amino acids) is sufficient to bind peptidoglycan *in vitro* (Lu et al., 2006).

ELISA assays revealed that ALE-1 SH3b domain specifically binds *S. aureus* PG. The presence of 5 glycine residues in the PG is required for binding. It has therefore been suggested that SH3b specifically recognises the pentaglycine motif in the PG. It was proposed that the pentaglycine stem could bind a deep and narrow groove in the *N*-terminal region of the domain (**Fig. 19**). Mutations of residues in this groove support this hypothesis (Lu et al., 2006).

SH3b domains are conserved in bacteria. Interestingly, some bacteria producing proteins with SH3b domains have PG crossbridges (e.g. L-Ala-L-Ala in *E. faecalis* and *S. agalactiae*), but some others have a direct crosslink (eg., *Anabaena variabilis*). How different SH3b domains recognise different PG structures is unknown.

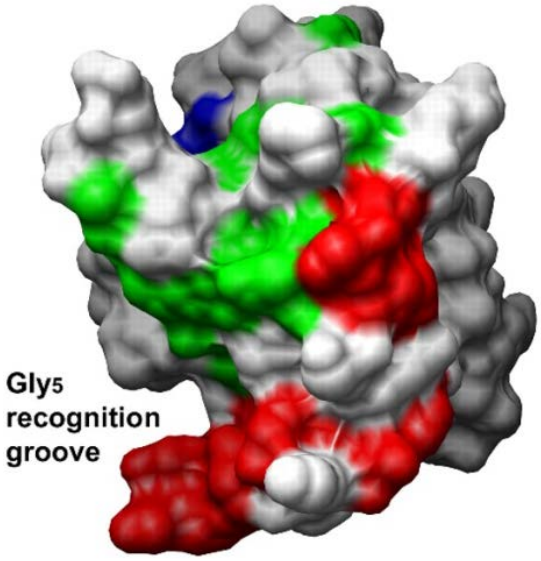

Figure 19. Crystal structure of the ALE-1 SH3b cell wall-targeting domain. ALE-1 SH3b domain specifically binds *S. aureus* PG. The presence of 5 glycine residues in the PG is required for binding. SH3b specifically recognises the pentaglycine motif in the PG. A deep and narrow groove in the *N*-terminal region of the domain has been proposed to bind the pentaglycine stem (Lu et al., 2006).

1.2.3.2.4. WxL

This domain was recently identified based on sequence analysis of secreted proteins in *E. faecalis* (Brinster et al., 2007a). Sequence comparisons revealed the presence of two WxL motifs separated by 80 to 120 residues. This consensus is found in 27 *E. faecalis* proteins mostly grouped in 8 clusters on the chromosome (Brinster et al., 2007a).

WxL domains are sufficient for PG binding but the motif they recognise in PG has not been identified yet. WxL proteins are only present in low GC Gram-positive bacteria including some pathogens (*Listeria monocytogenes*, *E. faecium* and *Bacillus cereus*) and for these species, the number of WxL proteins can vary between strains.

Some WxL proteins have been reported to contribute to virulence. One example is the *E. faecalis* internaline ElrA that contributes to stimulate the host inflammatory response (Brinster et al., 2007b). More recently, it was proposed that in *E. faecium*, WxL proteins interact to form surface complexes involved in interactions with the host extracellular matrix proteins (Galloway-Pena et al., 2015).

1.3. Peptidoglycan hydrolases (PGHs)

1.3.1. Definition

Peptidoglycan can be cleaved by enzymes called peptidoglycan hydrolases (PGHs). Some PGHs can cause cell lysis and in this case they are called autolysins. This chapter will describe the enzymatic activities of PGHs, their physiological function and give examples of PGHs well studied in Gram-positive bacteria that have been used as model systems.

1.3.2. Classification

Several types of PGHs have been described based on the PG bond they cleave: (i) glycosyl hydrolases: (*N*-acetylglucosaminidases and *N*-acetylmuramidases), (ii) *N*-acetylmuramoyl-L-Alanine amidases, and (iii) peptidases (**Fig. 20**).

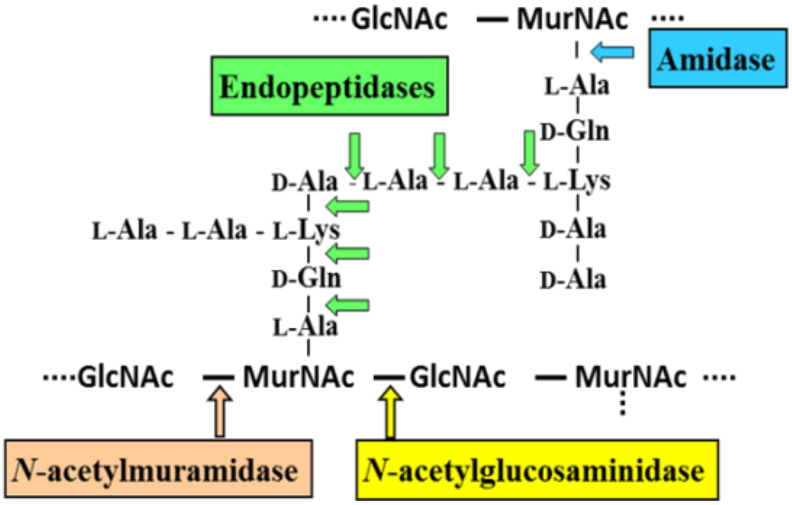

Figure 20. Schematic representation of PGHs cleavage sites (*E. faecalis* PG is given as an example). Glycosyl hydrolases including *N*-acetylglucosaminidases and *N*-acetylmuramidases cleave the glycan chains. *N*-acetylmuramoyl-L-Alanine amidases cleave between the Mur*N*Ac residues and the peptide stem. Peptidases cleave within the peptide stems. More details on these enzymes are provided below.

1.3.2.1. Glycosyl hydrolases

Three classes of glycosyl hydrolases are able to cleave PG glycan strands: *N*-acetylglucosaminidases, *N*-acetylmuramidases (also called lysozymes), and lytic transglycosylases. The latter two cleaving the same glycosidic bond (**Fig. 21**) (Vollmer et al., 2008).

***N*-acetylglucosaminidases** hydrolyse the glycosidic bond between Glc*N*Ac residues and adjacent Mur*N*Ac and generate a reducing Glc*N*Ac end (**Fig. 21, cleavage 1**).

A large number of PGHs with glucosaminidase activity belong to the CAZy family GH73. This catalytic domain is often associated with one or several cell wall-binding domains (e.g. the LysM domain).

***N*-acetylmuramidases** (also called lysozymes) hydrolyse the glycosidic bond between Mur*N*Ac and Glc*N*Ac residues and generate a reducing Mur*N*Ac end (**Fig. 21, cleavage 2**).

Lytic transglycosylases have the same cleavage site as muramidases but are formally not glycosylhydrolases as they do not use a water molecule. Instead of a reduced Mur*N*Ac extremity, they generate anhydroMur*N*Ac residues (**Fig. 21, cleavage 3**). This activity is rare in Gram-positive bacteria. The digestion product of lytic transglycosylases has been reported in *B. subtilis* (Atrih et al., 1999), but the enzyme responsible for this activity has not been identified.

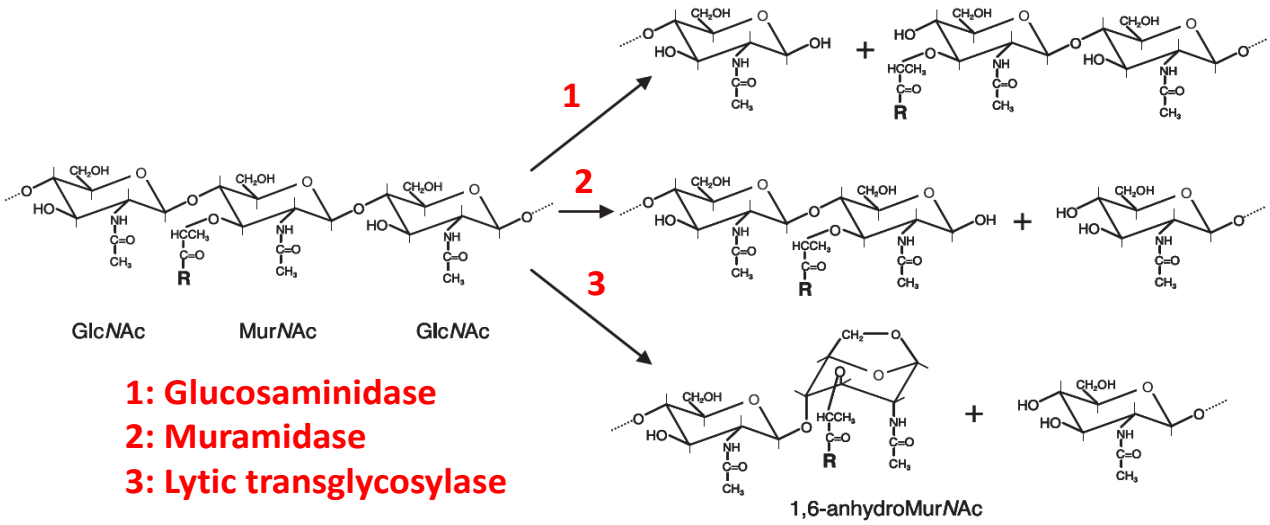

Figure 21. Cleavage of PG bonds by glycosyl hydrolases. The bonds cleaved by *N*-acetylglucosaminidases, *N*-acetylmuramidases and lytic transglycosylases and the corresponding products are described.

1.3.2.2. *N*-acetylmuramyl-L-alanine amidases

N-acetylmuramyl-L-alanine amidases cleave the amide bond between Mur*N*Ac and the *N*-terminal L-alanine residue of the stem peptide (**Fig. 22,** Ami). These enzymes, also known as amidases, are present in bacterial and bacteriophage/prophage genomes (Young, 1992; Lopez et al., 1981).

1.3.2.3. Peptidases

Several classes of PGHs can cleave the bonds between amino acids in the stem peptides (Vollmer et al., 2008) .Two major classes can usually be distinguished:

Endopeptidases cleave the bonds within the peptide stems or the crosslinks generated by PBPs and can therefore cause cell lysis (Shockman and Höltje, 1994). They can recognise several types of bonds. L,D endopeptidases cut between the first L-Ala and the γ-D-Gln residue. D,L endopeptidases cut between the γ-D-Gln residue and the diamino acid or at the end of the lateral chain in crosslinked peptide stems. A summary of the different types of peptidases is presented in **Fig. 22**.

Carboxypeptidases cleave the extremity of peptide stems and can therefore not trigger cell lysis. They can be D,D-carboxypeptidases (cleaving between D-Ala in position 4 and D-Ala in position 5) or L,D-carboxypeptidases (cleaving between the L-diamino acid in position 3 and D-Ala in position 4).

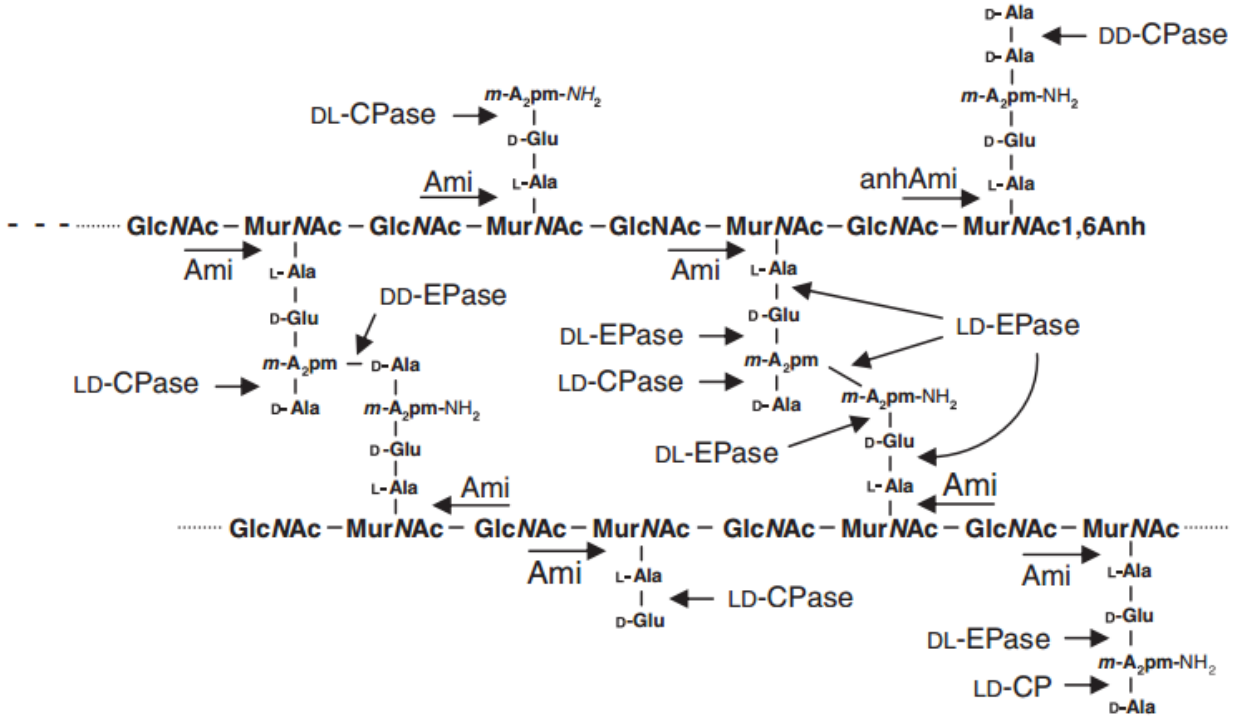

Figure 22. Cleavage of PG bonds by peptidases. *N*-acetylmuramoyl-L-alanine amidases (Ami) hydrolyse the amide bonds between the lactyl group of *MurN*Ac and the L-alanine of the stem peptide. Some amidases (anhAmi) specifically cleave at 1,6-anhydroMur*N*Ac residues, which are the hallmarks of PG turnover products in many species. Endopeptidases (DD-EPase, LD-EPase, DL-EPase) cleave amide bonds in the peptides. The cleavage sites for LD- or DL-endopeptidases are indicated in a dimeric (cross-linked) peptide, but there are also cleavage sites for these enzymes in monomeric peptides. Carboxypeptidases (DD-CPase, LD-CPase, DL-CPase) hydrolyse peptide bonds to remove C-terminal D- or L-amino acids, (*B. subtilis* PG is given as an example) (Vollmer et al., 2008).

1.3.3. The physiological role of the PGHs

The enzymatic activity of PGHs contributes to several functions during growth and also modulates some properties of bacterial cell populations.

1.3.3.1. Contribution to peptidoglycan biosynthesis

During cell growth, the PG molecule undergoes partial hydrolysis. Breaking PG bonds is required to allow the incorporation of new precursors in the existing network. This process involves lytic transglycosylases in *E. coli* and some endopeptidases such as LytE in *B. subtilis* (Carballido-Lopez et al., 2006).

It is widely accepted that some PGHs are part of the PG synthetic machinery complexes involving PBPs and cytoskeleton elements such as MreB and FtsZ (den Blaauwen et al., 2008). During growth, the activity of carboxypeptidases depends on the availability of precursor with pentapeptide stems used by the PBPs to polymerise PG. These enzymes regulate the degree of crosslinking in the PG sacculus and also contribute to the subcellular localisation of other proteins involved in cell division (Morlot et al., 2004).

1.3.3.2. Role during sporulation and germination

After asymmetric division (the first step required for sporulation), the asymmetric septum is digested by PGHs such as SpoIID (Gutierrez et al., 2010). This allows the engulfment process to take place. Later during sporulation, the spore peptidoglycan undergoes maturation, a process which leads to the formation of δ-lactam Mur*N*Ac residues. This step requires the activity of amidase CwlD which cleaves the peptide stem, and the Mur*N*Ac deacetylase PdaA which forms the lactam ring (Vollmer et al., 2008).

In *B. subtilis*, the L-alanyl-D-glutamate endopeptidase LytH removes the remaining peptide stems, a modification required for increased heat resistance (Horsburgh et al., 2003). Once the spore is formed, the mother cell is lysed by PGHs which act in synergy (LytC, CwlC and CwlH). Finally, germination of spores also requires the combined activity of several PGHs (CwlJ and SleB) (Moir, 2006).

1.3.3.3. Septum cleavage during cell division

Towards the end of the cell division process, the septum has to be hydrolysed to release two daughter cells. This requires the activity of PGHs. In some cases, several enzymes have been reported to be important for this process (Sle1 and Atl in *S. aureus*; (Yamada et al., 1996; Kajimura et al., 2005). In several Gram-positive bacteria, one particular PGH is dedicated to septum cleavage and plays a major role. This is the case of AtlA in *E. faecalis* (Mesnage et al., 2008), Cse in *S. thermophilus* (Layec et al., 2009) LytB in *S. pneumoniae* (de las Rivas, 2002) or AcmA in *L. lactis* (Buist et al., 1995).

1.3.3.4. Resuscitation of dormant cells

Some bacteria can enter a viable but non-culturable state. This corresponds to a physiological state where the cells don not divide and display a very low metabolic activity, usually following prolonged stationary phase. This is well established for *Micrococcus luteus* and *Mycobacterium tuberculosis* which can be found as "dormant" cells. Some PGHs called resuscitation-promoting factors (Rpf) can induce the growth of dormant cells (Mukamolova et al., 1998). In *Mycobacterium tuberculosis*, five Rpf proteins have been described (Keep et al., 2006).

1.3.3.5. Contribution to natural competence

Some bacteria are naturally competent, which means they can be transformed by exogenous DNA. This is the case of *S. pneumoniae* and *B. subtilis*. In *S. pneumoniae*, cell lysis by PGHs is an important step that promotes integration of new genes in the chromosome. It has been shown that within a population, competent cells are producing both an immunity factor and a bacteriocin that can activate autolysins (Guiral et al., 2005). As a result, competent cells are able to trigger the lysis of non-competent cells, a phenomenon known as allolysis.

1.3.3.6. PGHs as toxins to lyse competitors

PGHs can be involved in the cell lysis of competitors. One of the most studied examples is lysostaphin (Thumm and Gotz, 1997). This enzyme is produced by *S. simulans* biovar *staphylolyticus*. It cleaves the pentaglycine crossbridge specifically found in *S. aureus* PG. The lysostaphin gene is encoded by a plasmid, which also contains genes encoding immunity factors. These immunity factors modify the PG crossbridges in *S. simulans* by incorporating Serine residues instead of glycine. The lysostaphin is no longer able to cleave these modified crossbridges.

1.3.4. *E. faecalis* PGHs

The *E. faecalis* genome encodes 21 putative peptidoglycan hydrolases (PGHs), including 3 amidases, 5 endopeptidases, 6 glucosaminidases, and 7 proteins related to muramidases (**Fig. 23**).

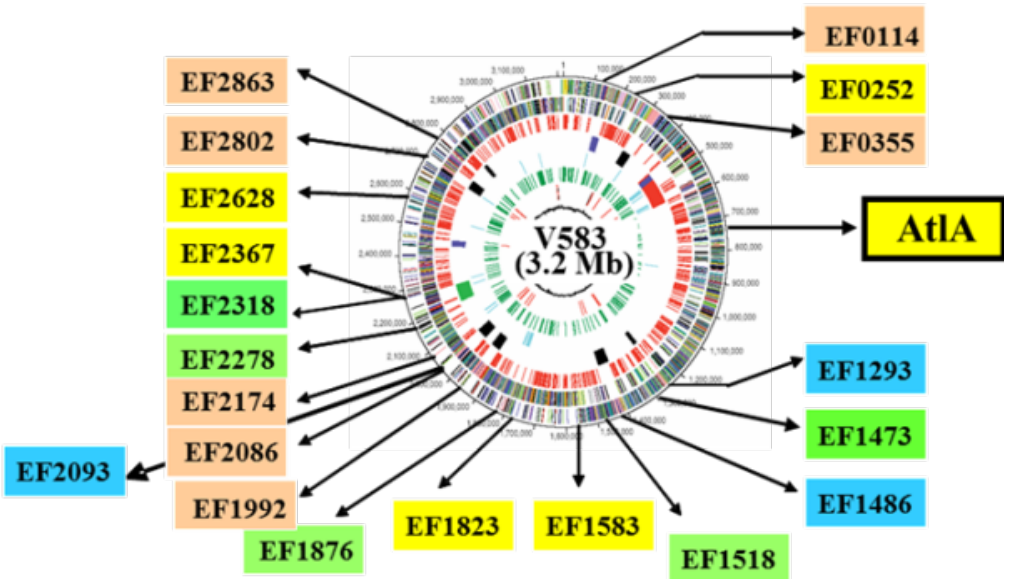

Figure 23. Putative PGHs encoded by *E. faecalis* V583. *E. faecalis* V583 genome encodes 21 putative peptidoglycan hydrolases (PGHs), including 3 amidases (blue boxes), 5 endopeptidases (green boxes), 6 glucosaminidases (yellow boxes), and 7 proteins related to muramidases (pink boxes).

Analysis of a limited set of strains suggested that only a 7 these genes are ubiquitous EF0114, EF0252, EF0799 (AtlA), EF1293, EF1518, EF1583, EF2367.

Analysis of PGH activities in cell extracts and supernatants by zymography indicates that only a limited number of the enzymes encoded by *E. faecalis* can be detected (Mesnage et al., 2008). In the strain JH2-2, three activities have been reported: AtlA, AtlB and AtlC. Another enzyme encoded by a prophage (EF1473, EnpA) has been expressed as a recombinant protein in *E. coli* and its PGH activity has been studied (Reste de Roca et al., 2010).

1.3.4.1. AtlA

AtlA is a 737 amino acid-long modular protein (**Fig. 24A**) composed of:

- A signal peptide (residues 1-53); although AtlA signal peptide is unusually long, it has all the expected properties (a charged *N*-terminal sequence followed by a hydrophobic segment and a canonical AEA cleavage sequence, where cleavage takes place after the last alanine).

- An *N*-terminal domain (residues 54-171) rich in Serine/Threonine/Glutamic acid and Proline (11%, 27%, 14% and 12%, respectively). Unpublished results in the laboratory have shown that this domain is glycosylated and that this modification inhibits the activity of the enzyme (Bartek Salamaga, unpublished). This domain is cleaved by proteases in *E. faecalis*, and this cleavage (which also removes AtlA glycosylation) increases the activity of the enzyme.
- A catalytic domain (residues 172-334) that displays an *N*-acetylglucosaminidase activity (Eckert et al., 2006). This domain belongs to the CAZy family GH73 that contains a very large number of bacterial glucosaminidases (Lipski et al., 2015).
- A C-terminal LysM domain made of 6 imperfect repeats (**Fig. 24B**) responsible for the peptidoglycan binding activity of the enzyme. The presence of this domain is crucial for the activity of the enzyme, and its truncation reduces the activity AtlA by approximately 500-fold (Eckert et al., 2006).

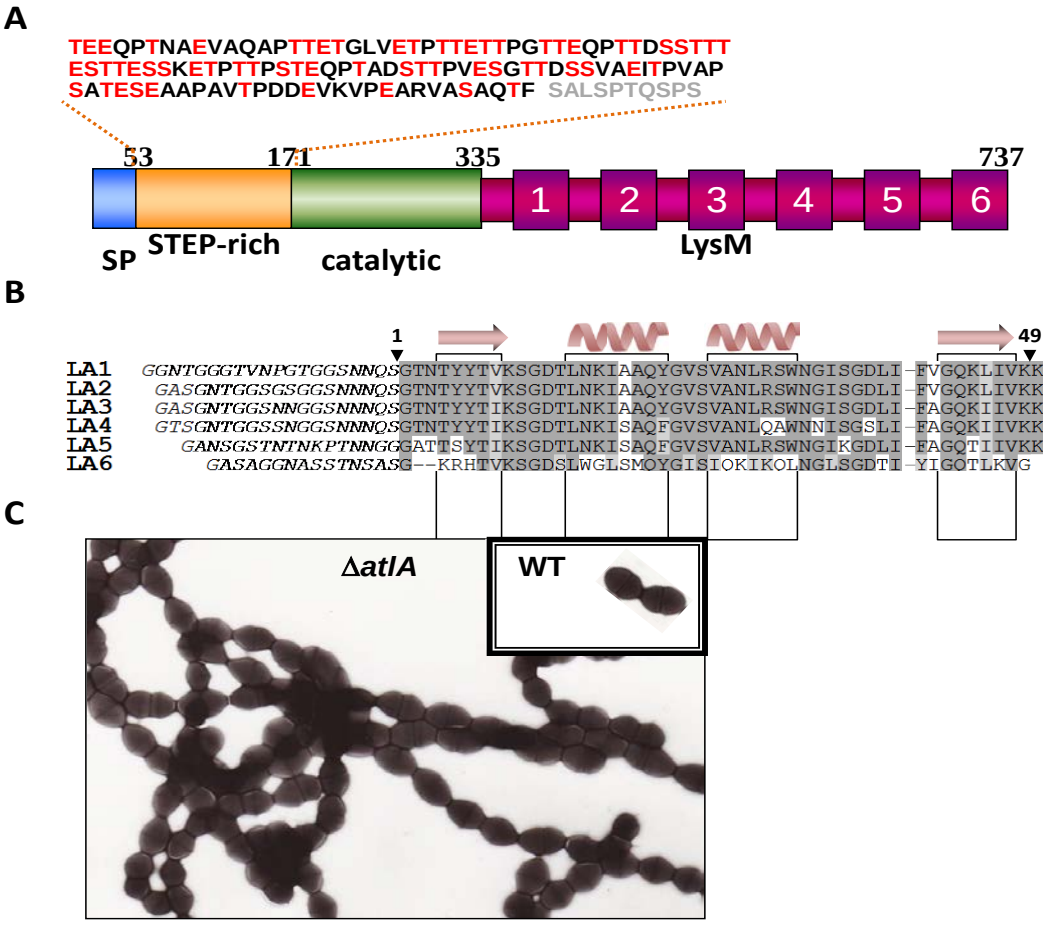

Figure 24. Modular organization of *E. faecalis* AtlA. (**A**), Domain organization of *E. faecalis* AtlA. Amino acid numbers refer to the transition between domains. SP, signal peptide; STEP-rich, catalytic and LysM domain. (**B**), Sequence alignment of the six AtlA LysM repeats. Numbering refers to residues corresponding to the beginning of each LysM fold, linker sequences are in italics. Identical amino acids in at least four modules are in dark grey boxes, conserved amino acids are in light grey boxes. (**C**), Chain-forming phenotype of the *E. faecalis atlA* mutant.

AtlA was originally identified during the screening of an expression library built in *E. coli* (Xu et al., 1997). In this work, a screen was carried out to identify recombinant *E. coli* colonies producing *E. faecalis* antigens recognized by human antisera from patients suffering from endocarditis caused by *E. faecalis*. Following this study, AtlA enzymatic activity was shown using zymogram assays (Qin et al., 1998). It was also reported that AtlA was able to cause cell lysis when the cells were re-suspended in phosphate buffer, as opposed to the *atlA* mutant which did not lyse at all. These results represent the first characterization of AtlA showing that it is the major autolysin in *E. faecalis* (Qin et al., 1998). AtlA is active against *E. faecalis* cells (Emirian et al., 2009) but has a relatively low activity as compared to AtlB (see below).

AtlA is required for the separation of daughter cells after cell division. This was confirmed as a result of the long chains that formed by Δ*atlA* mutant (**Fig. 24C**).

It has been reported that AtlA is essential for biofilm development (Kristich et al., 2008). This role is due to the autolytic activity of AtlA which is critical for the release of extracellular DNA (eDNA), a key component for the biofilm formation.

1.3.4.2. AtlB

In strain JH2-2, AtlB can be detected as a 45 kDa band with autolytic activity on a zymogram containing *E. faecalis* cells as a substrate (Mesnage et al., 2008). It was purified from culture supernatants using ammonium sulfate precipitation and ion exchange chromatography. The gene encoding AtlB (EF0355) was identified based on mass spectrometry analyses of tryptic digests of the protein. Deletion of the candidate gene and complementation of the mutant confirmed that AtlB is encoded by *EF0355*. The *N*-acetylmuramidase activity of AtlB was identified using mass spectrometry analysis of muropeptides solubilized by the recombinant enzyme produced in *E. coli*. AtlB is a 433 amino acid-long modular protein (**Fig. 25**) encoded by a prophage that is not present in all *E. faecalis* strains. This PGH is composed of:

- A canonical signal peptide (residues 1-22).
- An *N*-terminal catalytic domain (residues 23-226) that belongs to the CAZy family GH25; the model enzyme corresponding to this family of muramidases is the mutanolysin produced by *Streptomyces coelicolor* (Rau et al., 2001).
- Two C-terminal LysM repeats separated by a very short sequence and with a lower pI than AtlA (4.6 and 8.3). The biological significance of this lower pH is unknown.

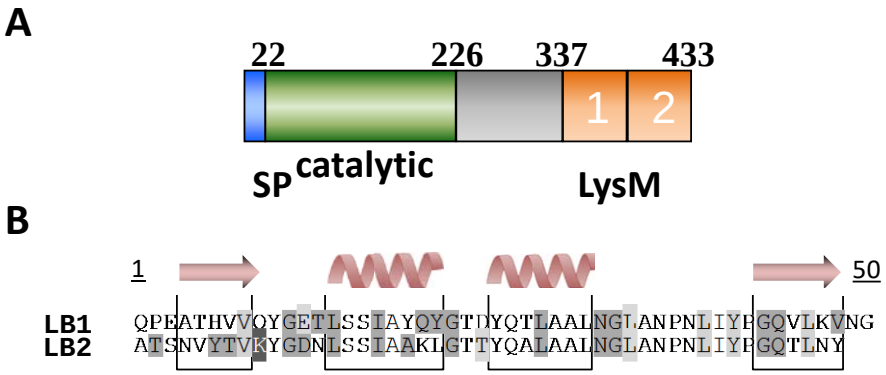

Figure 25. Modular organization of *E. faecalis* AtlB. (**A**), Domain structure of *E. faecalis* AtlB. Amino acid numbers refer to the transition between domains. SP, signal peptide. (**B**), Sequence alignment of the two AtlB LysM repeats. Numbering refers to residues corresponding to the beginning of the LysM fold. Conserved amino acids are in light grey boxes.

The physiological role of AtlB is poorly understood. In the absence of AtlA, AtlB contributes to septum cleavage converting long cell chains into diplococci but is not very active (Mesnage et al., 2008). This was confirmed *in vitro* using recombinant AtlB enzyme to cleave the septum of long cell chains of a Δ*atlA* mutant. Incorporation of 14C-Glc*N*Ac in PG during growth indicated that AtlB is not required for the insertion of novel PG precursors during growth. AtlB was found to be associated with the release of a small proportion of PG fragments into the growth media during stationary phase (Mesnage et al., 2008).

1.3.4.3. AtlC

In strain JH2-2, AtlC can be detected as a 42 kDa band with autolytic activity on a zymogram containing *E. faecalis* cells as a substrate (Mesnage et al., 2008). The gene encoding AtlC was identified using BLAST searches in order to find PGHs similar to AtlB. The gene encoding AtlC was deleted and complemented to confirm that it encodes the 42k Da band with PG hydrolytic activity detected in *E. faecalis* crude extracts. AtlC shares 69 % identity with AtlB (**Fig. 26**) and its physiological role is unknown.

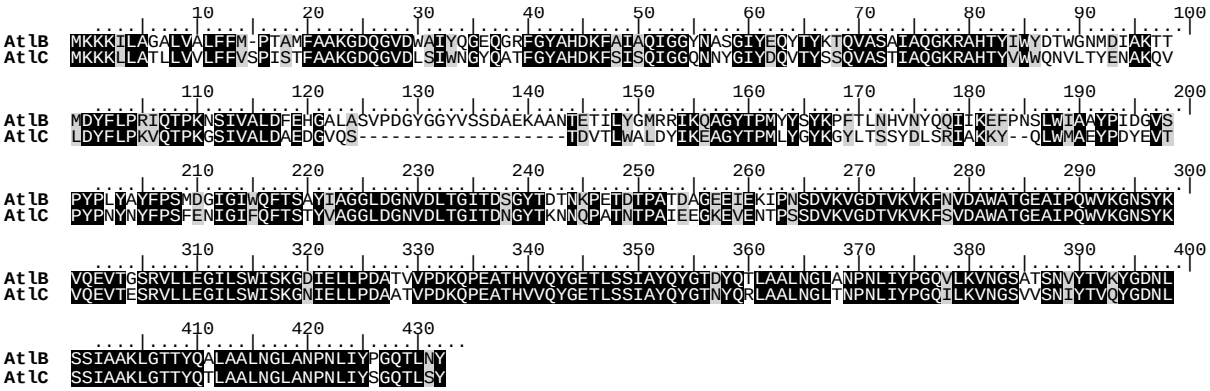

Figure 26. Amino acid sequence alignments of V583 EF0355 (AtlB) and EF1992 (AtlC). AtlC shares 69 % identity with AtlB.

1.3.4.4. EnpA

EnpA (EF1473) was identified based on the genome sequence analysis. It is a large protein of 1721 residues encoded by a prophage that is only present in some *E. faecalis* strains. The only EnpA domain recognized by the pfam database corresponds to a short C-terminal sequence of approximately 90 residues similar to endopeptidases belonging to the M23 family of peptidases (**Fig. 27**). These enzymes include lysostaphin (see paragraph 1.3.3.6). EnpA is poorly active against whole sacculi but displays a high activity against soluble disaccharide-peptides (Reste de Roca et al., 2010). Enzymatic assays using purified peptidoglycan fragments showed that EnpA cleaves the amide bond generated by PBPs, i.e. between the end of the PG crosslink and the D-Ala4 of the donor stem. Unlike lysostaphin that only cleaves *S. aureus* PG, EnpA can cleave disaccharide-peptides from a wide range of bacteria, but is not active against directly crosslinked muropeptides (Reste de Roca et al., 2010). The inactivation of the *enpA* gene, alone or in combination with the inactivation of *atlA*, *atlB* and *atlC* has no phenotype, suggesting that this enzyme may be specifically produced during the excision of the prophage encoding it.

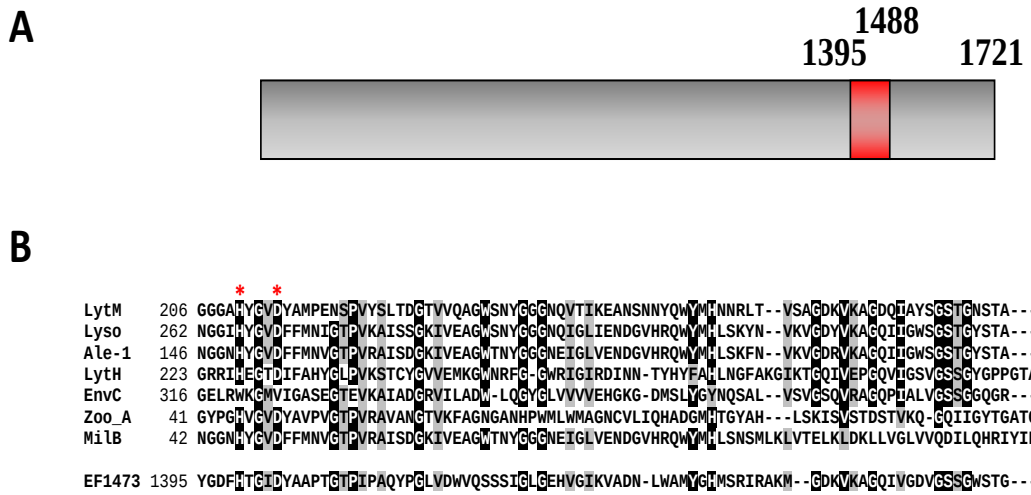

Figure 27. Schematic representation of *E. faecalis* EnpA (**A**), Domain structure of *E. faecalis* EnpA. Amino acid numbers refer to the identified M23 peptidase domain shown in red. (**B**), Sequence alignment of EnpA with other peptidases belonging to the M23 peptidase family.

1.4. Aims and objectives

AtlA is a peptidoglycan hydrolase which can cause autolysis when the cells are resuspended in phosphate buffer (Qin et al., 1998). The potentially lethal activity of AtlA therefore has to be tightly controlled during cell growth and division. How this is achieved is unknown. Recent work in the laboratory has shown that the formation of long chains in the *atlA* mutant is associated with a lack of virulence in the zebrafish model of infection (**Fig. 28**). When zebrafish embryos (20h post fertilization) are infected with *ca.* 1000 CFUs of *E. faecalis* OG1RF (WT) strain, approximately 60% of the larvae die within 96h (red curve in Fig. 28). The injection of a similar number of cells forming long chains only causes 20% mortality (blue curve in Fig. 28), indicating that septum cleavage defect is associated with a loss of virulence. Sonication of the long chains, which separated cells without impairing viability, restores *E. faecalis* virulence (green curve in Fig. 28).

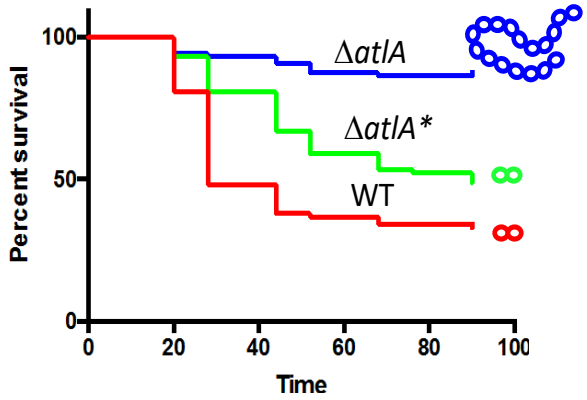

Figure 28. Virulence of *E. faecalis* forming long chains in the zebrafish model of infection. Survival of zebrafish larvae (n>20) following infection with *E. faecalis* OG1RF (WT) and *atlA* isogenic deletion mutant before (Δ*atlA*) and after (Δ*atlA**) sonication to disperse long chains.

Altogether, these results indicate that AtlA is a potential therapeutic target to control enterococcal infections, either by deregulating or abolishing its activity.

The aim of this work was to identify the mechanisms responsible for the control of AtlA activity. We used two distinct phenotypes associated with AtlA activity: (i) the formation of diplococci/short chains and (ii) the cell surface enzymatic activity of this enzyme that can be detected on agar plates containing autoclaved cells as a substrate.

Three objectives were identified:

1. Isolate and characterise spontaneous mutants with impaired septum cleavage.

2. Construct and screen a random transposon mutant library based on the Mariner transposon

3. Analyse the role of the genes identified in the control of AtlA activity

Chapter 2

Materials and Methods

2.1. Chemicals and enzymes

All chemicals used in this project were purchased from Sigma or Fisher Scientific. Restriction and modification enzymes and buffers for molecular biology were purchased from New England Biolabs.

2.2. Antibiotics

All antibiotics used and their concentrations are listed in Table 3. Antibiotic stock solutions were prepared by dissolving the antibiotics in the corresponding solvent, filter-sterilised and stored at -20°C.

Antibiotic	Stock concentration (mg/mL)	Working concentration (μg/mL)	Dissolved in
Ampicillin (Amp)	100	100	dH_2O
Chloramphenicol (Cm)	30	10	90% (v/v) ethanol
Erythromycin (Ery)	30	200[a]/30[b]	90% (v/v) ethanol
Gentamycin	128	128	dH_2O

Table 3. Antibiotic stock solutions and concentrations used in this project.

[a] concentration for *E. coli*

[b] concentration for *E. faecalis*

2.3. Media

All media were prepared using distilled water (dH_2O). Sterilisation was performed by autoclaving for 20 min at 121°C. Heat-sensitive compounds were sterilised by filtration through 0.45μm filters (Sartorius) and added to the autoclaved media cooled down to 55°C.

2.3.1. Brain heart infusion (BHI)

BHI broth was prepared according to manufacturer's instructions (37g/L) and eventually supplemented with 1.2% (m/v) bacterial agar No. 1 (Oxoid).

2.3.2. Super optimal broth with catabolite repression (SOC**)**

SOC buffer was prepared according to (Sambrook and Maniatis, 1989). The composition is as follows:

Tryptone (Oxoid)	2% (w/v)
Yeast extract (Oxoid)	0.5% (w/v)
NaCl	10 mM
KCl	2.5 mM

Once autoclaved, filter-sterilized $MgCl_2$, $MgSO_4$ and glucose were added at a final concentration of 10 mM, 10mM and 20mM, respectively..

2.3.3. Semi-solid medium for the isolation of spontaneous mutants

THY broth (Todd Hewitt 37g/L containing 5% [m/v] yeast extract) was prepared and supplemented with a low concentration of agar 0.06% (m/v). The medium was poured into flasks and left at 4°C for 1h to set before inoculation with dilutions of pre-cultures suitable to see individual colonies. The cells were grown at 37°C without agitation and the appearance of spontaneous mutants with altered colony morphology followed over a period of 96h

2.3.4. Agar plates to detect AtlA activity

BHI-agar was autoclaved in the presence of freeze-dried *M. luteus* plates at a final optical density at 600 nm of 1.5.

2.3.5. M17-Glu

M17 broth was prepared according to manufacturer's instructions (37g/L), autoclaved and supplemented with filter-sterilised glucose at a final concentration of 0.5% (m/v).

2.3.6. SGM17

M17-Glu broth was supplemented with 0.5 M sucrose and 2% (m/v) glycine and the pH ws adjusted at 7.0.

2.4. Bacterial strains, plasmids and oligonucleotides

All bacterial strains, plasmids and oligonucleotides used in this project are listed in Table 4.

Strains, plasmids and oligonucleotides	Relevant properties or genotype[a]	Source
Strains		
Enterococcus faecalis		
OG1RF	Plasmid-free, virulent laboratory strain isolated from the oral cavity	(Dunny et al., 1978)
JH2-2	Plasmid-free laboratory strain	(Jacob and Hobbs, 1974)
V583	Clinical isolate, first *E. faecalis* sequenced	(Paulsen et al., 2003)
M. lysodeikticus		
ATCC4698	Reference strain for PG hydrolase activity assays	ATCC
Escherichia coli		
NEB5α	Cloning strain	New England Biolabs
BL21(DE3)	BL21 derivative for protein expression	Novagen
Plasmids		
pET2817	pET28a derivative for overexpression of *N*-terminally His-tagged proteins (Amp^R)	(Eckert et al., 2006).
pGhost9	Thermosensitive plasmid for targeted gene replacement in *E. faecalis* (Erm^R)	P. Serror
pZXL5	Thermosensitive plasmid for transposon mutagenesis (Gm^R)	(Zhang et al., 2012b)
pJEH11	Replicative plasmid for *E. faecalis* complementation experiments (Erm^R)	M. Arthur
pET-AdmA	pET2817 derivative expressing AdmA (residues 26 to172)	This work
pTetH	Replicative plasmid for complementation experiments (Erm^R)	Lab stock
pAtlA_WT	pTetH derivative encoding a tetracycline-inducible wild-type *atlA* allele	This work
pAtlA_E212Q	pTetH derivative encoding a tetracycline-inducible *atlA*_E_{212}Q allele	This work
pAtlA_LysM	pTetH derivative encoding a tetracycline-inducible LysM domain	This work
pAtlA_WT	pTetH derivative encoding a tetracycline-inducible wild-type *atlA* allele	This work
pSecA_WT	pTetH derivative encoding a tetracycline-inducible wild-type *secA* allele	This work
pSecA_ΔE377	pTetH derivative encoding a tetracycline-inducible *secA*_ΔE377 allele	This work
pSecA_R548H	pTetH derivative encoding a tetracycline-inducible *secA*_R548H allele	This work
pSecY_WT	pTetH derivative encoding a tetracycline-inducible wild-type *secY* allele	This work
pSecY_L337S	pTetH derivative encoding a tetracycline-inducible *secY*_L337S allele	This work
Oligonucleotides [a] (Sequence 5'→3')		
EF0018_H11	TCACTATAGGGCGAATTGGGTACCATGAAGCGGATTGAAAAAATCTATC	
EF0018_H12	CGACATCAAAAGTTCTGGATTATGC	
EF0018_H21	GCATAATCCAGAACTTTTGATGTCGATTCCTTTGTCCATTGTAAATATG	
EF0018_H22	GAGGATCCCACCGCGGTGGCGGCCGCTTAATCTAGTGTATCAATTTCGG	
EF0018_H110	TTTCATGAAAGGGTTTTTAGTGT	
EF0018_H220	CGTGCCAACTTTAGTGTATCGG	
EF0018_up	AAAGGTCTCCCATGAAGCGGATTGAAAAAATCTATC	
EF0018_dn	AAAGGATCCATCTAGTGTATCAATTTCGGTGA	
EF0954_H11	TCACTATAGGGCGAATTGGGTACCGTTAGACATTCTGTCACATTTGC	
EF0954_H12	CCAAATTCCGTGCTGTCATATTTG	
EF0954_H21	CCAAATATGACAGCACGGAATTTGCCTCACAAATTAATTAAGCGTGA	
EF0954_H22	GAGGATCCCACCGCGGTGGCGGCCGCTTTAGATGTTCATTTAATGCG	
EF0954_H110	CCAATTGAGGCCACCATCACCTACC	
EF0954_H220	GTTATTCGTCGCTTGGAATTAACG	
EF0954_up	AAACCATGGAAGCAATTACAGTAAAAGATGTCGCT	
EF0954_dn	AAAGGATCCATGAATAGGAATAACTGTTTCACG	
EF0782_H11	ACTCACTATAGGGCGAATTGGGTACCTTGTAAGTGGATTATTTTGGCTA	
EF0782_H12	TTCCGTATTAAATTGTAAAATTTG	
EF0782_H21	CAAATTTTACAATTTAATACGGAAGGCATGGAAATATCCCGACGAACGG	
EF0782_H22	AGAGGATCCCACCGCGGTGGCGGCCGCGTACAAATGGCGATTGTGTCGC	
EF0782_H110	GAATGAAAACGGACCACGTATTGG	
EF0782_H220	GCGTCACCGAAATTAAGGCGCCG	
EF0782_up	AAACCATGGAATCCCAACAACAAAAACAAGTCCAG	
EF0782_dn	AAAGGATCCCTCATATCGTTTTCGTTTAGATG	
EF0773_H21	CCACTTCATTATTTTAAAGCGATTA	
EF0773_H12	AATCGCTTTAAAATAATGAAGTGGACCGACCATTCCGGCGATAAAAACA	
EF0773_H11	GGCGAATTGGGTACCGGGCCCCCCCTCGAGTGACCAGCTGTTAATAAGAAG	
EF0773_H22	TAGCTAGTGGATCCCCCGGGCTGCAGGAATTCATAATTTTCTTAGTTTTGTTC	
EF0773_1	TTTCCATGGGTTTTGTTTTTATCGCCGGAATG	
EF0773_3	AAACCATGGGTTCATCTTACAAAGAGCGAAAAGAAG	
EF0773_2	AAAGGATCCTTTAATCGCTTTAAAATAATGAAG	
AtlA_G_Rev	CTTTAGTGATGATGGTGATGGTGATGGTGGGATCCAACTTTTAAAGTTTGACCAATATAAATT	
AtlA_G_Fw	AACAGATCTGAGCTCAAGGAGGAGACTGACCATGGGAAAAAAAGAATCAATGTCACGTATCGA	
SecA_G_Fw	CAGATCTGAGCTCAAGGAGGAGACTGACCATGGCAAATTTTTTGAAAAAAATGATTGAAAACG	
SecA_G_Rev	TCTTTAGTGATGATGGTGATGGTGATGGTGGGATCTAGCGTTTCTTCCATGACAATTTTTG	
SecY_G_Fw	AACAGATCTGAGCTCAAGGAGGAGACTGACCATGGAGTTCAAGCTATTAAAGAACGCCTTT	
SecY_G_Rev	CTTTAGTGATGATGGTGATGGTGATGGTGGGATCCCTTATTGATAAAGCCGACATATTGAC	

[a] Amp^R, resistant to ampicillin; Erm^R, resistant to erythromycin;

Table 4. Bacterial strains, plasmids and oligonucleotides

2.5. Growth conditions

2.5.1. *E. faecalis*

2.5.1.1. Routine cultures of *E. faecalis*.

Strains were streaked from glycerol stocks and grown on BHI-agar plates. Plates were stored for up to two weeks at 4°C for short-term storage, before being re-streaked from glycerol stocks. For long-term storage, a single colony was spread onto a BHI agar plate containing relevant antibiotics and grown overnight at 37°C. A loopful of cells was re-suspended in 2 × 1mL BHI containing 15% (v/v) glycerol in a sterile 1.5 mL microfuge tube. These glycerol stocks were stored at -80°C. Liquid cultures were prepared by inoculation of culture medium with a single isolated colony. Unless otherwise stated, cultures were grown overnight in sterile plastic 25 mL universals or conical flasks without agitation.

E. faecalis plates or liquid medium cultures were grown at 37°C unless otherwise stated.

2.5.1.2. Selection of spontaneous mutants in semi-solid medium

THY broth - agar 0.06% (m/v) was poured into 250 mL cell culture flasks and left at 4°C for 1h to set before inoculation with dilutions of pre-cultures made overnight in BHI suitable to see individual colonies. The cells were grown at 37°C without agitation and the appearance of spontaneous mutants with altered colony morphology followed over a period of 96h

2.5.1.3. Analysis of sedimentation profiles in standing cultures

A falcon tube (15 mL) containing 6 mL of a BHI broth medium was inoculated with a single colony of *E. faecalis*. The tubes were then incubated overnight (O/N) at 37°C without agitation before taking a picture of all tubes.

2.5.2. *Micrococcus luteus*

M. luteus cells were grown in BHI at 37°C with agitation at 250 rpm. Alternatively, freeze-dried *M. luteus* ATCC46498 was purchased from Sigma, resuspended in dH_2O and autoclaved. Cells were incorporated in BHI agar plates at a final OD_{600} between 0.5 and 2.5.

2.5.3. *Escherichia coli*

E. coli strains were grown at 37°C in LB media eventually supplemented with antibiotics to ensure selection of plasmids. Plate cultures were stored at 4°C for up to two weeks before re-streaking from glycerol stocks. Strain storage, inoculation of medium and growth cultures were carried out as for *E. faecalis* except for the use of LB instead of BHI media.

2.6. Buffers and stock solutions

All buffers were prepared using milliQ water and stored at room temperature unless stated. Solutions for use in microbiological work and molecular biology experiments were sterilised by autoclaving (20min, 121^{0}C, 15 psi).

2.6.1. 10× DNA loading buffer

Bromophenol blue	0.25% (w/v)
Glycerol	50% (v/v)

2.6.2. Phosphate buffered saline (PBS)

NaCl	8 g/L
Na_2HPO_4	1.4 g/L
KCl	0.2 g/L
KH_2PO_4	0.2 g/L

The pH was adjusted to 7.4 using NaOH.

2.6.3. TAE (50x)

Tris Base	242 g/L
Acetic acid	0.57% (v/v)
EDTA (pH 8.0)	0.05M

1× TAE buffer was made by diluting 50× TAE buffer 1:50 with dH_2O.

2.6.4. SDS-PAGE solutions

2.6.4.1. 4× SDS-PAGE loading buffer

Tris-HCl (pH 6.8)	0.25 M
SDS	20 % (w/v)
Glycerol	40 % (v/v)
Bromophenol blue	0.4 % (w/v)

β-mercaptoethanol (βME) was added just before use at a concentration of 50mM.

1× SDS-PAGE loading buffer was made by diluting 4× SDS-PAGE buffer 1:4 with dH_2O

2.6.4.2. SDS-PAGE

10% (w/v) Resolving gel

1.5 M Tris-HCl (pH 8.8)	2.5 mL
10% (w/v) SDS	100 µL
30% (w/v) Acrylamide/Bis (37.5:1)	4.0 mL
10% (w/v) Ammonium persulphate	50 µL
TEMED (N,N,N'N'-tetramethyl-ethylenediamine)	10 µL
dH_2O	3.5 mL

The components were mixed by gentle swirling and loaded into the gel casting apparatus using a 10 mL pipette. A layer of isobutanol was carefully pipetted on top of the gel to isolate it from the air. After the gel had solidified, the stacking gel was made up as follows;

4% (w/v) Stacking gel

0.5 M Tris-HCl (pH 6.8)	2.5 mL
10% (w/v) SDS	100 µL
30% (w/v) Acrylamide/Bis (37.5 : 1)	1.3 mL
10% (w/v) Ammonium persulphate	50 µL
TEMED (N,N,N'N'-tetramethyl-ethylenediamine)	10µL
dH_2O	6.1 mL

The components were mixed by gentle swirling and pipetted on top of the resolving gel. A plastic comb was inserted into the gel to create wells. After the gel had solidified, it was transferred to the gel-running tank and submerged in 1× SDS-PAGE electrophoresis buffer.

2.6.4.3. 10× SDS-PAGE electrophoresis buffer

Glycine	144	g/L
Tris base	30.3	g/L
SDS	10	g/L

1× SDS-PAGE buffer was made by diluting 10× SDS-PAGE buffer 1:10 with dH_2O.

2.6.4.4. Coomassie Blue staining solution

Coomassie Blue R-250	0.25%	(w/v)
Acetic acid	10%	(v/v)
Methanol	50%	(v/v)

Coomassie stain was stored in a foil-wrapped Duran bottle (light sensitive).

2.6.4.5. Destain solution

Acetic acid	10%	(v/v)
Methanol	5%	(v/v)

2.6.4.6. Zymogram solutions renaturing solution

Triton X-100	0.2 %	(v/v)
NaCl	50 mM	

Depending on the pH, the following buffers were used:

50 mM Citrate	pH 5.0
50 mM HNa_2PO_4	pH 6.25
50 mM Tris-HCl	pH 7.4
50 mM Tris-HCl	pH 8.4

2.6.5. TE

Tris-HCl	100 mM
EDTA	10 mM

The pH was adjusted to 7.5 using 1M HCl before autoclaving.

2.6.6. Solutions to prepare *E. coli* competent cells

RF1

RbCl	1.2 g
$MnCl_2.4H_2O$	9.9 g
Potassium acetate	30 mL of 1M stock (pH 7.5)
$CaCl_2 \cdot 2H_2O$	1.5 g
Glycerol	150 mL

The constituents were dissolved in 800 mL sterile dH_2O and the pH was adjusted to 5.8 using 0.2 M acetic acid before made up to 1 L. The solution was filter sterilized and stored at 4°C.

RF2

MOPS	20 mM of 0.5M stock (pH 6.8)
RbCl	1.2 g
$CaCl_2.2H_2O$	11 g
Glycerol	150 mL

The constituents were dissolved in 800 mL sterile dH_2O and the pH was adjusted to 6.8 using 0.1 M NaOH before made up to 1 L. The solution was filter sterilized and stored at 4°C.

2.6.7. Suc-Gly

Sucrose	0.5 M
Glycerol	10% (v/v)

The pH was adjusted to 7.0 using 1M HCl before autoclaving.

2.6.8. SM17MC

SM17MC corresponds to M17-Glu supplemented with:

Sucrose	0.5 M
$MgCl_2$	10 mM
$CaCl_2$	10 mM

The pH was adjusted to 6.9 using 1M HCl before filter-sterilization.

2.7. Molecular biology techniques

2.7.1. Polymerase chain reaction (PCR)

2.7.1.1. High-fidelity PCR using Phusion DNA polymerase (Thermofisher Scientific)

Phusion DNA polymerase was utilised when high sequence fidelity was required, such as when DNA was being used for cloning. Reactions were performed in a Biorad T100 thermal cycler. 25µl 2x Phusion master mix was mixed with an amount of 0.4µM of each oligonucleotide and template of DNA was (10-100 ng) in a final volume of 50µl. 2.5µl DMSO was added when necessary. The PCR machine was pre-set as follows:

1. Initial denaturation set up: 98 °C for 10 s
2. Denaturation set up: 98 °C for 10 s
3. Annealing set up: 56 °C for 20 s (reduced to 50 °C if necessary)
4. Extension time: 72 °C for 15-30s per kilobase
5. Repeat steps between 2- 5 30 cycles
6. Final extension set up: 72 °C for 5 minutes

2.7.1.2. Routine PCR Taq DNA polymerase

When high sequence fidelity was not necessary, such as when screening plasmids for inserts, Taq polymerase was used. Reactions were carried out in a Biorad T100 thermal cycler. 10µl taq master mix (lab stocks) was mixed with 0.4µM of each oligonucleotide and part of an *E. coli* or *E. faecalis* colony in a final volume of 20µl. The PCR machine was programmed as follows:

1. Initial denaturation time: 90 °C for 5 minutes
2. Denaturation temperature and time: 94 °C for 20 s
3. Annealing temperature and time: 56 °C for 20 s
4. Extension temperature and time: 72 °C for 1 minute per kilobase
5. Repeat steps between 2- 5 for 30 cycles
6. Final extension temperature and time: 72 °C for 5 minutes

2.7.2. PCR purification

PCR products were purified using a GeneJET kit (Fisher Scientific), according to the manufacturer's instructions. An equal volume of binding buffer was added to the PCR product. The DNA solution was applied to the column and centrifuged at 13,000 × g for 30 sec. The flow-through was discarded and the column placed back in the same collection tube. The column was washed twice with 0.75 mL Buffer PE by centrifugation (as before). The flow-through was discarded and the column placed back in the same collection tube and centrifuged (13,000 × g) for 2 min. The column was placed in a clean micro centrifuge tube to elute the DNA by adding 30 µL TE. The concentration of the eluate was determined by measuring the absorbance at 260 nm using a Nano-drop device and stored at -20 °C until further use.

2.7.3. Gel extraction

The DNA was excised from an agarose gel with a clean, sharp scalpel and purified using a GeneJET kit (Fisher Scientific), according to the manufacturer's instructions.. The gel slice was weighed and 3 volumes of binding buffer were added. The mixture was then applied onto the column and the washing and elution steps carried out as previously described above (see 2.7.2).

2.7.4. Plasmid purification

Plasmid DNA was purified following alkaline lysis using a GeneJET kit (Fisher Scientific). Briefly, the pellet corresponding to 3 mL of an overnight culture in LB was re-suspended in 250µl of resuspension buffer (50mM Tris-HCl [pH 8.0], 50mM EDTA, RNase A 100 µg/mL). 250µl of lysis buffer (1% [m/v] SDS, 0.2 M NaOH) was added, the tube mixed by inversion 4-6 times and incubated for 5 min at room temperature. 350µl of neutralisation buffer (3 M potassium acetate [pH 5.5]) was added and the tube mixed thoroughly by inverting until the precipitation was evenly dispersed.

The solution was centrifuged for 10min at 15,000 *x g*) and the supernatant applied to a spin column. The DNA was subsequently purified according to the manufacturer's instructions (see 2.7.2).

2.7.5. Genomic DNA extraction

Genomic DNA was isolated and purified from *E. faecalis* using a QIAGEN DNeasy™ kit according to the manufacturer's instructions. A single colony of *E. faecalis* was used to inoculate 5 mL of BHI in a 30 mL sterile universal tube and grown overnight at 37°C. 1.5 mL of cells was harvested by centrifugation (4,000 rpm, 5 min, room temperature). Cells were re-suspended in 180 µl enzymatic lysis solution containing 50 mM phosphate buffer (pH 6.0,) 50 mM EDTA, 10 mg/mL RNase and 5 µL mutanolysin (5 mg/mL). After 1h incubation at 37°C, the protocol was continued as per the manufacturer's instructions. Genomic DNA was eluted into clean 1.5 mL microfuge tubes using two 200 µL aliquots and the two eluates were pooled. The DNA concentration was estimated using a Nano-drop device and stored at 4°C until further use.

2.7.6. Enzymatic digestion of DNA

Digestion of DNA was performed according to the manufacturer's instructions, with the buffers supplied in volumes. Analytical digestions (to check plasmid maps) were made using 200 ng of DNA in a final volume of 15 µL in the presence of 4 units of each enzyme. Preparative digestions (to generate vectors or insert for ligation or Gibson assembly) were made using 5µg of DNA in a final volume of 50 µL in the presence of 30 units of each enzyme. The reaction volume was made up with dH_2O. The restriction digests were incubated at 37°C for 45 minutes (PCR products or plasmids) or 1h30 in the case of genomic DNA.

2.7.7. DNA ligation

Each ligation reaction contained approximately a 1:3 molar ratio of vector to insert. The final ligation volume (15 µL) contained 100ng of vector, an appropriate amount of insert (variable depending on the size), 1.5 µl 10× DNA ligase buffer, and 200 µL of T4 DNA ligase. The final volume was made up to 15 µl with sterile MilliQ water and incubated overnight at 16°C. Ligation mixtures were directly transformed into *E. coli* competent cells without purification.

2.7.8. Gibson assembly

Restriction-free cloning was carried out using the Gibson Hi-Fi assembly kit (NEB) according to the manufacturer's instructions. Oligonucleotides were designed to amplify the insert using Snapgene. They contained 32 bases homology with the vector. 100 ng of vector DNA cut by restriction enzymes was incubated in the presence of PCR-amplified insert (1:3 molar ratio of vector to insert) in a volume of 4 µL before adding an equal volume of NEB Hi-Fi 2x mastermix. The reaction was incubated for 30 minutes at 50°C and 4 µL were directly used to transform electro- or chemically-competent *E. coli* cells.

2.7.9. Agarose gel electrophoresis

DNA fragments were separated by horizontal gel electrophoresis using various size electrophoresis tanks (Fisher Scientific). Appropriate volume of agarose gel (1% [w/v]) was dissolved in TAE by microwaving. For the visualisation of DNA, ethidium bromide was added to the melted agarose at a final concentration of 0.5µg/mL. DNA loading dye was added to a 1× final concentration with the samples before loading in the gel wells. The gel was run at 5V/cm for 1h and visualised using a UV transilluminator at 305 nm. To estimate the sizes of DNA fragments, DNA markers were also loaded onto the gel.

2.7.10. Agarose gel photography

A record of agarose gels was obtained by photographing the UV- illuminated gels using BioDoc-It system (UVP) and printed by Sony Video Graphic Printer using Thermal Print Media (UPP-110HA).

2.8. Spectrophotometric measurement (OD_{600})

To follow bacterial growth, spectrophotometric measurements at 600 nm (OD_{600}) were performed using a Fisher Scientific spectrophotometer. When necessary, the culture samples were diluted in unused sterile corresponding culture medium to give a reading within the range of this type of spectrophotometer.

2.9. Protein expression and purification

2.9.1. Expression of recombinant proteins in *E. coli* BL21(DE3)

Recombinant plasmids (pET2817 derivative) were used to transform *E. coli* BL21(DE3). A starter culture was prepared by inoculating 15 mL of LB containing Ampicillin (100 µg/mL) in a universal tube.

The culture was incubated at 37°C with shaking (250 rpm) overnight. 7.5 mL of the starter culture was added to 750 mL LB containing ampicillin (100 µg/mL) in a 3L flask, and incubated at 37°C with shaking (250 rpm) until OD_{600} 0.7. At this stage, IPTG was added at a final concentration of 1 mM, and incubation continued for 4 h. Cells were harvested by centrifugation (6,000 × *g*, 15 min, 4°C). Supernatant was discarded and the pellet stored at -70°C.

2.9.2. Preparation of protein extracts

Induced cells were thawed and re-suspended in 25 mL of buffer A (50 phosphate buffer [pH 7], 250 mM NaCl, 20% glycerol (v/v), and 2mM DTT). A crude extract was prepared by sonication on ice using setting 10 for 5 cycles (25 sec on, 30 sec rest). An aliquot was taken and the rest of the lysate was centrifuged at 45,000 × g for 20 min at 4°C. The protein concentration in the soluble fraction was determined using the protein Bio-Rad assay according to the manufacturer's instructions, with BSA as a standard. The concentration of the crude extract was assumed to be the same as the one of the soluble fraction. Protein samples were prepared at a concentration of 1 mg/mL and heated for 3 min at 95°C before being loaded on an SDS-PAGE.

2.9.3. Protein purification using immobilized metal affinity chromatography (IMAC)

Two mL of Ni-NTA resin (Qiagen) was washed in distilled water and equilibrated twice with 12 mL of buffer A (see 2.9.2). The soluble fraction was incubated in the presence of the equilibrated beads in a 50 mL Falcon tube for 1h at 4°C under agitation. His-tagged proteins were purified "in batch" once transferred into a 15 mL Falcon tube using a centrifuge. After centrifugation of the loaded beads, the fraction containing proteins not bound to the resin was recovered (flow through). The beads were then washed successively four times with 13 mL of buffer A, twice with 13 mL of buffer A (see 2.9.2) with 5 mM imidazole and eluted with 10 mL of buffer A with 400 mM imidazole (twice 3 mL and twice 2 mL). The elution fractions were pooled and filtered before further purification by size exclusion chromatography.

2.9.4. Protein purification using size exclusion chromatography

Proteins from IMAC purification were loaded on a Superdex 75 26/60 chromatography column (GE Healthcare) pre-equilibrated in buffer A and eluted with an isocratic gradient. The proteins with the expected retention time were pooled and the concentration calculated using the value predicted by the Expasy server (web.expasy.org/protparam/).

2.10. Preparation of cell walls as a substrate in agar plates

2.10.1. *M. luteus* cells

See section 2.5.2.

2.10.2. *E. faecalis* cells

To increase the sensitivity of the assay for PG hydrolase activity, we used a mutant with multiple deletions in *pbp* genes (Δ4; Δ*ponA*Δ*pbpF*Δ*pbpZ*Δ*pbp5*) [M. Arthur, unpublished results]. Large volume cultures (4.5L in 5L flasks) were grown in BHI broth (OD_{600} ~ 2.5) O/N at 37°C. Cells were harvested (7,500 x *g* for 10 min at 4°C), re-suspended in 35mL of dH_2O and autoclaved.

2.10.3. Unbroken cell walls

Cells corresponding to 1.5 L of culture were boiled in 4% (w/v) SDS for 30 min in a total volume of 25 mL, washed 6 times in dH_2O, re-suspended in 10 mL of dH_2O and autoclaved.

2.10.4. *E. faecalis* broken cells

Δ4 mutant cells corresponding to 3 L of culture were re-suspended in 20 mL of dH_2O and broken by 3 passages through a French press at a pressure of 1,000 psi. Broken cells were recovered by centrifugation (45,000 x g, 20 min, 20°C), washed 3 times with dH_2O, re-suspended in 10 mL of dH_2O and autoclaved.

2.10.5. Preparation of broken cell walls

Broken cells (see 2.10.4.) were boiled in 4% (m/v) SDS for 30 minutes min in a total volume of 25 mL, washed 6 times in dH_2O, re-suspended in 10 mL of dH_2O and autoclaved

2.11. Sodium Dodecyl Sulphate-Polyacrylamide gel electrophoresis (SDS-PAGE)

2.11.1. SDS-PAGE

Discontinuous SDS-PAGE was performed using Bio-Rad minigels (70 mm (L) × 80 mm (W) × 1 mm thickness) following the manufacturer's instructions (Bio-Rad). Reagents for SDS-PAGE were prepared as described in (Chapter 2.6.). The resolving and stacking gel contained 10% (w/v) and 4% (w/v) acrylamide respectively. Samples were prepared in sample buffer and heated at 95°C for 5 min. Electrophoresis was performed at RT with constant voltage of 190 V for 50 min.

2.11.2. Coomassie blue staining

After electrophoresis, protein gels were placed in approximately 30 mL Coomassie blue stain for 30-60 min and destained in two volumes of approximately 30 mL destain solution (Chapter 2.6.) overnight. Molecular masses were determined by comparison to a molecular mass protein marker of known sizes.

2.11.3. Renaturing SDS-PAGE

PGH activity was detected by renaturing gel electrophoresis using purified cell walls as the substrate then incorporated into the acrylamide gel to a concentration corresponding to an OD_{600} between 0.5-3 (see result section). Electrophoresed gels were rinsed three times 5 min in 250 mL dH_2O to remove SDS and then in 200 mL of renaturing solution (chapter 2.6.) at RT for 30 min, followed by incubation overnight at 37°C in another 200 mL of renaturing solution. After de-staining in dH_2O, PGHs activity was visualised as zones of clearing in the opaque background. Molecular masses were determined by comparison to protein standards of known sizes that were run on the same gel, cut off and Coomassie blue stained.

2.11.4. Protein sample preparation for zymogram analysis

Protein samples were prepared from 10 mL of an overnight standing culture. Bacterial pellets were re-suspended in 600 µL of PBS and 250µl of glass beads (106µm in diameter). The cells were broken using a Fast Prep machine (6.5 speed, 5 cycles of 30 seconds with 2 min pauses between each cycle to avoid heating). Protein concentration was measured spectrophotometrically at 595nm using a Bio-Rad protein assay kit. Protein samples were adjusted at 1mg/mL using 1x SDS-PAGE buffer.

2.12. Isolation of transposon mutants impaired in AtlA activity

The screening for the transposon mutants was performed on an agar plate containing *M. luteus*. Mutants did not have a halo around the clones on *M. luteus* plates were isolated, interrupted genes were identified by reverse PCR.

2.12.1. Construction of the transposon library

pZXL5 was introduced into *E. faecalis* by electroporation. Transformants harbouring pZXL5 were selected on BHI agar plates containing 128 mg/mL gentamycin (Gm^{128}) and 10 mg/mL chloramphenicol (Cm^{10}) at a permissive temperature (28°C). A transformant was grown overnight in 200 mL BHI broth containing Gm^{128} and Cm^{10} at 28°C. Transposition was induced by inoculating 200µl of the overnight culture in 200mL of BHI broth containing Gm^{128} supplemented with nisin (25ng/mL). This culture was incubated overnight at 42°C. The nisin-induced culture containing transposon mutants was used to inoculate BHI broth (200µl in 200mL) containing Gm^{128} and incubated at 42°C

2.12.2. Identification of *atlA* deficient mutants

Transposon mutants were plated on BHI agar plates containing Gm^{128} and *M. luteus* as a substrate. 300 colonies per plate was found to be the optimal density; this corresponds to plating 100µl of a 10^{-3} dilution of the library (Fig. 49).

2.12.3. Mapping of the transposon insertions sites

The transposition site was identified by reverse-PCR using self-ligated chromosomal DNA that had been digested by SspI and two divergent primers on the transposon. The detailed experimental strategy is described in the result section (see 3.2.3.2, Fig. 53).

2.13. rp-HPLC analysis of peptidoglycan structure

2.13.1. Purification of cell walls

Unbroken cell walls were extracted from 500 mL of exponentially growing culture (OD_{600}=0.7) as described in section 2.10.3. The material was further treated with 2 mg/mL pronase for 5h at 60°C and washed 6 times with MilliQ water. Insoluble, protease-treated cell walls were freeze-dried and re-suspended in MilliQ water at a concentration of 20 mg/mL.

2.13.2. Preparation of disaccharide-peptides

One mg of purified cell walls was digested by mutanolysin (0.25 mg/mL) in a final volume of 100 µL containing 50 mM phosphate buffer (pH 6.0) for 16h at 37°C. The digestion mixture was heated for 5 min at 95°C to inactivate mutanolysin and soluble disaccharides-peptides were recovered by centrifugation (20,000 x*g*, room temperature, 10 min). Soluble muropeptides were reduced by addition of 100 µL of 250 mM borate buffer (pH 9.0) and 2 mg/mL of sodium borohydride. After 20 min at room temperature, the pH was adjusted at 4.5.

2.13.3. rp-HPLC separation of disaccharide-peptides

20 µL of soluble, reduced muropeptides (*ca.* 100 µg) were analysed by rp-HPLC on a Dionex Ultimate 3000 system. Following injection on a Hypersil GOLD aQ column (C18; 2.1 by 200 mm, Thermo Scientific), muropeptides were separated at a flow rate of 0.3 mL/min using 10 mM ammonium phosphate (pH 5.5) as a mobile phase (buffer A). After a 5 min isocratic step, muropeptides were eluted with a 45 min methanol gradient (0 to 30% linear gradient in buffer A). Elution was monitored by recording the Absorbance at 210 nm.

2.14. Transformation techniques

2.14.1. Transformation of *E. coli*

2.14.1.1. Preparation of *E. coli* competent cells (Hanahan, 1983)

1 L of pre-warmed LB medium in a 3 L conical flask was inoculated with 5 mL of an overnight culture and incubated at 37°C with shaking (250 rpm), until an OD_{600} of 0.5 - 0.8 was reached. The culture was transferred into a 1 L bottle and chilled on ice for 15 min. The cells were then harvested by centrifugation (6,500 x *g*, 10 min, 4°C), and the pellet was drained before re-suspended in 16 mL RF1 (chapter 2.6.9) and incubated on ice for 15 min. The cells were pelleted again, drained as before, re-suspended in 4 mL RF2 (chapter 2.6.9) and placed on ice for 15 min. The cells were divided into 50 µL aliquots and used immediately or the microfuge tubes were snap frozen in liquid nitrogen before storage at -80°C. The level of competence of the cells was determined by transformation with a 10 pg of pUC19 as a control plasmid.

2.14.1.2. Transformation of Hanahan competent *E. coli* cells by heat-shock

An aliquot of frozen Hanahan competent cells was thawed on ice for 10 minutes before adding 4µl of the ligation or Gibson assembly product. After 30 min on ice, the mixture was heat shocked at 42°C for 30 sec and immediately returned to the ice for a further 5 min. The volume was made up to 1 mL with SOC broth and the transformed cells were incubated for 1 hr at 37°C with shaking at 250 rpm to allow expression of plasmid-encoded antibiotic resistance markers. Transformed cells were spread using sterile glass beads onto agar plates containing appropriate antibiotics and incubated at 37°C for 18-48 h.

2.14.2. Transformation of *E. faecalis*

2.14.2.1. Preparation of *E. faecalis* electro-competent cells

A single colony of *E. faecalis* was used to inoculate 10 mL of BHI broth and incubated overnight at 37°C without shaking. This culture was used to inoculate 200 mL of fresh pre-warmed SGM17 in a 250 mL conical flask to an OD_{600} of 0.05 and grown at 37°C without shaking until log phase (OD_{600} 0.5-0.6). Cells were harvested by centrifugation (5,000 x g, 10 min, room temperature) and washed 3 times with 50 mL of cold Suc-Gly buffer. Cells were finally re-suspended in 500 µL of Suc-Gly and snap-frozen in 50 µl aliquots using liquid nitrogen and stored at -80°C. The level of competence of the cells was determined by electroporation with 10ng of pAT18 as a control plasmid.

2.14.2.2. Transformation of *E. faecalis* by electroporation

0.2-1 µg of plasmid DNA dialysed against MilliQ water to ensure the complete removal of salt. The DNA was then added to an aliquot of electro-competent cells, which had been thawed on ice for 5 min and added to a chilled 1 mm electroporation cuvette. The plasmid/cell mix was electroporated at room temperature at 200 ohms, 25 µF and 2.4 kV using a Bio-Rad Gene Pulser. Cells were recovered by adding 1 mL of cold SM17MC buffer and kept 5 min on ice before incubation for 3 h at 28°C (pGhost derivatives) or 37°C (non-thermosensitive plasmids). Cells were spread on selective media as described above and incubated at 28°C or 37°C for 18-96 h.

Chapter 3

Results

3.1. Isolation and characterization of spontaneous mutants with altered AtlA activity

3.1.1. Experimental strategy to isolate mutants forming long chains in semi-solid media

The screening used was based on the sedimentation properties of *Enterococcus faecalis* cells. This screen was previously also used with *Lactococcus lactis* to identify mutants with impaired septum cleavage (Mercier et al., 2002) during division. A flask containing THY broth (Todd Hewitt containing 5% [m/v] yeast extract) supplemented with a low concentration of agar (0.06% (m/v)) was inoculated with diluted pre-cultures of the wild type or its isogenic mutant (*atlA*$_{E212Q}$-*gfp*) to see individual colonies. The cells were grown at 37°C without agitation and the appearance of spontaneous mutants with altered colony morphology followed over a period of 96h (**Fig. 29A**). The corresponding mutants were isolated and analysed.

E. faecalis wild type cells are typically found as diplococci or form short chains (4 to 6 cells), they form "comets" as they grow in semi solid medium (**Fig. 29B**); however, *atlA* mutants form long chains and are immobilized in the medium and they appear as "clumps" (**Fig. 29C**).

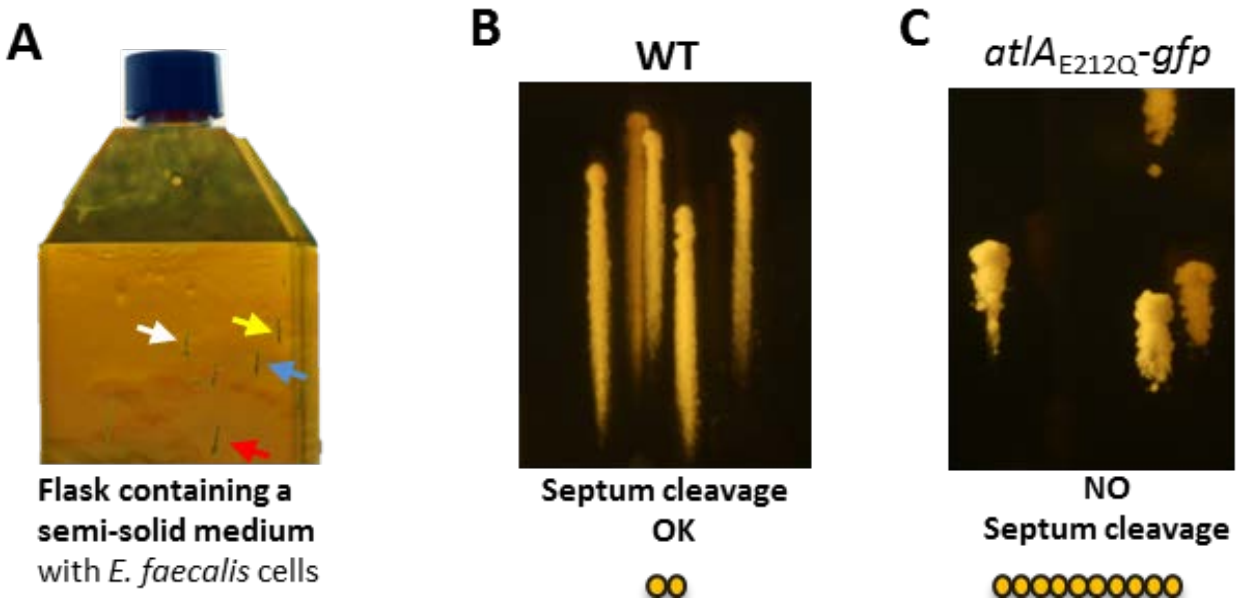

Figure 29. Strategy used to isolate spontaneous mutants with altered chain forming phenotypes. (**A**), A flask containing semi-solid medium was inoculated with *E. faecalis* cells and incubated at 37°C without agitation. Arrows show colonies growing in the medium. (**B**), Wild type colonies made of diplococci and short chains form "comets" as they are mobile in the semi-solid medium. (**C**), *atlA* mutants form long chains and are immobilized in the medium; they appear as "clumps".

3.1.2. Identification of mutants with impaired septum cleavage

3.1.2.1. JH2-2 mutants forming long chains

After several attempts, it was not possible to isolate spontaneous mutants forming long chains from the wild type strain *E. faecalis* JH2-2 (**Fig. 30A**). Although AtlA mutants form distinctive colonies in the semi solid media (**Fig. 29C**), it is possible that the appearance of colonies forming clumps is not easy to see in the background formed by wild type comets. Another possibility is that we did not screen enough colonies to identify an AtlA mutant.

3.1.2.2. *atlA* derivatives forming very long chains (group A)

As an alternative strategy, we decided to use an *atlA* mutant forming long chains as a parental strain. We used a JH2-2 derivative (called *atlA*$_{E212Q}$-*gfp*) expressing inactive AtlA allele with a point mutation in the catalytic residue (substitution of glutamic acid in position 212 by a glutamine; fused to the GFP. We isolated 4 mutants forming more compact colonies than the parental *atlA*$_{E212Q}$-*gfp* strain. These mutant were defined as **group A mutants** (**Fig. 30BA**).

3.1.2.3. Mutants supressing the long chain phenotype of group A mutants (group B)

One of the group A mutants (clone 14) was selected to isolate suppressor mutations leading to the formation of shorter chains again. Nine derivatives were isolated; defining **group B mutants** (**Fig. 30C**).

3.1.2.4. Mutants supressing long chain phenotype from *atlA*$_{E212Q}$-*gfp* mutants (group C)

We also tried to identify mutants that suppress the *atlA* phenotype (forming short chains from *an atlA*$_{E212Q}$-*gfp* strain forming long chains) unlike strain *atlA*$_{E212Q}$-*gfp* that is immobile and forms clumps, suppressor mutants restored a WT phenotype and formed comets in the semi-solid medium. Twenty one derivatives forming short chains were isolated and named **group C mutants (Fig. 30D).**

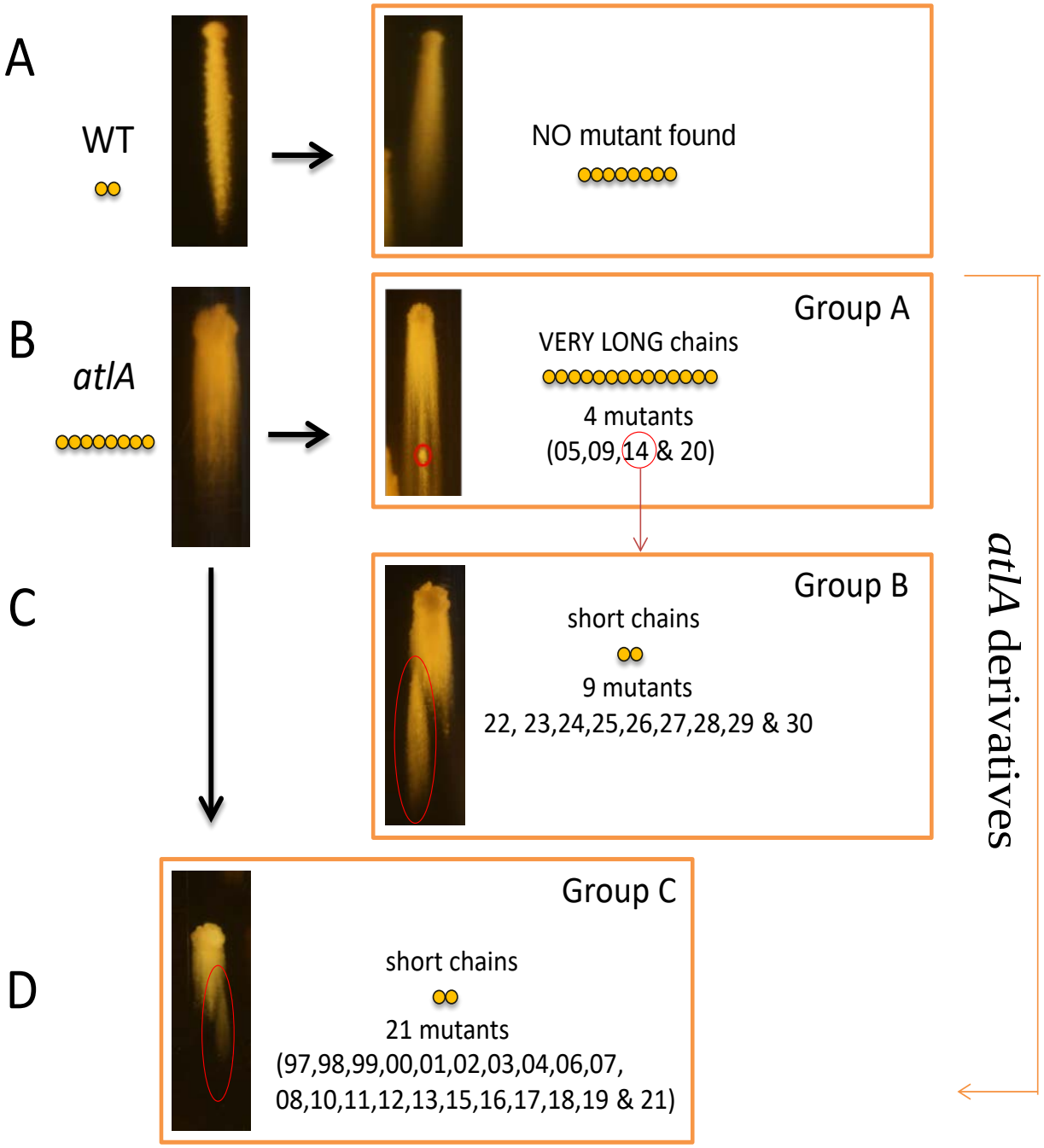

Figure 30. Description of the screen used to isolate spontaneous *E. faecalis* in semi-solid medium. (**A**), No JH2-2 derivatives forming long chains were isolated. (**B**), Identification of *atlA*$_{E212Q}$-*gfp* derivatives forming very long chains (class A mutants). (**C**), Identification of class A derivatives (clone 14) forming short chains. (**D**), Identification of *atlA*$_{E212Q}$-*gfp* derivatives forming short chains.

3.1.3. Analysis of the sedimentation profiles of *E. faecalis* mutants

The size of cell chains has an influence on the sedimentation profile of the culture. This property was therefore used as a method to compare the sedimentation profiles of the spontaneous mutants isolated in comparison to the wild type. A falcon tube containing a BHI broth medium was inoculated with the *E. faecalis* cells and incubated overnight (O/N) at 37°C without agitation. The results corresponding to the control strains are shown in (**Fig. 31**). Wild-type cells forming essentially diplococci did not sediment and the corresponding culture was homogeneously turbid with most cells in suspension (planktonic growth; (**Fig. 31A**). A mutant with a deletion in two genes encoding autolysins previously described (AtlB and AtlC; ΔBC) showed a sedimentation profile very similar to WT with planktonic growth (**Fig. 31B**). By contrast, the strains harbour an *atlA* mutation (either the $atlA_{E212Q}$-*gfp* mutation or the *atlA* deletion) sedimented (**Fig. 31C**), the triple deletion mutant Δ*ABC* (**Fig. 31D**) showing the most extreme sedimentation.

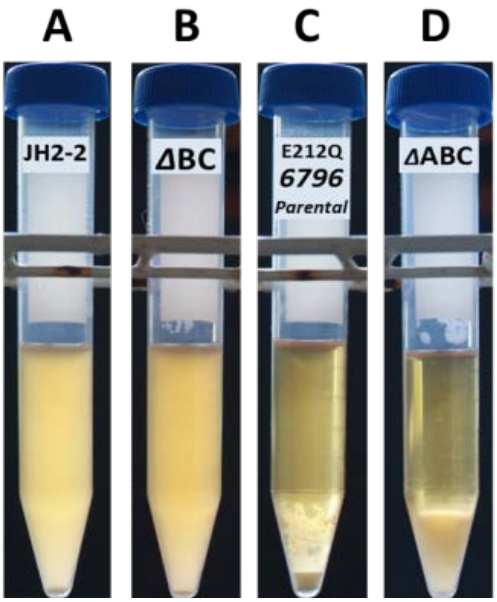

Figure 31. Sedimentation profiles of *E. faecalis* control strains. Falcon tubes containing BHI broth were inoculated with controls strains and grown O/N at 37°C without agitation. (**A**), wild type JH2-2 strain (WT) essentially forms diplococci and short chains that do not sediment (planktonic growth). (**B**), the double Δ*atlB* Δ*atlC* mutant strain (ΔBC) displays a sedimentation profile similar to the WT strain, indicating that when AtlA is produced, the enzymatic activities of AtlB and AtlC do not contribute significantly to septum cleavage. (**C**), the $atlA_{E212Q}$-*gfp* mutant forms long chains that sediment at the bottom of the tube. (**D**), the Δ*ABC* mutant forms extremely long chains and shows a dramatic sedimentation profile.

The spontaneous mutants isolated were analysed using the same strategy as described above and their sedimentation profiles are shown in (**Fig. 32**).
Three of the 4 clones in group A (5, 9 and 20) had a more pronounced sedimentation than the wild type, as expected, clone 9 having a similar profile as the Δ*ABC* mutant. Clone 14 was similar to the parental strain.

Most of the clones in group B, suppressing the long chain-forming phenotype of mutant 14 presented more planktonic growth than the parental strain. Surprisingly, mutants 23, 25 and 30 had sedimentation profiles similar to the parental mutant 14 (**Fig. 32**).

All mutants from group C were isolated based on their mobility in semi-solid medium greater than the $atlA_{E212Q}$-*gfp* strain. As expected for mutants forming shorter chains than the *atlA* mutant, most of the group C mutant cultures appeared more turbid than the parental Δ*atlA* strain (more planktonic growth). Mutants 97, 98, 01, 03, 07, 08, 19 and 21 displayed a sedimentation profile similar to the wild type JH2-2 strain with a planktonic growth. A second set of mutants 99, 4, 6, 10, 11, 12, 13, 15, 16, 17 and 18 showed no obvious difference with their parental strain $atlA_{E212Q}$-*gfp*. A third set of mutants 00 and 02 showed surprisingly more sedimentation than the parental strain.

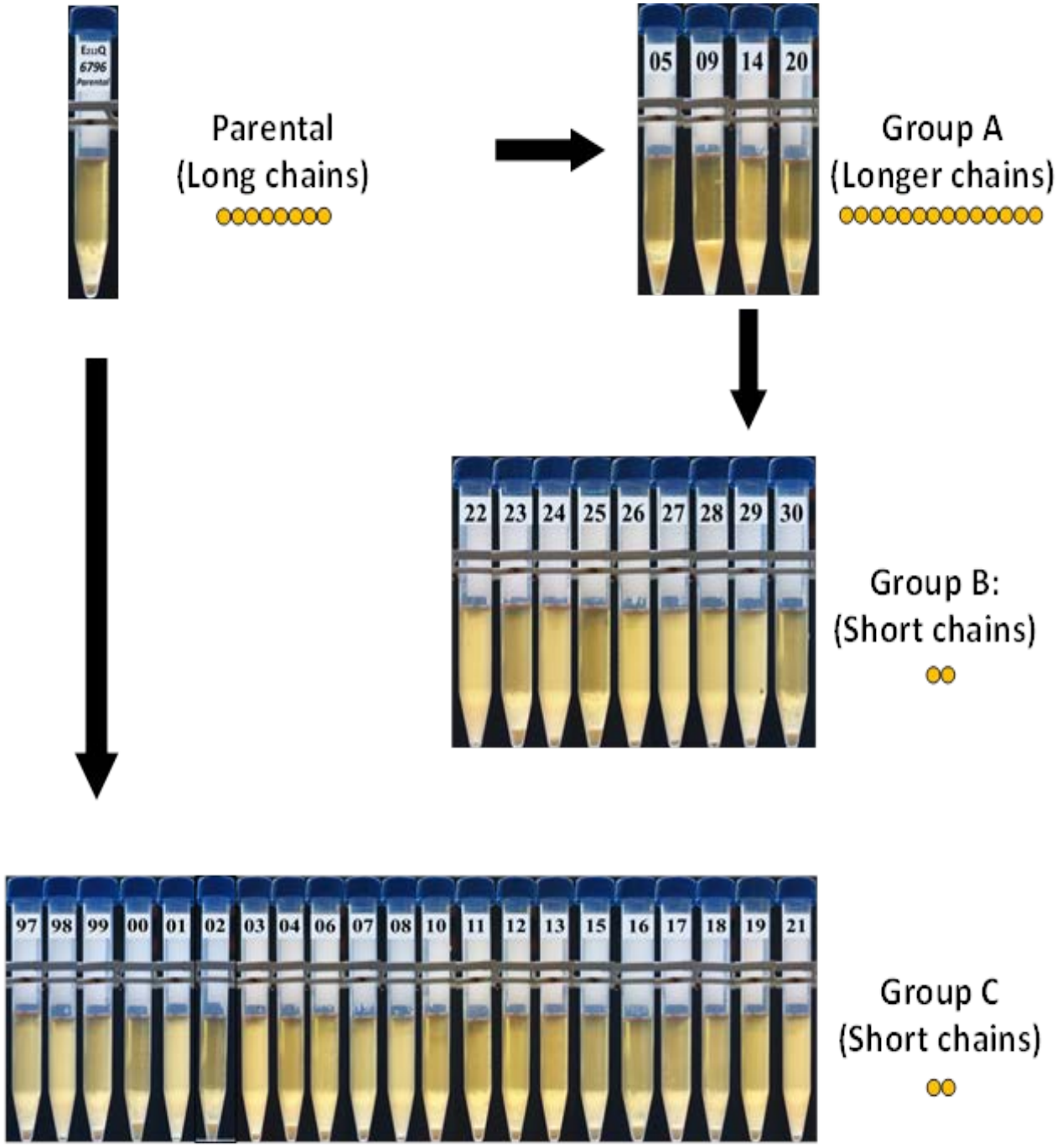

Figure 32. Sedimentation profiles of spontaneous mutants in BHI standing cultures. In group A mutants, sedimentation associated with clone 14 was similar to the parental strain whilst other mutants (clones 5, 9 and 20) showed a more pronounced sedimentation. In group B mutants, sedimentation profiles of clones 23, 25 and 30 were similar to that of the parental strain (clone 14) whilst the other mutants (22, 24, 26, 27, 28 and 29) showed more planktonic growth indicating that they formed smaller cell chains. In group C mutants, clones 97, 98, 01, 03, 07, 08, 19 and 21 were similar to the planktonic growth of the wild type. Mutants 99, 4, 6, 10, 11, 12, 13, 15, 16, 17 and 18 showed no obvious difference with the parental *atlA*$_{E212Q}$-*gfp* strain. Mutants 00 and 02 showed a more pronounced sedimentation than the parental *atlA*$_{E212Q}$-*gfp* strain.

3.1.4. Detection of hydrolytic activities PGHs produced by mutants on agar plates

3.1.4.1. Detection of AtlA activity on *M. luteus* agar plates

The PGH enzymatic activity at the surface of the cells can be visualized on agar plates that contain autoclaved cells as a substrate. In *E. faecalis*, AtlA activity can be specifically detected using *M. luteus* cells as a substrate. The hydrolysis of *M. luteus* autoclaved cells leads to the formation of a halo formed around the colonies, indicating that the enzymes are also able to diffuse in the medium. It has been shown that AtlA is the only PGH produced by *E. faecalis* able to hydrolyse *M. luteus* cells as colonies from the *atlA* mutant are not surrounded by any halo (Qin et al., 1998).

To compare the activity of the spontaneous mutants isolated with that of the control strains, all strains were grown in 96-well plates. Cells were grown overnight at 37°C and inoculated at the surface of agar media that containing *M. luteus* autoclaved cells with a 96-pin replicator. The following strains were used as controls:

- JH2-2, a wild-type strain (WT);
- Δ*atlA* (ΔA), a mutant harbouring an in-frame deletion of the *atlA* gene;
- *atlA*$_{E212Q}$-*gfp*, the catalytically inactive mutant used for our screen.
- A-GFP, a JH2-2 derivative expressing a translational fusion between AtlA and the GFP;
- Δ*atlB*Δ*atlC* (ΔBC), a JH2-2 derivative with in frame deletion in the two genes encoding the PGHs AtlB and AtlC;
- Δ*atlA*Δ*atlB*Δ*atlC* (ΔABC), a JH2-2 derivative with in frame deletion in the genes encoding the PGHs AtlA, AtlB and AtlC.

As expected, halos were observed around colonies of the WT, A-GFP, and ΔBC strains which produce an active AtlA (**Fig. 33A**). No halo was detected around the colonies of strains ΔA, *atlA*$_{E212Q}$-*gfp* and ΔABC, confirming that AtlA is the only autolysin produced by *E. faecalis* that can hydrolyse *M. luteus* peptidoglycan (**Fig. 33A**). None of the spontaneous mutants isolated so far formed a halo on *M. luteus* plates, even after long incubation after (48h) (**Fig. 33B)** and after (72h) (**Fig. 33C)**. This result indicated that the increased septum cleavage activity of mutants in group B and C was not due to a reversion of the mutation, *atlA*$_{E212Q}$-*gfp* present in the parental strain or to the expression of another PGH which can cleave *M. luteus* peptidoglycan.

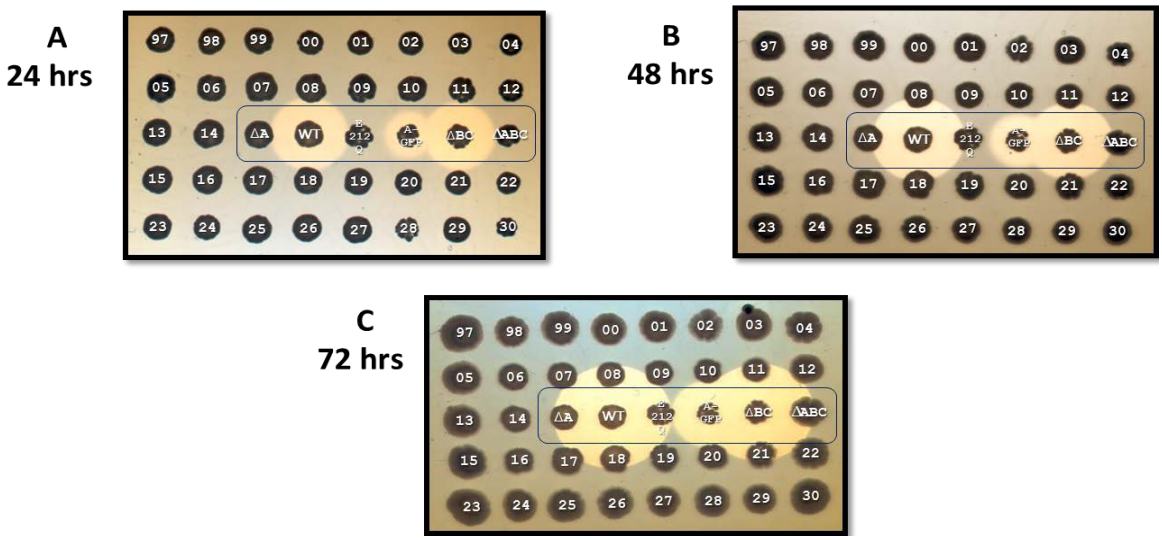

Figure 33. Detection of AtlA hydrolase activity on plates containing *M. luteus* cells after 24 hours (A), 48 hours (B) or 72 hours (C). Control strains (boxed) include the *atlA* deletion mutant (ΔA), JH2-2 (WT), the *atlA*$_{E212Q}$-*gfp* parental strain, a JH2-2 derivative expressing an AtlA-GFP fusion (A-GFP), the double mutant Δ*atlB*Δ*atlC* (ΔBC) and the triple Δ*atlA*Δ*atlB*Δ*atlC* mutant (ΔABC).

3.1.4.2. Detection of PGH activities on *E. faecalis* agar plates

We further analysed the surface-associated PGH activities of the spontaneous mutants isolated using *E. faecalis* autoclaved cells as a substrate. Previous studies revealed that this substrate was suitable to detect AtlA, AtlB, and AtlC activities (Mesnage et al., 2008).

3.1.4.2.1. Protocol optimization

Our first attempts to detect PGH activities around the colonies on agar were inconclusive (data not shown). It was not possible to visualise a clear halo on *E. faecalis* plates. The halo was relatively small and the contrast was not good enough to take pictures.

We hypothesized that the poor contrast of the halo could be due to two factors: (i) the relatively high cross-linking index of *E. faecalis* peptidoglycan as compared to *M. luteus*; (ii) the fact that autoclaved cells incorporated in the plates contain not only peptidoglycan, but lipids, proteins, carbohydrates and nucleic acids that cannot be digested by autolysins. To improve the sensitivity of the assay and to increase the contrast of the background in the plates, the experiment was repeated using an *E. faecalis* mutant with a less cross-linked PG (a more sensitive substrate for PGHs). This mutant (called Δ4) has four deletions in *pbp* genes responsible for PG polymerisation: three class A Pbps (PonA, PbpF, and PbpZ) and a class B Pbp (PbpB).

Cell preparations of the Δ4 substrate were used to test the impact of two treatments: cell disruption using the French Press and cell disruption followed by ebullition in SDS and extensive washes in water (**Fig. 34A**). The comparison of plate assays using these two different substrates revealed that breaking cells without treating with SDS was not sufficient to detect clear halos (**Fig. 34B**). Cell disruption followed by SDS treatment clearly improved the sensitivity of the assay. We found that cell walls at a final concentration of OD_{600}=1.5 gave the best results as shown in (**Fig. 34C**).

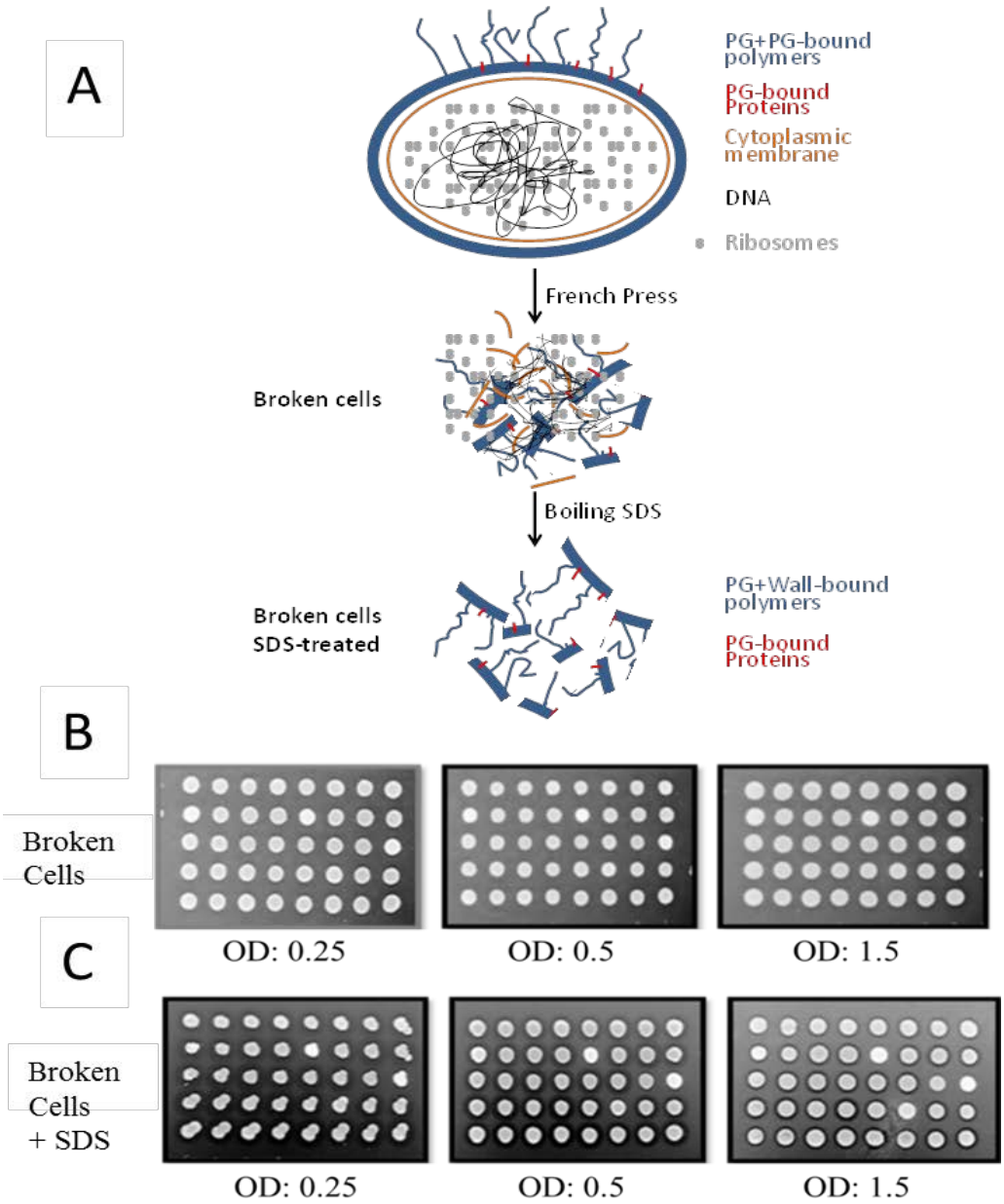

Figure 34. Detection of autolytic activities on agar plate containing broken *E. faecalis* cells. (**A**), Strategy followed to produce broken cell extracts or cell walls. (**B**), Plates containing various concentrations of broken cells (left: OD_{600}=0.25; middle: OD_{600}=0.5; right: OD_{600}=1.5) gave a poor halo contrast. (**C**), plates containing broken cells treated with SDS (*ie* cell walls) at various concentrations (left: OD_{600}=0.25; middle: OD_{600}=0.5; right: OD_{600}=1.5) allowed a good detection of autolytic activities.

3.1.4.2.2. Analysis of PGHs activities

The same control strains as those described in section 3.1.4.1 were analysed using the optimized method. JH2-2, A-GFP and the two *atlA* mutants (ΔA and *atlA*$_{E212Q}$-*gfp*) showed a halo of a similar size (**Fig. 35**) indicating that AtlA does not significantly contribute to the surface activities digesting *E. faecalis* PG. The ΔBC mutant showed a very small halo indicating that the two enzymes AtlB and AtlC are the most active enzymes produced by *E. faecalis* able to digest this substrate. The triple ΔABC mutant colonies showed no halo, indicating that AtlA, AtlB, and AtlC are the only PGHs that can be detected by this assay. The activity of spontaneous mutants from the three groups A, B and C previously described was analysed. A halo was identified around the colonies for all mutants except for two of them (**Fig. 35**).

In group A, mutants 05 and 14 had a halo similar to the *atlA*$_{E212Q}$-*gfp* parental cells ($E_{212}Q$). Mutants 09 and 20 showed no activity, a phenotype similar to that of the ΔABC mutant. This suggested that the very long chains formed by these two mutants could result from a mutation in *atlB* and *atlC* (**Fig. 35**).

In group B, all mutants had a halo with a size similar to the parental strain *atlA*$_{E212Q}$-*gfp*, with the exception of mutant 27 which displayed a slightly bigger halo at 24 hours and mutant 23 which displayed a slightly smaller halo (**Fig. 35A**). The overexpression of a PGH digesting *E. faecalis* substrate could explain the suppression of the phenotype of the class A mutant. The lower expression of surface-exposed PGH activities in mutant 23 remains unexplained.

In group C mutant 18 seemed to form a bigger halo than the parental strain. The increased enzymatic activity detected is in agreement with the smaller cell chains formed by mutant 18 as compared to the parental *atlA*$_{E212Q}$-*gfp* strain.

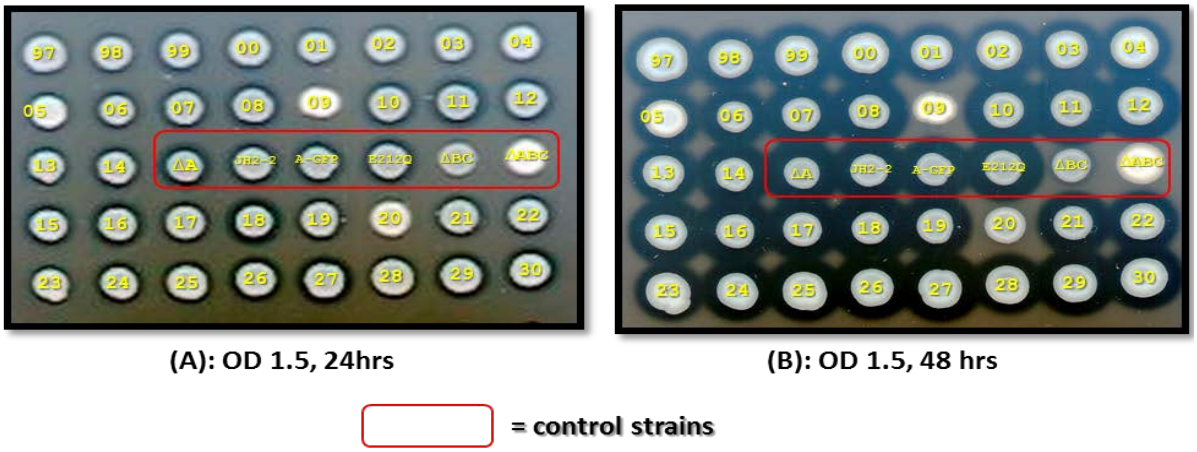

Figure 35. Detection of cell surface PGH activities on agar plates containing *E. faecalis* cell walls after 24 hours (A) or 48 hours (B). Control strains (boxed) are described in (**Fig. 33**).

3.1.5. Identification of PGH hydrolytic profiles by zymogram analysis

3.1.5. Identification of PGH hydrolytic profiles by zymogram analysis

3.1.5.1. Detection of PGHs activities in control strains

Our previous plate assays with *M. luteus* as a substrate indicated that none of the mutants displayed PGH activity against this heterologous substrate. To further analysis the PGH activities produced by spontaneous mutants, we carried out zymogram experiments using exclusively *E. faecalis* as a substrate. The principle of this method is to separate proteins under denaturing conditions on a SDS-PAGE containing purified cell wall as substrate. Proteins are then renatured in a buffer containing a non-ionic detergent (triton X-100) and the bands with hydrolytic activities are detected as a clearing zone in the gel.

Two types of protein samples were tested (crude extracts and supernatants) using different pHs pH 5.0, 6.2, 7.4 and 8.5 and different incubation times to maximize the possibility to detect all PGHs produced by mutants. To increase the sensitivity of the assay, we used as a substrate, cell walls from the *E. faecalis* mutant with deletions in 4 genes encoding PBPs (Δ4, see 3.1.4.2.1).

Using bacterial crude extracts, wild type hydrolytic profiles revealed two clear bands with activity (**Fig. 36A**). The band with the highest molecular weight corresponds to AtlA activity because it can be seen in WT (lane 1) and strain ΔBC, but disappears in all *atlA* strains (*atlA*$_{E212Q}$-*gfp*, lane 3; ΔA, lane 4 and ΔABC, lane 6). As no AtlA activity could be detected in the producing the AtlA-GFP fusion, (lane 2) we concluded that the fusion is not active. The band with the lowest molecular weight corresponds to AtlB activity as it is present in the WT (lane 1), A-GFP (lane 2), *atlA*$_{E212Q}$-*gfp* (lane 3) and ΔA (lane 4) strains, but it cannot be seen in all *atlB* crude extracts and supernatants: (strains ΔBC, lane 5 and ΔABC, lane 6). AtlC could be identified in some cases as a band just below AtlB activity. As expected, AtlC activity was no systematically detected because it is masked by AtlB.

Longer incubation (after 10 days) increased all bands intensity but no other band appeared except AtlB and AtlA. AtlA can be detected with all pHs (5.0, 6.2, 7.4 and 8.5), (**Fig. 36B, C and D**) AtlB could be detected with pH 5.0, 6.2 and 7.4 but poorly at pH 8.5 as previously described (Mesnage et al., 2008).

Similar results were found when culture supernatants were used instead of crude extracts (**Fig. 37**).

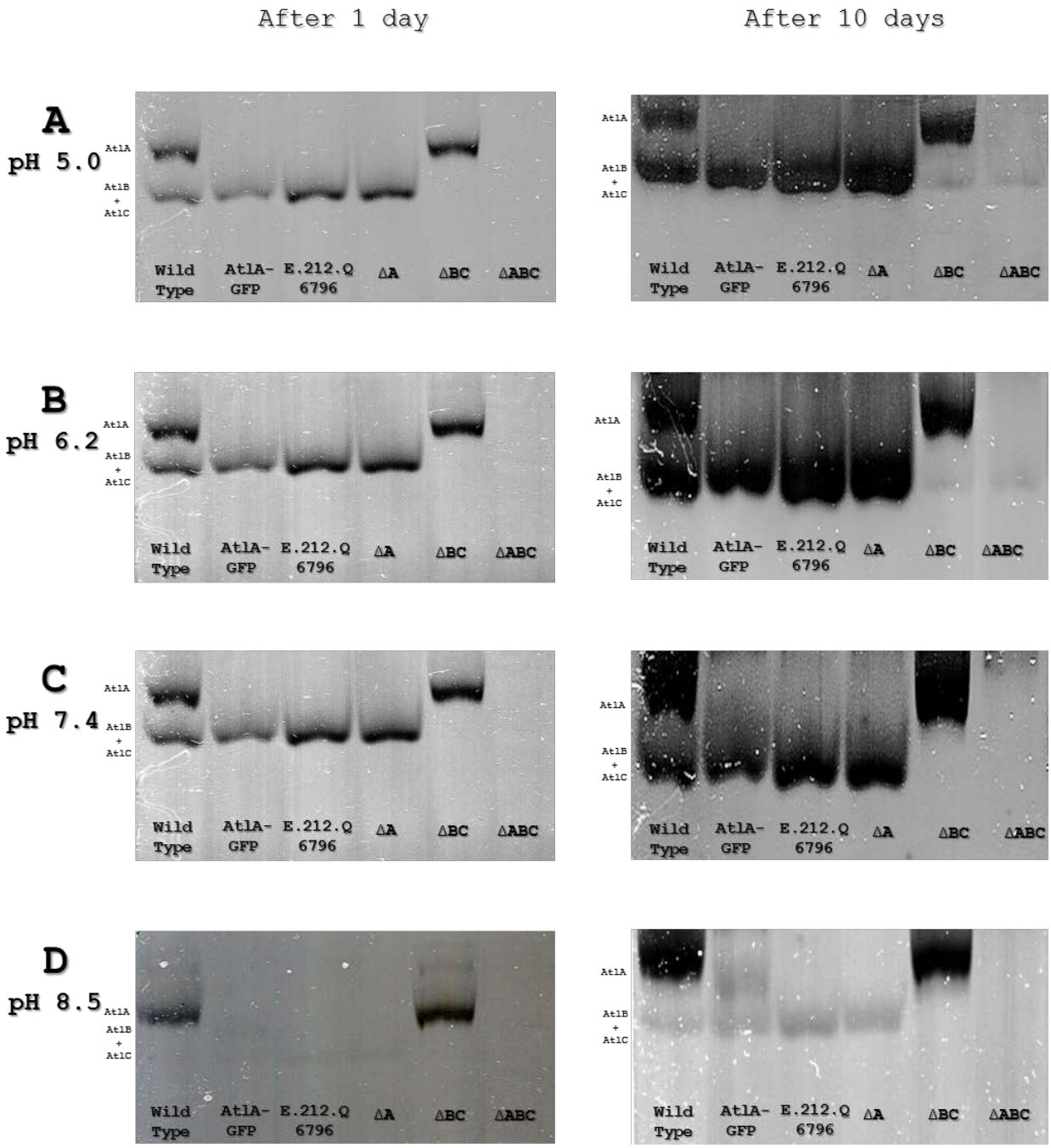

Figure 36. Zymogram detection of PGH activities in control strains using crude extract samples and *E. faecalis* autoclaved cells as a substrate. The same buffer was used at different pHs: 5.0 in (**A**), 6.2 in (**B**), 7.4 in (**C**) or 8.5 in (**D**). For each buffer condition, a picture was taken after 1 day (left handside gel) or 10 days (right handside gel) of incubation at 37°C.

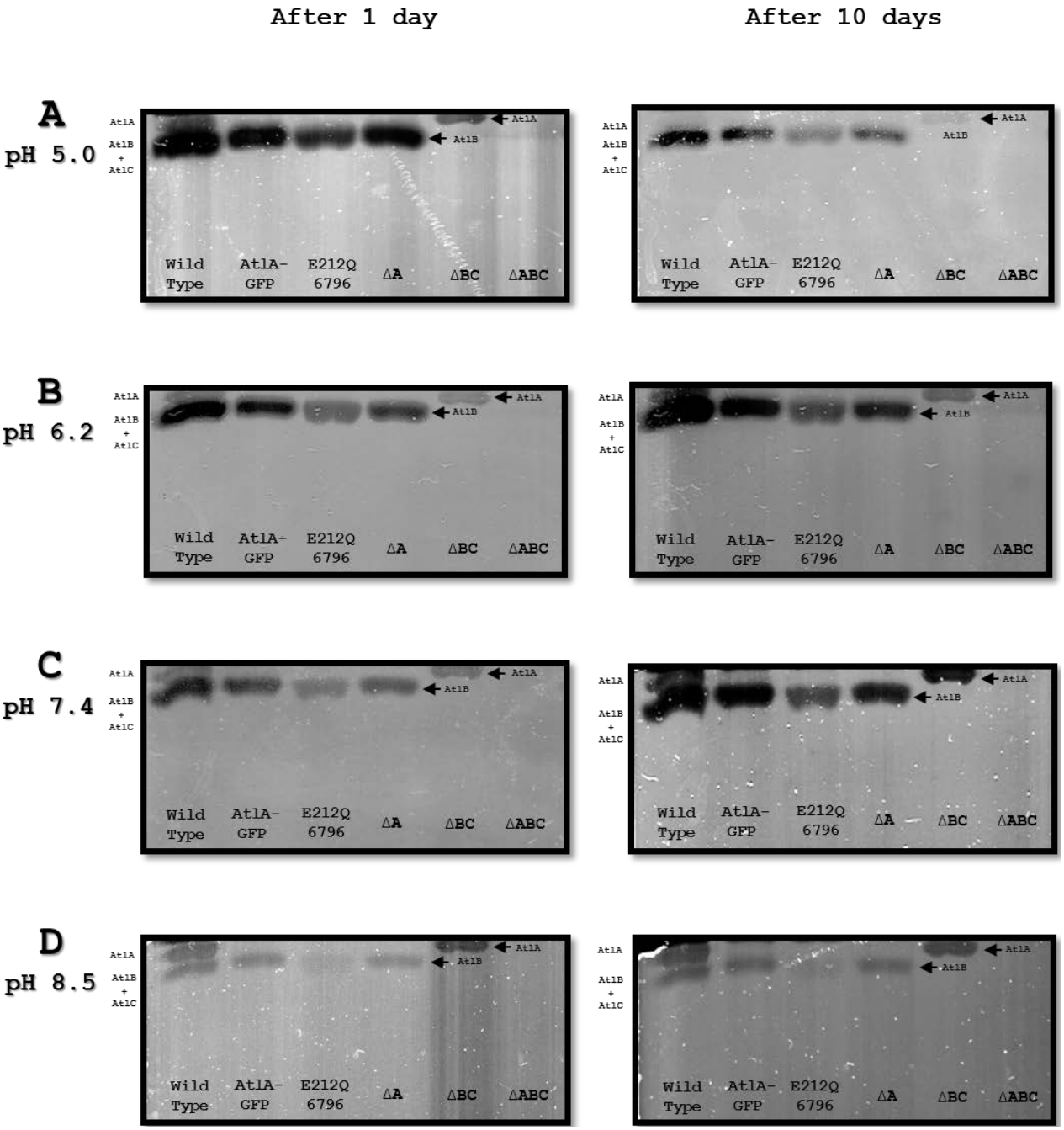

Figure 37. Zymogram detection of PGH activities in control strains using culture supernatants. The same buffer was used at different pHs: 5.0 in (**A**), 6.2 in (**B**), 7.4 in (**C**) or 8.5 in (**D**). For each buffer condition, a picture was taken after 1 day (left hand side gel) or 10 days (right hand side gel) of incubation at 37°C.

3.1.5.2. Detection of PGH activities in mutant strains

The PGHs activities produced by the mutants were analysed by zymogram using *E. faecalis* Δ4 cell walls as a substrate using crude extract (**Fig. 38**) and supernatants (**Fig. 39**), different pHs and incubation times.

The same autolytic profile as the parental strain was detected in nearly all mutants (32/34). Generally, the only activity detected was AtlB and in some case AtlC (**Fig. 38B**) and there was no difference using different pHs or incubation time.

This suggested that the formation of shorter chains was not associated with the production of a novel autolysin or an increase in AtlB activity. Only two mutants (9 and 20) showed no or less AtlB activity, respectively. This result is in agreement with the plate assay (**Fig. 35**) indicating that mutants 9 and 20 have no halo.

Altogether, the zymogram data suggested that the long chains in mutants 9 and 20 (class A) are due to a defect in AtlB activity.

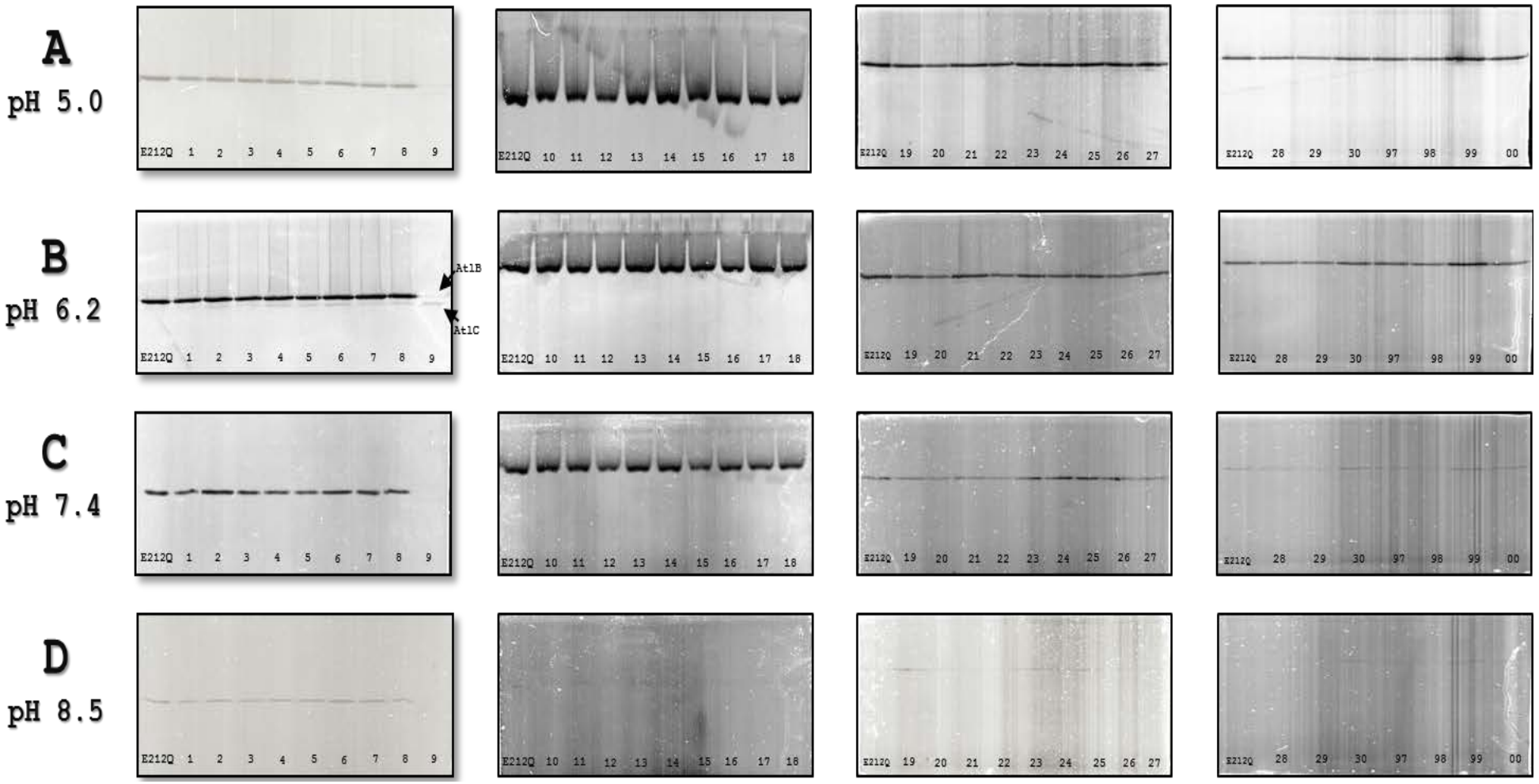

Figure 38. Zymogram detection of PGH activities in mutant crude extracts. The same buffer was used at different pHs: 5.0 in (**A**), 6.2 in (**B**), 7.4 in (**C**) or 8.5 in (**D**). For each buffer condition, a picture was taken after 1 day (left hand side gel) or 10 days (right hand side gel) of incubation at 37°C.

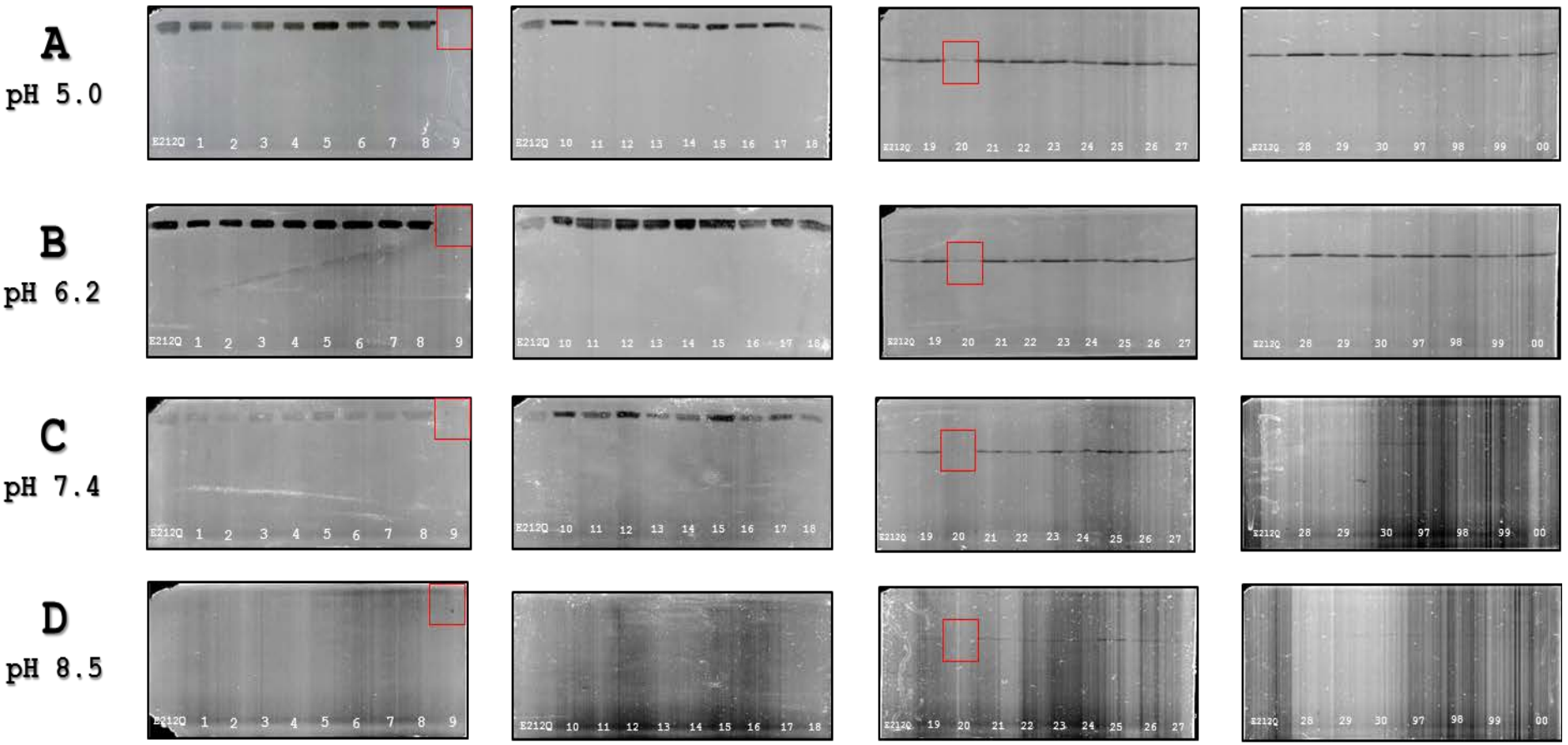

Figure 39. Zymogram detection of PGH activities in mutant culture supernatants. The same buffer was used at different pHs: 5.0 in (**A**), 6.2 in (**B**), 7.4 in (**C**) or 8.5 in (**D**). For each buffer condition, a picture was taken after 1 day (left hand side gel) or 10 days (right hand side gel) of incubation at 37°C.

3.1.6. rp-HPLC analysis of mutant peptidoglycan structure

Zymogram did not reveal any change in the autolytic profile of most spontaneous mutants, so we hypothesized that it may not be the PGHs which are altered in the mutants, but the PG structure that is less digested by PGHs. To test this hypothesis, we analysed the PG structure of all mutants. PG was purified using established methods and digested with mutanolysin (Bouhss et al., 2002). PG soluble fragments (disaccharides-peptides) were separated by reversed phase HPLC as described in the materials and methods section.

Overall, all mutants traces were virtually identical to that of the parental strain see **Fig. 40** as an example. Only one trace appeared different (mutant 3), with a high proportion of muropeptides containing tripeptides stem (indicated with an arrow) (**Fig. 41**), however, a repeat of the experimental did not reveal any difference (**Fig. 42**).

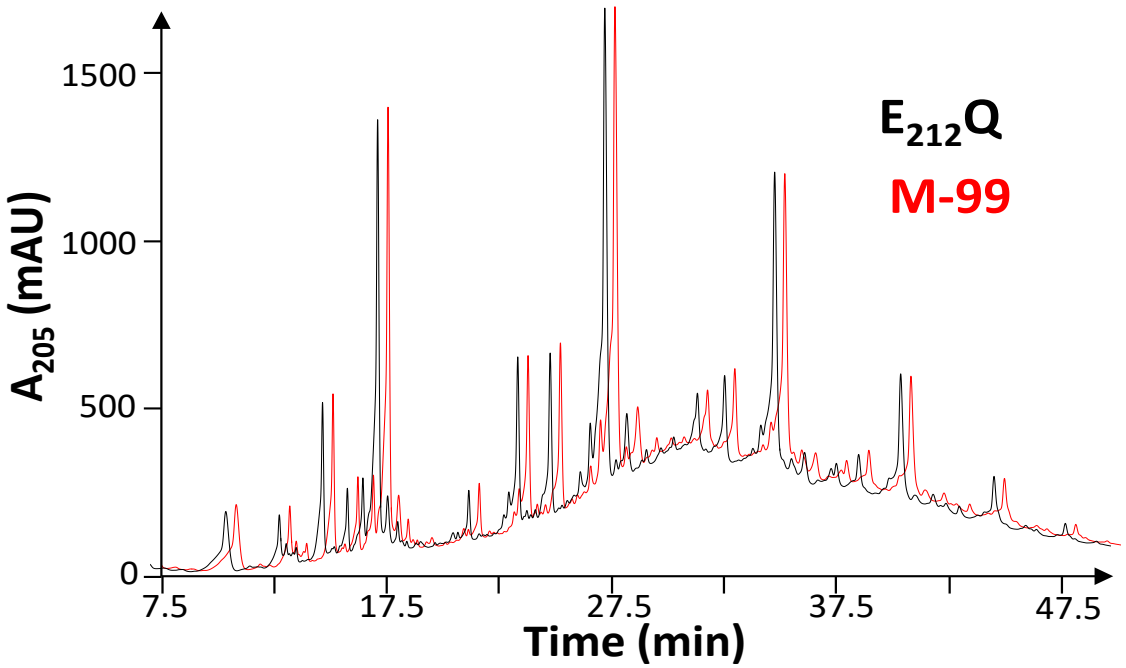

Figure 40. rp-HPLC muropeptide comparison of the parental strain with a spontaneous mutant. The parental trace (black) is superimposed with that of mutant 99 to show the reproducibility of the muropeptide separation and illustrates the lack of significant differences between the two samples, a property that also applied to most samples analysed.

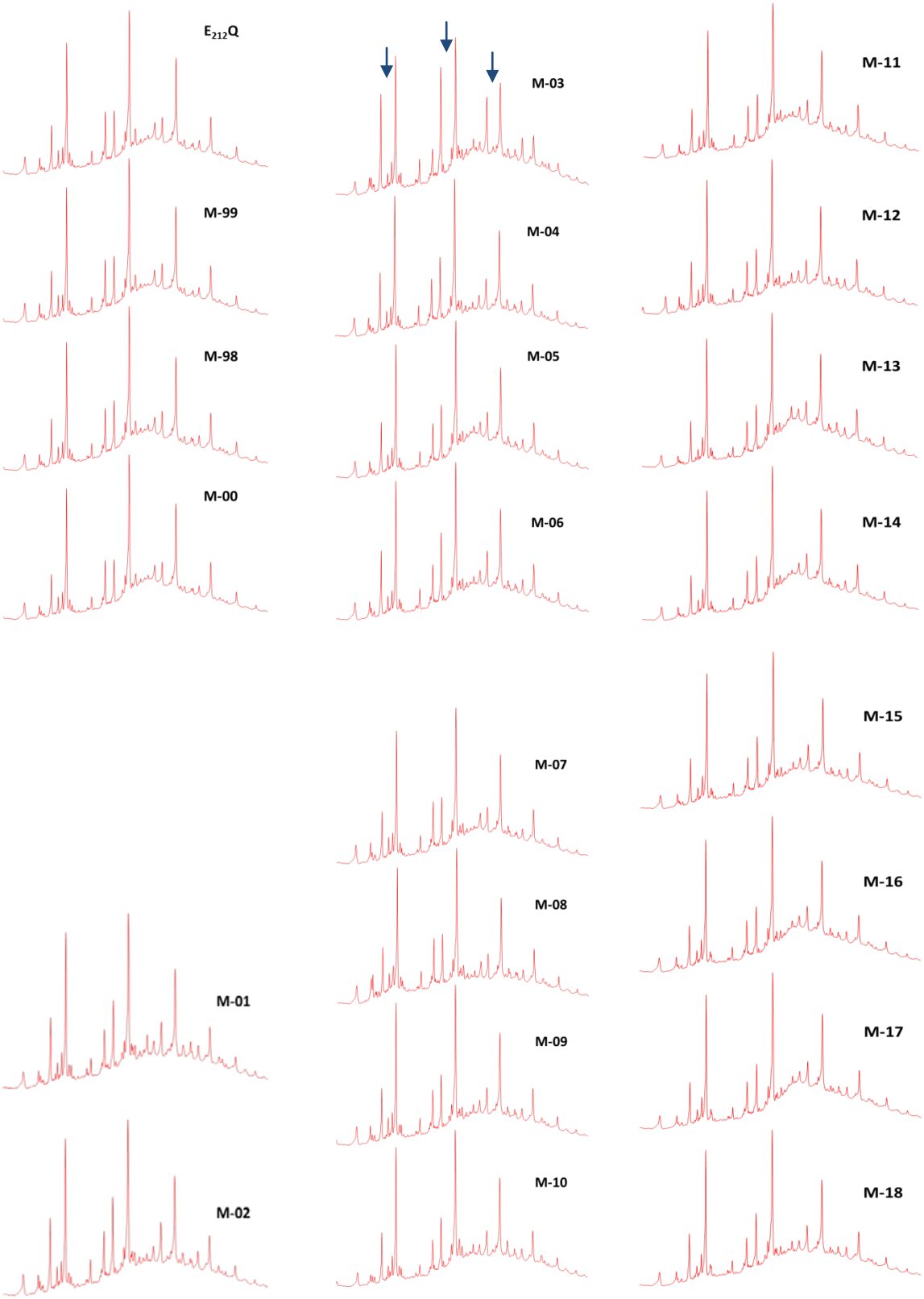
$E_{212}Q$
M-99
M-98
M-00
M-01
M-02
M-03
M-04
M-05
M-06
M-07
M-08
M-09
M-10
M-11
M-12
M-13
M-14
M-15
M-16
M-17
M-18

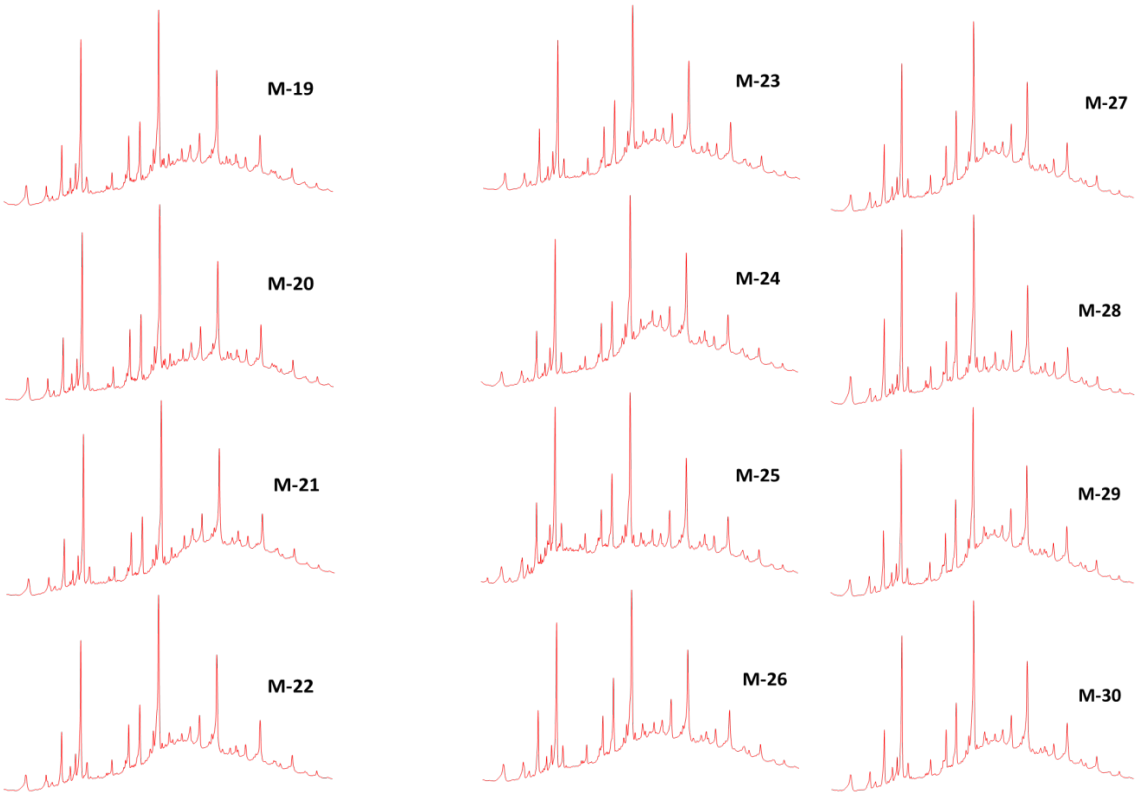

Figure 41. rp-HPLC analysis of PG muropeptide profiles of spontaneous mutants. All traces were virtually identical, except mutant 03 which revealed a higher abundance of disaccharide-tripeptide stems indicated by arrows.

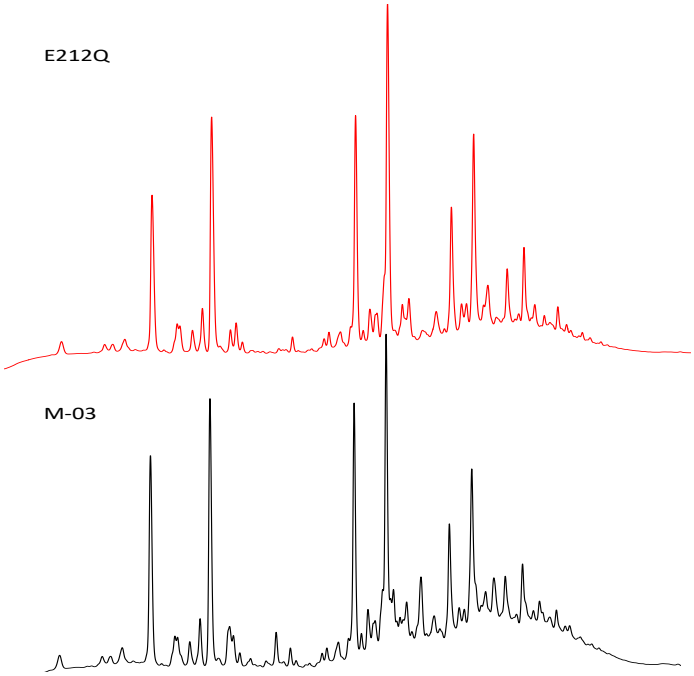

Figure 42. Biological replicate of the comparative muropeptide analysis of WT and mutant 03. Only one mutant had a muropeptide profile that seemed different from that of the parental strain (mutant 03). The PG was extracted and analysed again, but did not show any difference.

3.1.7. Whole genome sequencing of spontaneous mutants

The genomes of spontaneous mutants were sequenced to identify mutations responsible for the phenotype observed. The chromosomal DNA was extracted and its integrity was tested on agarose gel (**Fig. 43A**). Although samples were contaminated by RNA high molecular weight DNA was detected for all samples, confirming the integrity of the samples. All DNAs were completely digested using the HindIII restriction enzyme as judged by the disappearance of the high molecular weight DNA (**Fig. 43B**).

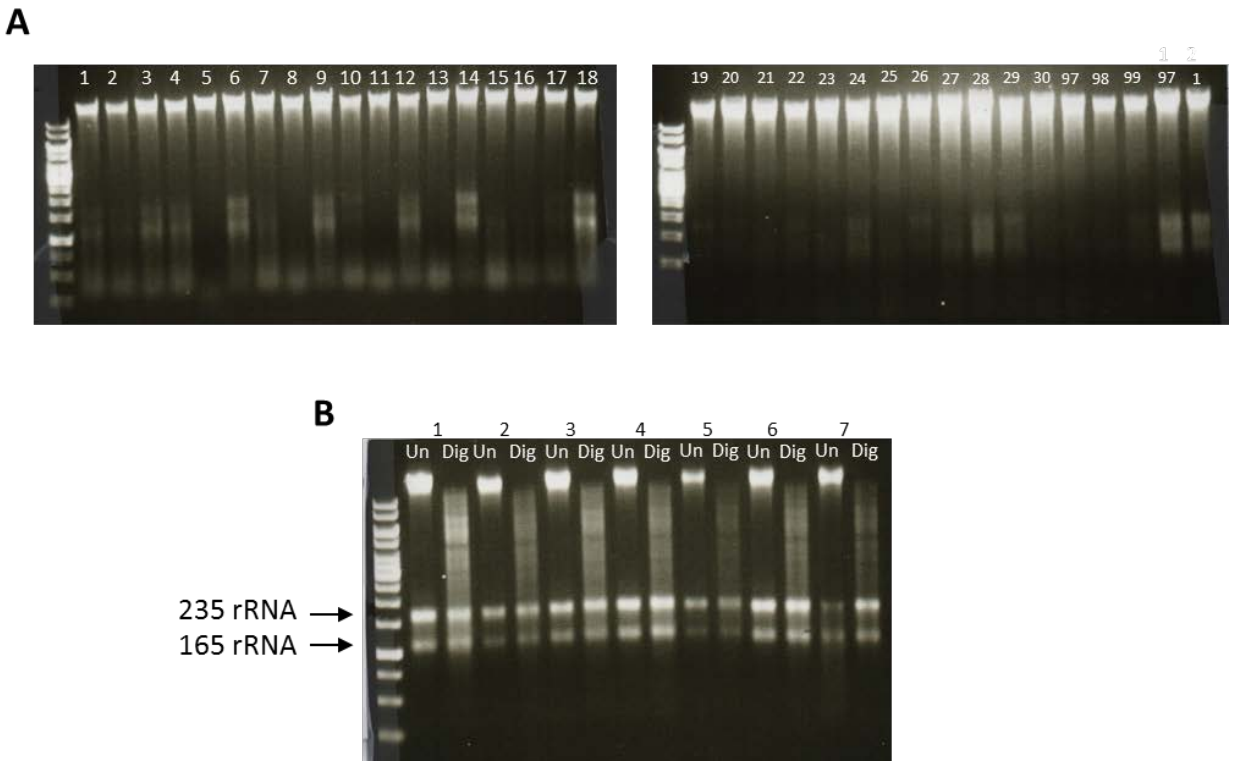

43. Agarose gel electrophoresis of purified chromosomal DNA of spontaneous mutants. (**A**), One µg of undigested DNA was loaded on a gel**.** (**B**), A subset of mutant DNAs was further digested with HindIII.

DNA libraries were prepared by Dr Paul Health at the Sheffield Institute for Translational Neuroscience (SITraN) and sequenced on an ILLUMINA HiSeq sequencer. Reads were assembled by Dr Roy Chaudhuri in the department of Molecular Biology and Biotechnology (MBB) against the JH2-2 draft genome available. Dual indexed DNA samples were prepared using the Illumina Nextera XT DNA kit and run on a HiSeq 2500 sequencer in high output run. Sequence reads were adapter trimmed using Cutadapt (Martin, 2011), and mapped to the reference genome using BWA-MEM (Li, 2013). SNPs were called using FreeBayes v0.9.20, run via Snippy 3.0 (https://github.com/tseemann/snippy) using default settings, which exclude reads with mapping quality below 60 and SNPs with less than 10-fold coverage.

3.1.7.1. Genome analysis of class A mutants

Two of the four group A mutants forming longer chains than the parental strain contained mutations that could account for their phenotype (mutants 5 and 9), whilst no mutations were identified in the two others (14 and 20) (table 5). Mutant 5 has a single base deletion in the open reading frame encoding an unknown protein (AdmA for **A**tlA **d**isplay **m**utant A) that leads to a premature stop codo. The resulting protein has a truncation of 43 C-terminal amino acids. In collaboration with S. Kulakauskas (INRA, Jouy en Josas, France), we have shown that AdmA is required for the surface translocation of AtlA in *E. faecalis* and its orthologue AcmA in *L. lactis* (**Fig. 44**). Mutant 9 harbours an entire deletion of prophage pp1 (Matos et al., 2013) that encodes AtlB.

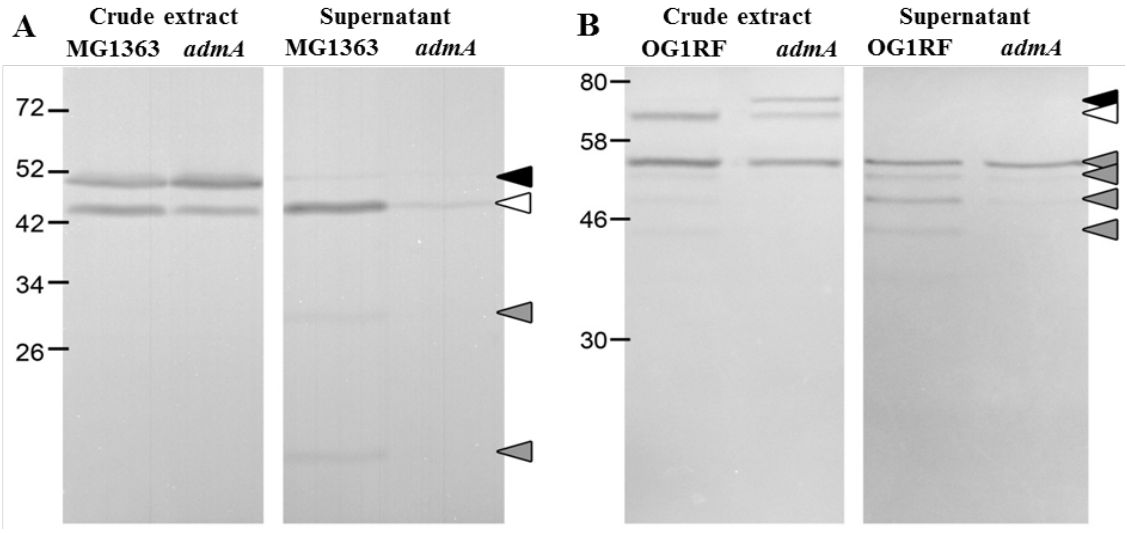

Figure 44. Zymogram analyses of *L. lactis* MG1363 and *E. faecalis* OG1RF. Crude extract and supernatants of *L. lactis* MG1363 (**A**) or *E. faecalis* OG1RF (**B**) and isogenic *admA* mutants were loaded on a 12% SDS-PAGE and activities were visualized after renaturation. Protein sizes in kDa are indicated on the left. Pre-proteins are indicated as black triangles, secreted proteins (after cleavage of the signal peptides) as white triangles, and proteolytically processed autolysins as grey triangles. Molecular weights in kDa are indicated on the left side of the gel.

3.1.7.2. Genome analysis of class B mutants

Group B mutants isolated from mutant 14 correspond to suppressors of the very long chain phenotype. Mutations potentially responsible for the short chain phenotype were identified in 9 out of the 10 group B mutants (table 5). 6 mutants had mutations in *atlA* including premature stop codons abolishing the production and/or surface display of AtlA (table 5). Two identical deletions of a single amino acid were found in *secA*. Finally, a single amino acid substitution was identified in a class B PBP (mutant 28).

3.1.7.3. Genome analysis of class C mutants

Group C mutants suppress the long chain phenotype due to the production of the inactive $AtlA_{E212Q}$-GFP allele. Five out of 19 class C mutants did not reveal any difference with the reference genome. Six mutants had mutations in *atlA*, five of them being identical to the ones found in group B mutants. Three mutations were found in *secA*, including one not previously found in group B mutants. One mutation was found in *secY* and two others in genes encoding an ABC transporter and a protein involved in biotin transport (table 5). Mutations in *secA* and *secY*, were mapped on the crystal structure of the SecAEGY complex (**Fig. 45**). This was achieved by aligning the *E. faecalis* sequences with the sequences corresponding to the sequences of the secAEGY components used to generate the 3D structure available in the PDB database (3DL8).

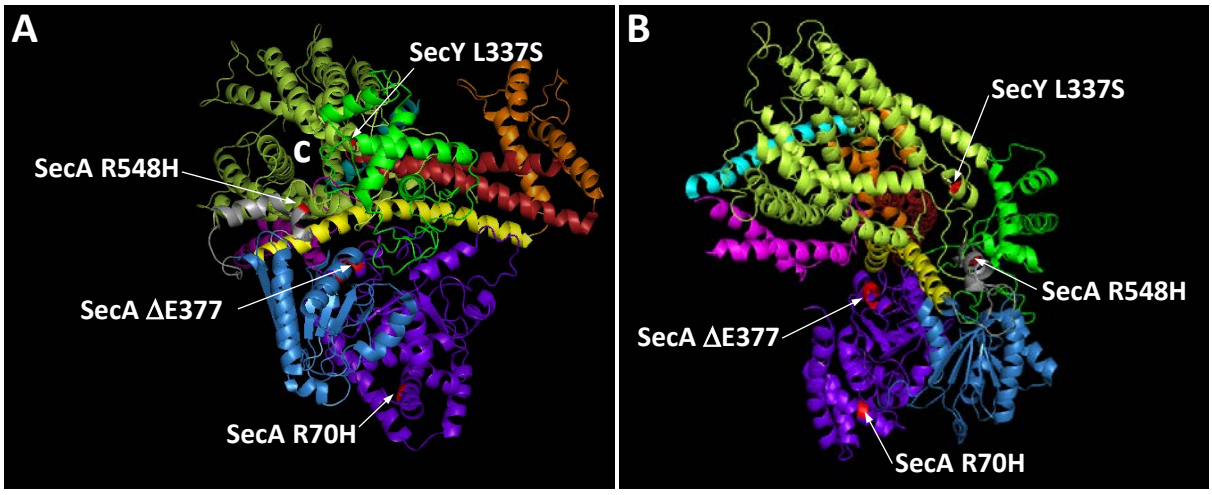

Figure 45. Mapping of *E. faecalis secA* and *secY* mutations on the crystal structure of the complex of *Aquifex aeolicus* SecYEG and *B. subtilis* SecA in its closed form (PDB 3DL8). (A) is a bottom view, showing the SecY channel (c) and (**B**) is a side view**.** The different domains are colored are as follows: bright blue, SecE; magenta, SecG, purple, NBD1 (nucleotide binding domain 1); blue, NBD2; yellow, helical scaffold domain (HSD); red, 2 HFD (Helix Finger Domain); orange, HWD (Helical Wing Domain); grey, "joint" region connecting SD and NBD2; bright green, pre-protein binding domain (PBD); light green, SecY. The mutations SecA R548H, SecA Δ377 and SecY L337S seem to group around the region where the HSD (yellow) meets the PDB (bright Green), at the entrance to the SecY channel.

		Coverage	Mutation	WT	Mut	Read Nb	NT position	Effect			Locus (gene name)	Function
Group A	5	41.2	del	ATT	AT	AT:32 ATT:1	416/519	Frameshift	L139 → stop	Truncation of 43 C-ter AA	JH2-2_0604 (*admA*)	Unknown
	9	70.6	Prophage excision (encodes *atlB*)					49,104 bp deletion			JH2-2_1253-1327 (*pp1*)	Septum cleavage
	14	67.4	NO SNP detected									
	20	42.0	NO SNP detected									
Group B	29	65.2	SNP	C	T	T:57 C:0	169/2937	Premature stop	Q57 → stop	Stop 4 AA after signal peptide	JH2-2_0632 (*atlA*)	Septum cleavage
	24	62.9	SNP	C	A	A:108 C:0	696/2937	Premature stop	Y232 → stop	Stop 50 AA after start of catalytic domain	JH2-2_0632 (*atlA*)	Septum cleavage
	22	27.5	SNP	C	T	T:43 C:0	1057/2937	Premature stop	Q353 → stop	Stop 5 AA before the 1st LysM	JH2-2_0632 (*atlA*)	Septum cleavage
	27	44.0	SNP	C	A	A:53 C:1	1508/2937	Premature stop	S503 → stop	Stop 10 AA after the start of the 3rd LysM	JH2-2_0632 (*atlA*)	Septum cleavage
	26	58.8	SNP	C	A	A:66 C:0	1682/2937	Premature stop	S561 → stop	Stop 1 AA after the start of the 4th LysM	JH2-2_0632 (*atlA*)	Septum cleavage
	21	71.2	SNP	C	A	A:59 C:0	2194/2937	AA substitution	Q732 → K	Subtitution 5 AA before the stop codon	JH2-2_0632 (*atlA*)	Septum cleavage
	23	35.8	Del	TCT TCT tct	TCT TCT	TCT:23 TCT tct:0	1130/2538	Inframe deletion	E377 deletion	Nucleotide binding domain 1	JH2-2_1593 (*secA*)	Protein secretion
	25	45.7	Del	TCT TCT tct	TCT TCT	TCT:29 TCT tct:0	1130/2538	Inframe deletion	E377 deletion	Nucleotide binding domain 1	JH2-2_1593 (*secA*)	Protein secretion
	28	47.7	SNP	G	T	T:71 G:0	1651/2229	AA substitution	A551 → S	Transpeptidase domain	JH2-2_0810 (*pbpC*)	PG polymerisation
	30	69.4	NO SNP detected									
Group C	1	22.8	SNP	C	T	T:14 C:0	169/2937	Premature stop	Q57 → stop	Stop 4 AA after signal peptide	JH2-2_0632 (*atlA*)	Septum cleavage
	8	51.2	SNP	C	T	T:58 C:0	169/2937	Premature stop	Q57 → stop	Stop 4 AA after signal peptide	JH2-2_0632 (*atlA*)	Septum cleavage
	19	42.6	SNP	C	A	A:87 C:0	696/2937	Premature stop	Y232 → stop	Stop 50 AA after start of catalytic domain	JH2-2_0632 (*atlA*)	Septum cleavage
	17	40.5	SNP	C	T	T:60 C:0	1057/2937	Premature stop	Q353 → stop	Stop 5 AA before the 1st LysM	JH2-2_0632 (*atlA*)	Septum cleavage
	6	18.3	Del/Ins	AGATT	CAATC	CAATC:10 AGATT:0	1814/2937	AA substitution	K604 → T	Subtitution 6 AA before theend of the 4th LysM	JH2-2_0632 (*atlA*)	Septum cleavage
	16	54.7	SNP	C	A	A:55 C:0	2194/2937	AA substitution	Q732 → K	Subtitution 5 AA before the stop codon	JH2-2_0632 (*atlA*)	Septum cleavage
	98	30.6	SNP	C	T	T:41 C:0	209/2538	AA substitution	R70 → H	Nucleotide binding domain 1	JH2-2_1593 (*secA*)	Protein secretion
	11	47.0	SNP	C	T	T:41 C:0	209/2538	AA substitution	R70 → H	Nucleotide binding domain 1	JH2-2_1593 (*secA*)	Protein secretion
	2	31.6	Del	TCT TCT tct	TCT TCT	TCT:24 TCT tct:0	1130/2538	Inframe deletion	E377 deletion	Nucleotide binding domain 1	JH2-2_1593 (*secA*)	Protein secretion
	18	100.9	Del	TCT TCT tct	TCT TCT	TCT:53 TCT tct:0	1130/2538	Inframe deletion	E377 deletion	Nucleotide binding domain 1	JH2-2_1593 (*secA*)	Protein secretion
	4	46.1	SNP	C	T	T:35 C:0	1643/2538	AA substitution	R548 → H	Joint region connecting NBD1 and NBD2	JH2-2_1593 (*secA*)	Protein secretion
	0	36.8	SNP	T	C	C:54 T:0	1010/1299	AA substitution	L337 → S	Entry of the SecY channel	JH2-2_0233 (*secY*)	Protein secretion
	3	61.4	SNP	G	A	A:48 G:0	1043/1569	AA substitution	G348 → D	?	JH2-2_0191	ABC transporter
	99	20.3	SNP	G	T	T:17 G:0	218/549	AA substitution	G73 → V	?	JH2-2_2551	Biotin transport?
	7	12.3	NO SNP detected									
	10	37.9	NO SNP detected									
	12	44.1	NO SNP detected									
	13	61.7	NO SNP detected									
	15	36.6	NO SNP detected									

Table 5. Summary of the mutations identified by whole genome sequencing.

3.1.8. Discussion

In this chapter, we identified and characterised 34 spontaneous mutants with altered septum cleavage based on a phenotypic screen of bacterial colony morphologies in semi-solid agar (**Fig. 30**). These included mutants forming chains longer or shorter than the parental strain. Putative mutations responsible for the cell separation changes were identified by whole genome sequencing.

Despite the clear phenotype difference between the colony morphology of the wild-type strain JH2-2 and the *atlA* derivative, we could not isolate any spontaneous mutants forming long chains from JH2-2. The fact that the *atlA* mutant is able to grow in the medium used for the screen suggests that mutants may have arisen, but we did not detect them in the fast growing "comets" formed by the parental cells. It would be interesting to explore other experimental conditions to re-do this experiment. For example, use lower concentrations of agar to exacerbate the phenotype difference between wild-type and chain forming mutants. Other conditions such as temperature or low osmolarity conditions to favour the emergence of mutants with a PG structure more resistant to mechanical stresses. Another possibility would be to repeat these experiments starting with a Δ*atlB*Δ*atlC* parental strain to isolate chain forming mutants. AtlB and AtlC have been shown to have a low septum cleavage activity so their absence could help to identify other genes involved in this process.

Using a strain deficient for AtlA activity (JH2-2 $atlA_{E212Q}$-*gfp*), we were able to identify several mutants forming longer chains (group A) or shorter chains (group C). We also identified mutants suppressing the extreme chaining phenotype of group A mutants. (group B). For 8 out of 34 mutants, we did not identify any mutation that was likely to be responsible for the change in the cell chain length.

<u>Mutations associated with a septum cleavage defect</u>

4 spontaneous mutants forming cell chains longer than the parental strains were isolated. Whole genome sequencing of 2 of them revealed mutations that could be responsible for this phenotype. Mutant 5 had a nonsense mutation in an unknown gene that we named *admA*. This gene was also identified in our transposon mutagenesis. Although AdmA does not show any similarity with sequences from the protein databases, structure predictions suggest that it is related to polysaccharide deacetylases see (**Fig. 54**).

Interestingly, the *admA* mutation does not alter AtlA activity but reduces AtlA surface localisation. The predicted cytoplasmic localisation of AdmA makes it unlikely to function as a peptidoglycan deacetylase, but it could potentially be involved in the modification of Epa. Surface polysaccharides are polymerised in the cytoplasm and then translocated onto the cell surface (Mistou et al., 2016). It is therefore possible that AdmA modifies the Epa polymer that contains glucosamine. The impact of Epa deacetylation on AtlA translocation remains difficult to explain. An alternative possibility is that the structure predictions are misleading and that AdmA does not display any Glc*N*Ac deacetylase activity. It is worth pointing out that the sequence predictions presented in (**Fig. 55**) introduce several long gaps in AdmA. Determining the crystal structure of AdmA will provide insights into its function.

The second mutation identified corresponds to a complete excision of prophage 1 encoding AtlB. This explains why AtlB activity cannot be detected in zymogram using protein crude extracts from mutant 9 (**Fig. 38**). Previous studies have shown that AtlB can cleave the septum in the absence of AtlA (Mesnage et al., 2008), therefore explaining the long chain phenotype of mutant 9.

<u>Mutation associated with an increased septum cleavage activity</u>

Most mutations associated with increased septum cleavage abolish the production or surface display of the $AtlA_{E212Q}$-GFP protein. Several mutations introduce a premature stop codon that prevent the production of a catalytically active AtlA or lead to the truncation of at least 2 LysM modules. Previous work indicated that removal of the LysM domain drastically reduces the activity of AtlA (Eckert et al., 2006). Although it has a less pronounced impact, truncation of 2 LysM modules or more also reduces the binding to PG significantly (B. Salamaga and S. Mesnage, unpublished). Two mutations associated with shorter chains (K604T and Q732K)

The impact of these mutations remains to be established, but we can hypothesize that they lead to a lower binding affinity to PG. Altogether, the mutations in AtlA associated with increased septum cleavage suggest that the absence of this protein at the cell surface allows other PG hydrolases to access the septum to cleave it. The enzymes involved include AtlB, AtlC and other(s) that remain to be identified (Mesnage et al., 2008). Interestingly, this result is in agreement with unpublished data indicating that the *atlA* deletion mutant forms cell chains shorter than the strain producing the $AtlA_{E212Q}$-GFP inactive enzyme (B. Salamaga and S. Mesnage, unpublished).

To confirm that the presence of $AtlA_{E212Q}$-GFP prevents other PG hydrolase from cleaving the septum, several experiments could be considered.

We will have to complement the *atlA* mutations described in (table 5) with the *atlA*$_{E212Q}$-*gfp* allele to show that this leads to an increased size of the cell chains. Using the complementation vector based on the tetracycline-inducible promoter recently built in the lab will allow complementing the mutations with increasing amounts of $AtlA_{E212Q}$-GFP. A similar complementation experiment could be carried out with the same inducible system to express the LysM domain alone to test if the saturation of PG glycan chains with this domain prevents other enzymes from cleaving the septum.

We identified 3 mutations in *secA* and one in *secY* in the mutants forming cell chains shorter than the parental strain. This may reflect the fact that AtlA is secreted via the general secretory pathway rather than a specific transporter which has been described for other autolysins (Lenz et al., 2003). This result is somewhat surprising since it has been proposed that the secretion machinery in *E. faecalis* forms a so-called exportal that is not localised at the septum (Kline et al., 2009). The mutation identified in *secA*, and *secY* have not been reported previously and their impact on the secretion of surface proteins awaits further analysis. Using proteomics, we could compare the proteins in culture supernatants and cell surface extracts from wild-type and *sec* mutants. Before doing these rather complex and costly experiments, we could use the inducible expression system that we will construct to complement mutations in *atlA*, (see previous paragraph), to compare the secretion rate of AtlA tagged with 6 C-terminal His residues in both the parental and *sec* mutants. A key question will be to figure out if the *sec* alleles in the mutants forming shorter cell chain length affect the secretion of AtlA and/or other proteins.

One mutation was found in a gene encoding a class B PBP that has not been studied to date. Although the mutation is not in the predicted active site, it could be associated with a slight decrease in PG crosslinking (**Fig. 42**). This result is extremely interesting as it suggests that PBPs play specific roles in *E. faecalis* PG polymerisation. Again, this mutation will have to be complemented to confirm the role of PbpC in septum cleavage. It is worth noting that a previous screen to isolate transposon mutants suppressing the chain forming of *L. lactis* AcmA identified several insertions in the gene encoding PonA, a class A Pbp (Mercier et al., 2002).

Spontaneous mutants with no detectable genetic difference

The overall sequence coverage was satisfactory for all the genomes that did not reveal any obvious mutation between (30x-70x) for most genome. Only mutants 6 and 7 had relatively low coverage (18.3 and 12.3) respectively. It is therefore tempting to assume that a re-sequencing of these samples would not identify any mutation. It must be pointed out that the algorithm that was used to identify mutations is primarily designed to identify single nucleotide polymorphism (SNPs), short deletions and/or insertions (such as in mutants 5, 23 or 26). Genome re-arrangements or larger deletions were not detected in the original analysis. For example, the 49.1 kbp deletion in mutant 9 was identified by "manual inspection" of the whole genome assembly. A careful and systematic analysis of small deletions, re-arrangements, or gene duplications is therefore required. Alternatively, other sequencing strategies such as PacBio sequencing involving much longer reads (>30kpb versus 150bp) could solve this problem. However, this is a relatively costly option (approx. £1.5k/genome for PacBio sequencing versus £60/genome using Illumina sequencing). Finally, another possibility could be that these ''mutants'' are not mutants and therefore have a genome identical to the parental strain. Bearing in mind the sedimentation profiles shown in **Fig. 32** it is likely that clones 10, 12, 13, 14, 15 and 30 are not true mutants as they are indistinguishable from the parental strains.

In parallel to the analysis of the genomic data available, several experiments could be carried out to understand why these mutants have an altered septum cleavage activity leading to the formation of extremely long (mutants 14 and 20) or short relatively short chains (mutants 30, 7, 10,12, 13 , 15).

- **Do the mutations affect AtlA$_{E212Q}$-GFP expression levels?**

Several mutants with mutations abolishing the production of AtlA$_{E212Q}$-GFP display an increased septum cleavage activity (Table 5). We could therefore quantify the expression level of AtlA$_{E212Q}$-GFP using flow cytometry or western blot analyses using in-gel fluorescence to quantify the GFP in cell extracts.

- **Do the mutations affect the localisation of *atlA*$_{E212Q}$-*gfp*?**

We could test the presence of AtlA$_{E212Q}$-GFP at the cell surface by immunofluorescence using anti-AtlA or anti-GFP antibodies. In parallel, deconvolution fluorescence microscopy could be used to localize the GFP distribution in the cell.

- **Do the mutations alter the cell wall composition and susceptibility to septum-cleavage enzymes?**

Although we did not identify any novel autolytic activity in protein extracts from the mutants with no detectable SNPs, we have not explored if their cell wall is more susceptible to septum cleavage activities. To test this possibility, we could use autoclaved cells corresponding to these mutants to do zymograms with wild-type extracts.

Alternatively, we could use these mutants as substrates to measure the septum cleavage activity by flow cytometry (Mesnage et al., 2008) again using wild-type protein extracts.

3.2. Isolation of transposon mutants impaired in AtlA activity

3.2.1. Construction of the transposon mutant library

3.2.1.1. pZXL5 as a transposon delivery system

The *Mariner* system has been selected. In this system, the transposon jumps into TA dinucleotides in the chromosome (Munoz-Lopez and Garcia-Perez, 2010). Because *E. faecalis* genome is AT-rich, the *Mariner* transposon system is able to generate a large variety of insertions, and is therefore considered as "random". The screening for the transposon mutants was performed on an agar plate containing *M. luteus* to detect of AtlA activity as a halo around the colonies. Once the mutants that did not have a halo around the clones on *M. luteus* plates were isolated, interrupted genes were identified by reverse PCR. The transposon system we used was recently described for *E. faecium* (Zhang et al., 2012a).

Plasmid pZXL5 used for the mutagenesis is described in (**Fig. 46**). This plasmid has a size of 11760 bp and contains the following elements:

- **An origin of replication in Gram negative bacteria** (Ori), for cloning purposes in *E.coli*;
- **A thermosensitive origin of replication in Gram-positive bacteria** (Ori^{ts}), which will be only functional at 28°C;
- **A gene conferring resistance to chloramphenicol** (Cm^{R}) in both Gram-positive and Gram-negative bacteria.
- **A *Mariner* transposon cassette** made of a gentamycin resistance gene flanked by two inverted repeats (IR);
- **A transposase gene under the control of a nisin- inducible promoter**;
- **A nisin-responsive two-component system (*NisRK*)** that will allow the expression of the transposase following addition of nisin (Mierau and Kleerebezem, 2005).

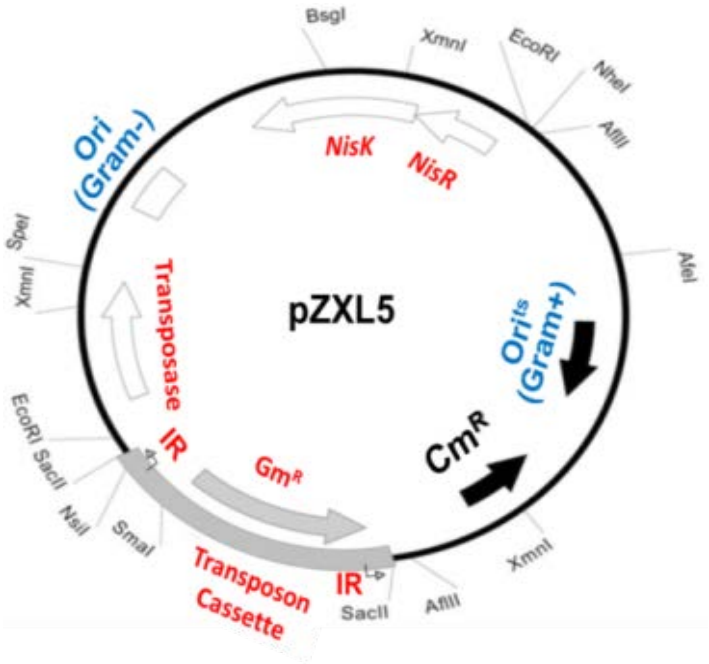

Figure 46. Plasmid map of pZXL5 used for transposon mutagenesis. The plasmid contains (i) an origin of replication in Gram negative bacteria (Ori) for cloning purposes in *E. coli*; (ii) a thermosensitive origin of replication in Gram-positive bacteria Ori^{ts}), which is non-functional at 42°C; (iii) a gene conferring resistance to chloramphenicol (Cm^{R}) in both Gram-positive and Gram-negative bacteria; (iv) a *Mariner* transposon cassette made of a gentamycin resistance gene (Gm^{R}) flanked by two inverted repeats (IR); (v) a transposase gene under the control of a nisin- inducible promoter; (vi) a nisin-responsive two-component system (*NisRK*) that will allow the expression of the transposase following addition of nisin.

3.2.1.2. Construction of the Transposon library

The transposon library was built using plasmid pZXL5 described above in four sequential steps (**Fig. 47**).

STEP 1: selection of transformants harbouring pZXL5. pZXL5 was introduced into *E. faecalis* OG1RF by electroporation. Transformants harbouring pZXL5 were selected on BHI agar plates containing 128 mg/mL gentamycin (Gm^{128}) and 10 mg/mL chloramphenicol (Cm^{10}) at a permissive temperature to allow plasmid replication (28°C). The presence of the plasmid was checked by antibiogram (using antimicrobial discs) and PCR using pZXL5 specific primers to check the presence of the plasmid in the transformed cells.

STEP 2: amplification of the population of pZXL5 transformants. A transformant was grown overnight in 200 mL BHI broth containing Gm^{128} and Cm^{10} at 28°C to amplify the population of pZXL5 transformants.

STEP 3: induction of transposition with nisin. Transposition was induced by inoculating 200µl of the overnight culture in 200mL of BHI broth containing Gm^{128} supplemented with nisin (25ng/mL). This culture was incubated overnight at 42°C. At this temperature, the plasmid cannot replicate and Gm^{R} colonies are in theory resulting from a transposition event onto the chromosome.

STEP 4: amplification the transposons library. The nisin-induced culture containing transposon mutants was used to inoculate BHI broth (200µl in 200mL) containing Gm^{128} and incubated at 42°C to amplify the population of mutants.

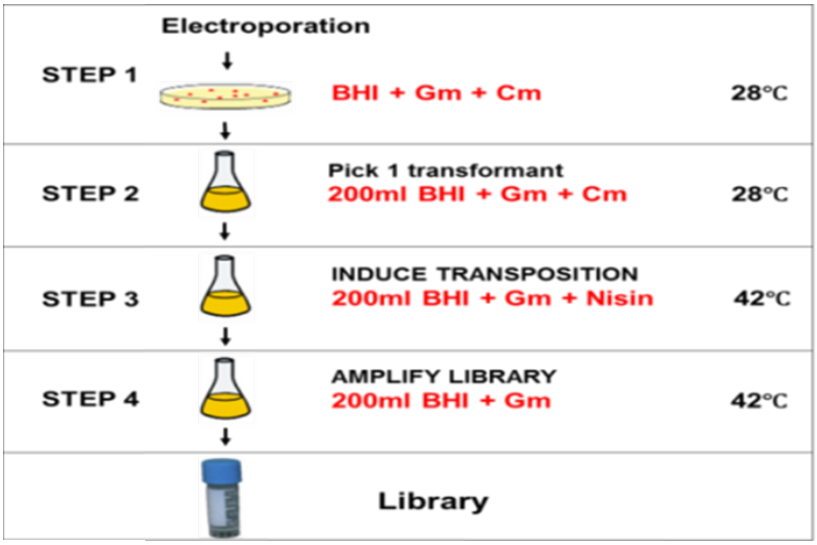

Figure 47. Steps followed to construct the transposon library. See paragraph 3.2.1.2. For a detailed description of the protocol used.

3.2.1.3. Analysis of the Library

The transposon library was analysed to estimate the efficiency of transposition. Mutants were grown in BHI agar containing gentamycin (Gm^{128}) or chloramphenicol (Cm^{10}) to estimate the number of colonies resulting from a transposition event (**Fig. 48**). Growth at 42°C should in theory eliminate the plasmid, which is thermosensitive. Cells growing at 42°C in the presence of chloramphenicol can result from an insertion of the whole plasmid on the chromosome or from a mutation on the plasmid allowing its replication at a non-permissive temperature. By comparing the number of CFUs on gentamycin and chloramphenicol plates, we determined that less than 5% of the Gm^{R} colonies were resistant to chloramphenicol. This indicated that the transposition was efficiently induced by nisin.

A

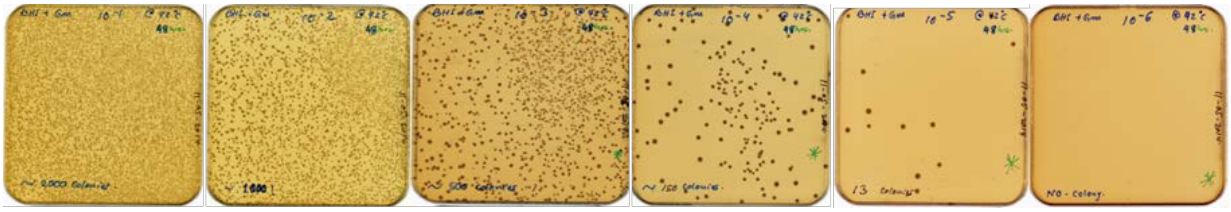

B

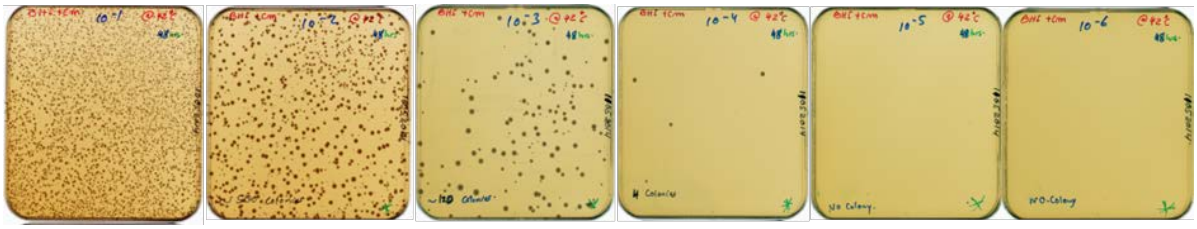

Figure 48. Analysis of the elimination of the plasmid in the mutant library. (A), Serial dilution of the library were plated on selected media containing gentamycin (Gm^{128}) chloramphenicol (Cm^{10}) (**B**) and grown at 42°C. Comparison of CFU numbers between condition A and B indicate that more than 95% cells lost the plasmid.

3.2.2. Identification of *atlA* deficient mutants

The dilution of the library before plating was optimized to visualise the AtlA activity around individual colonies. Transposon mutants were plated on BHI agar plates containing Gm^{128} *M. luteus* PG as a substrate to detect AtlA activity as a halo around the colonies. We determined that approximately 200-300 colonies per plate were an optimal density to analyse halos around colonies. This corresponds to plating 100µl of a 10^{-3} dilution of the library Plastic Petri Dishes (100 mm x 15 mm) (**Fig. 49**).

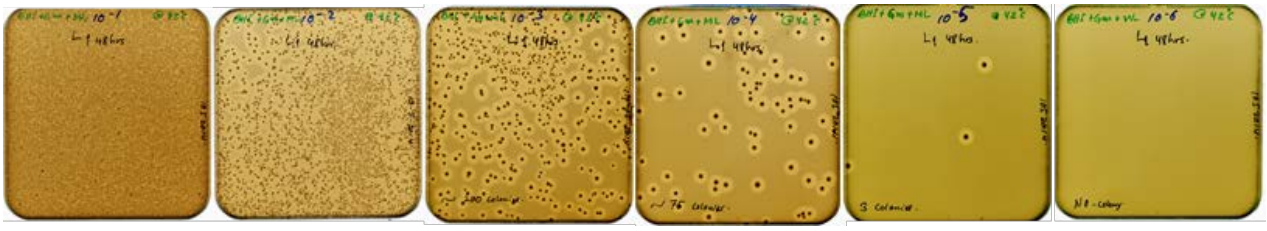

Figure 49. Optimisation of dilution factor to be used to plate the library on selective media. 100µl of a 10^{-3} dilution of the library was found to give the most suitable colony density to visualise AtlA activity.

Three series of screens were performed, each corresponding to approximately a hundred plates containing 200-300 colonies per plate. Altogether, we screened an estimated number of 60,000 transposon mutants. We finally isolated 106 mutants including 3 clones with a bigger halo than the parental strain. An example of a screening plate is shown in **Fig. 50**.

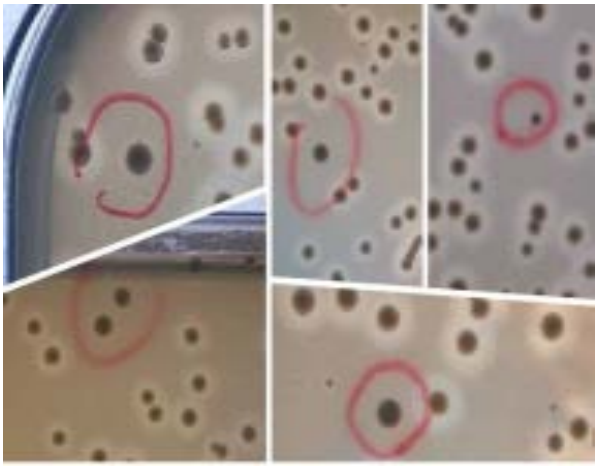

Figure 50. Screening of transposons mutants on agar plate containing *M. luteus*). *atlA* mutants showing no halo around the colony are circled in red.

3.2.3. Mapping of the transposon insertions sites

3.2.3.1. Identification of mutants with an insertion in the *atlA* gene

To find out whether the transposon inactivated *atlA*, we used two primers (AtlA_FW and AtlA_REV) flanking the *atlA* gene (**Fig. 51A**). In the absence of the transposon in the *atlA* gene, the expected size of the PCR product is 3kb. In contrast, if the transposition event has occurred in the *atlA* gene, the estimated amplification size is 5kb (**Fig. 51B**). To identify the site of insertion in *atlA*, we used a primer on the transposon (T7) and one in the *atlA* gene (AtlA_FW) (**Fig. 51A**). The PCR products (**Fig. 51C**) were sequenced.

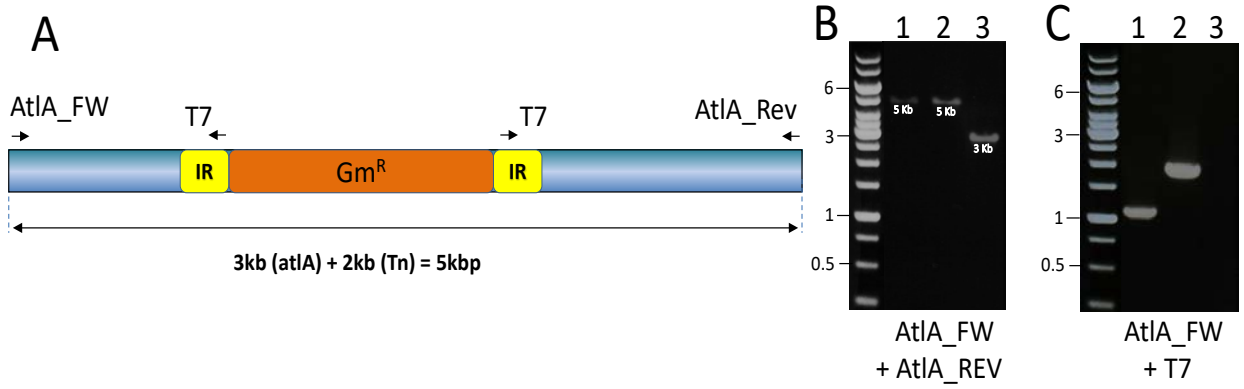

Figure 51. Identification of mutants with a transposon insertion in *atlA*. (**A**), schematic diagram of a mutant with a transposon insertion in *atlA*. (**B**), Amplification of *atlA* gene containing a transposon insertion (lanes 1 and 2) or no insertion in *atlA* (lane 3). (**C**), analysis of the same clones as in (**B**) with oligonucleotides AtlA_FW and T7. Only clones in lanes 1 and 2 have a transposon inserted in *atlA* and give a positive PCR signal. Molecular weights in kbp are indicated on the left side of the gel.

The nucleotide sequences of the PCR products were aligned with the sequence of the inverted repeat of the transposon to identify the first base corresponding to the insertion site in the *atlA* (**Fig. 52A**). The sequence starting after the last IR nucleotide aligned with the *atlA* sequence to identify the exact position of the insertion (**Fig. 52B**). All the insertions that have been identified in *atlA* are summarized in (**Fig. 52C**). The insertion site of 23 additional *atlA* transposon mutants was not identified.

A

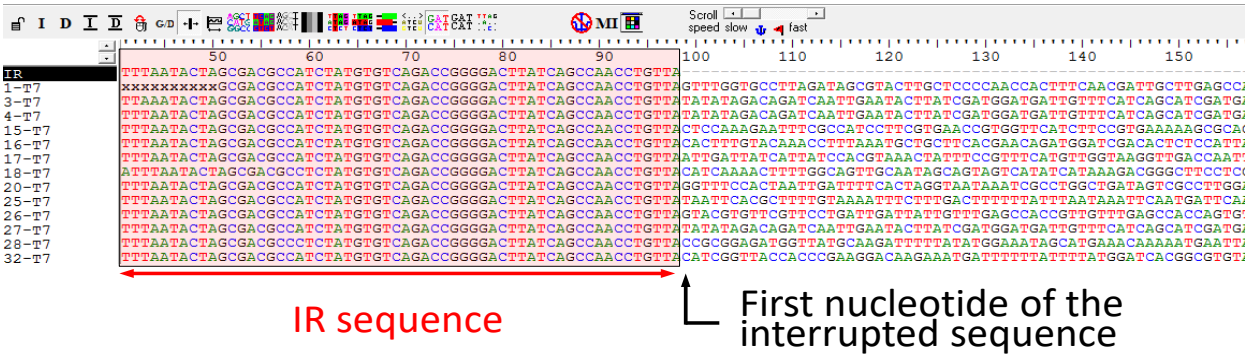

B

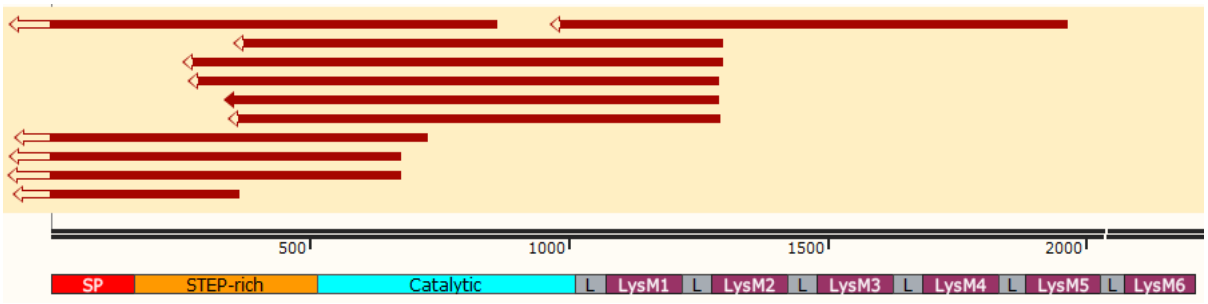

C

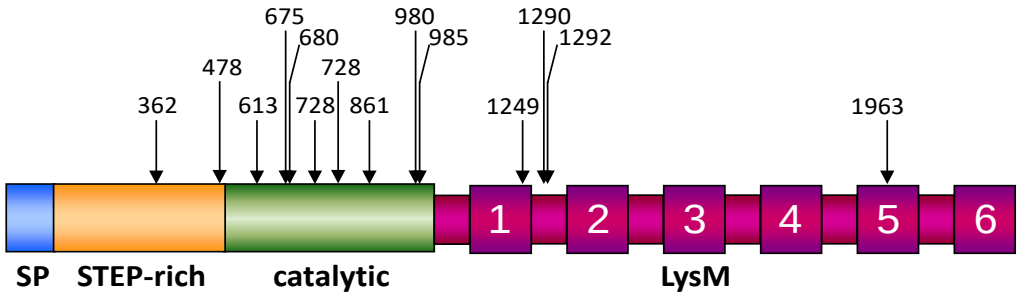

Figure 52. Identification transposition sites in *atlA*. Nucleotide sequences of the PCR products amplified with oligos T7 and AtlA_FW were aligned with the inverted repeat sequence of the transposon to identify the first base corresponding to the insertion site. (**A**), Alignment of the sequences starting after the inverted repeat sequences were aligned to the *atlA* sequence to identify precisely the insertion site. (**B**), Alignment of the sequences starting after the IR with the *atlA* ORF. The plain arrows indicate sequences identical to the *atlA* reference gene. (**C**), Summary of the transposon insertion sites mapped in the *atlA* gene. 23 other atlA mutants were not mapped.

3.2.3.2. Identification of insertion sites on the *E. faecalis* chromosome

Transposition sites on the chromosome have been mapped using a reverse PCR strategy described in (**Fig. 53A**). The chromosomal DNA was extracted from each mutant. Purified DNA was diluted to 4ng/µl and digested with SspI restriction endonuclease (New England Biolabs) which cleaves in the gentamycin resistance cassette and frequently in the chromosome (the genome contains 3600 SspI restriction sites).

Digested products were diluted to a concentration of 1ng/µl and self-ligated with T4 DNA ligase. PCR was carried out on 5µl of the ligation products using two divergent primers on the transposon (Mar_up, and Mar_dn). PCR products were gel extracted and sent for sequencing using the primer T7.

An example of PCR products is shown in (**Fig. 53B**). The genes that have been interrupted by a transposon insertion were identified using *E. faecalis* V583 genome as a reference sequence and using the blast software (http://blast.ncbi.nlm.nih.gov/Blast.cgi).

The results of the sequence analysis of the transposon mapping are described in (table 6).

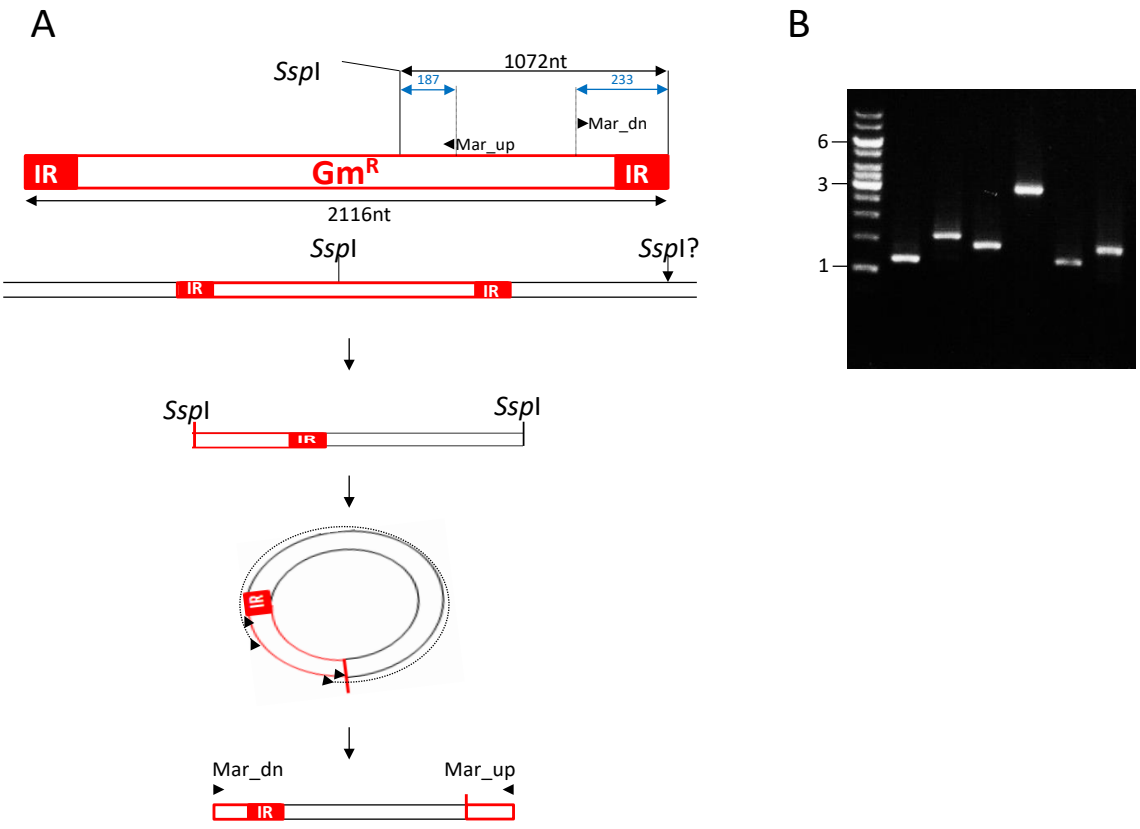

Figure 53. Strategy used to map the transposition sites by reverse PCR. (**A**), Chromosomal DNA was extracted, digested with SspI, self-ligated, used for a reverse PCR with oligos Mar_up, and Mar_dn. PCR products as shown in (**B**) were sent for sequencing with oligo T7. Molecular weights in kbp are indicated on the left side of the gel.

GENE ID[a] OG1RF	GENE ID[a] V583	Site of Insertion (nt)	Mutant ID	Gene
EF_10017	**EF_0018**	700 1239	32 94	sigma-54 factor interaction domain-containing protein
EF_10019	**EF_0020**	809	13, 108 & 109 [b]	PTS system mannose-specific transporter subunit IIAB
EF_10506	**EF_0773**	195	3, 4, 19, 27, 37, 39, 41, 42, 43, 44, 45, 46, 48, 49, 50, 51,53, 55, 56, 58, 59, 60, 69, 71,72,73, 75,77,78, 80, 81, 82, 84, 92, 93, 96, 98, 100,101, 101, 105, 106 and 107	*admA*
EF_10533	**EF_0799**	362 613 675 680 478 787 728 861 980 985 1249 1290 1292 1963 NI	33, 67 6 7 1 74 5 14, 40, 66, 11, 57 47, 64, 30 76 8, 22, 26, 29, 34, 36, 38, 31, 35, 12 21,33, 34, 35, 36, 38, 40, 47, 52, 64, 66,70, 74, 79, 83, 85, 90, 95, 97, 99, 103 & 104	*atlA*
EF_10679	**EF_0954**	325 508	18 17	Sugar-binding transcriptional regulator, LacI family
EF_12044	**EF_2674**	677	16	Oligoendopeptidase F
EF_12423	**EF_3156**	104	20	GntR transcriptional regulator
NI	**NI**	NI	63,65,86,87,89,91	No PCR product
NI	**NI**	NI	15, 28, 61, 62, 68, 88	No sequence data

Table 6. Description all transposon mutants identified. NI: Not identified.

[a] Gene ID relates to the annotated *E. faecalis* V583 genome, the corresponding OG1RF gene names are also labelled

[b] These mutants present a bigger halo, indicating an increased AtlA activity.

Transposon insertions in seven different loci were identified:

- ***EF_0018*** encodes a 962 amino acid protein annotated as a sigma-54 factor interaction domain-containing protein. ***EF_0018*** (***MptR***) is a putative σ^{54} (*rpoN*)-associated activator (Hechard et al., 2001). It has been shown that *EF_0018* is required for sensitivity to mesenterin Y105, a class IIa pore-forming bacteriocin (Abee et al., 1995) but the mechanism of this resistance is unknown. Transposon insertion in *EF_0018* is associated with a lack of AtlA activity.
- ***EF_0020*** encodes a 331 amino acid protein corresponding to the subunit IIA from a phosphotransferase system (PTS) specific for mannose. This gene is located downstream of *EF_0018* and has been proposed to be under the transcriptional control of *EF_0018*. Interestingly, the transposon insertion in *EF_0020* leads to an increased AtlA activity. Given that *EF_0018* inactivation is associated with a decrease in AtlA activity, this suggests that EF_0018 is a repressing the expression of *EF_0020*.
- ***EF_0773*** (*admA*) encodes a 172 residues protein containing no obvious homology to any known domain in the Pfam database. AdmA contains a putative membrane anchor consisting of 22 hydrophobic amino acids predicted by the TMHMM server (**Fig. 54**).

```
# EF0773 Length: 172
# EF0773 Number of predicted TMHs:  1
# EF0773 Exp number of AAs in TMHs: 22.69417
# EF0773 Exp number, first 60 AAs:  22.65698
# EF0773 Total prob of N-in:        0.16851
# EF0773 POSSIBLE N-term signal sequence
EF0773  TMHMM2.0        outside      1     3
EF0773  TMHMM2.0        TMhelix      4    26
EF0773  TMHMM2.0        inside      27   172
```

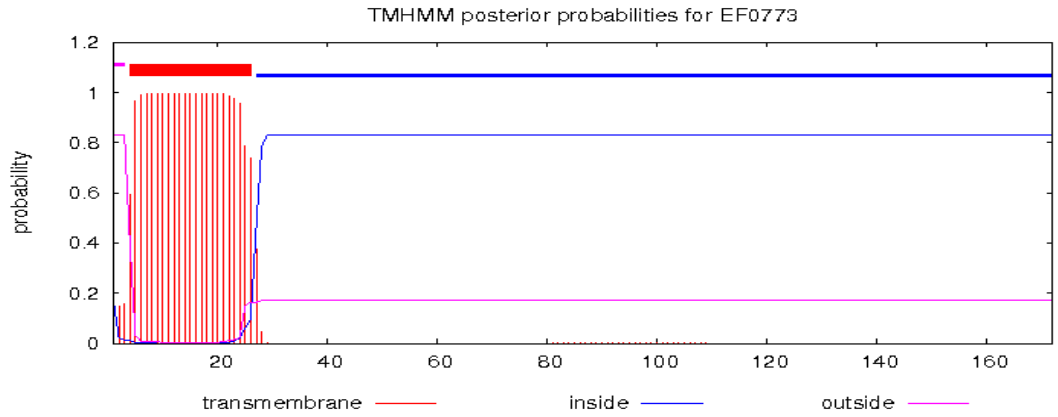


```
MFVFIAGMVG VIVGALIVTA SAALHSSYKE RKEVRYRELE HLVKEIESLN LLNKKVKEIL  60
QKRELYIDRS IEYLSMDDCF ISIDDFIYLE SFSAQNNFYL PTYLIEEFFK KIAHRKVILT 120
ASEVAEMGGH TYKGGRVILE NFSDEILAIIEDKKRKMQRL SNEPLHYFKA IK          172
```

Figure 54. Topology prediction of AdmA protein. The TMHMM Server v. 2.0 (http://www.cbs.dtu.dk/services/TMHMM/) was used to predict transmembrane helices which appear in red in the diagram shown above.

Although there is a canonical signal peptidase cleavage site after residue 22 (ASA↓A), the lack of a charged tail suggests that AdmA is not a secreted protein, but instead a cytoplasmic protein anchored on the membrane. AdmA homologs are found in *E. faecalis, E. gallinarum, E. italicus, E. faecium, E. casseliflavus* and other bacteria of the genus *Enterococcus* (identity ranging between 98 and 31%), in lactic bacteria such as *L. lactis* and in *L. garviae* (identity ranging between 84 and 82%) and in *Melissococcus plutonius* and *Tetragenococcus halophilus*. All strains carrying AdmA homolog thus belong to the *Enterococcaceae* family. A structural homology was detected between AdmA and a polysaccharide deacetylase of *Streptomyces coelicolor* using the Phyre server (**Fig. 55**). This server is predicting secondqry structures and matches them to a database of existing structures. Based on the similarities, a predicted 3D structure is generated.

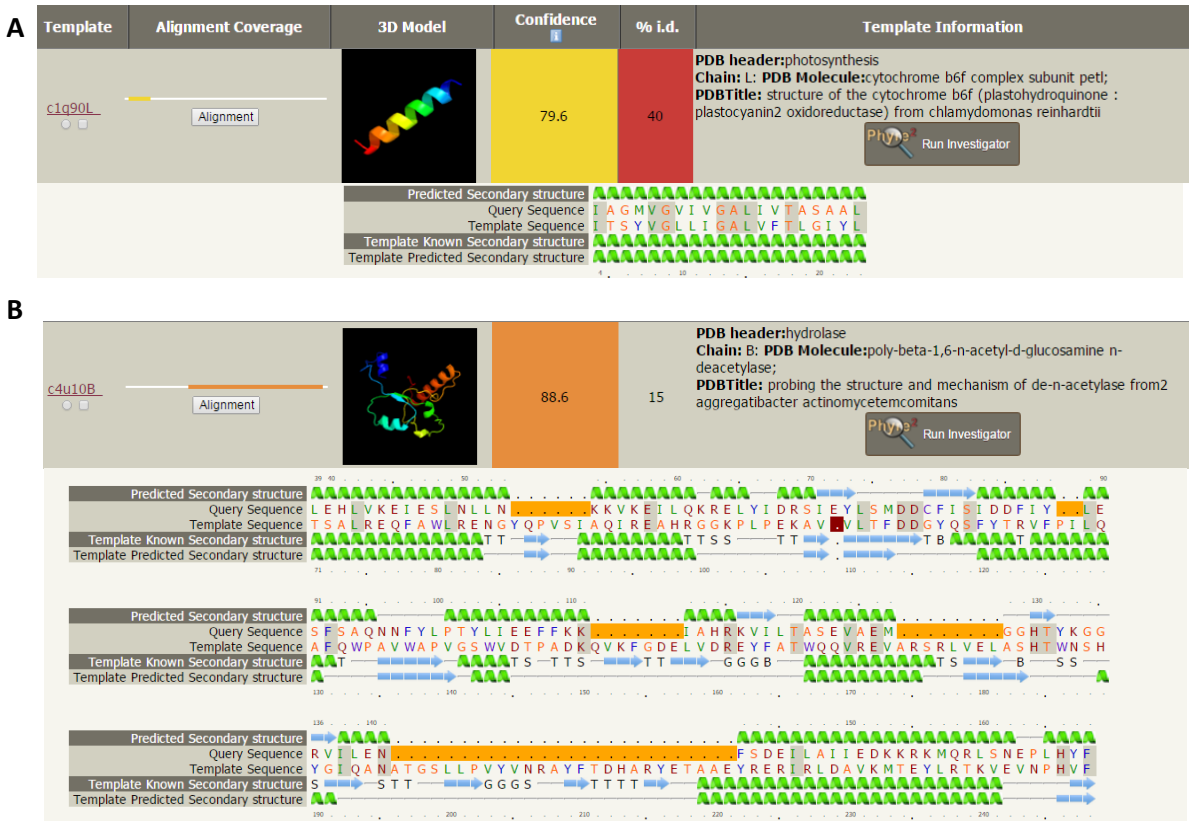

Figure 55. Structure prediction of the AdmA protein. The Phyre2 Server (http://www.sbg.bio.ic.ac.uk/phyre2/html/) was used to predict the 3D structure of AdmA based on secondary structure homologies with proteins in the PDB database. (**A**), Structure prediction and secondary structures of residues 5 to 24 of AdmA compared to the transmembrane domain of cytochrome b6. (**B**), structure prediction of residues 39-168 and comparison with the secondary structure of *E. coli* β-1,6 *N*-acetylglucosaminidase.

- ***EF_0954*** encodes a 337 residues protein with homology to a transcriptional regulator from the LacI family (Le Breton et al., 2005). This gene is located downstream of a putative operon involved in the metabolism of galactose, a carbohydrate present in *E. faecalis* cell wall-associated polymers (Hancock and Gilmore, 2002).
- ***EF_2674*** encodes a 604 amino acid-long protein homologous to oligoendopeptidases from *L. lactis* (Nardi et al., 1997). This gene is located upstream of a set of genes with unknown functions and downstream of genes involved in competence. The impact of the transposon insertion in *EF_2674* on AtlA activity remains unclear.
- ***EF_3156*** encodes a 238 amino acid-long protein with homology to transcription factors belonging to the GntR family. EF_3156 has a DNA-binding helix-turn-helix domain at its N-terminus and an effector-binding or oligomerisation domain at the C-terminus. *EF3156* is located in a region of the chromosome containing genes related to carbohydrate metabolism. It is therefore tempting to assume that this gene controls the expression of genes involved in the production of surface polysaccharides which have been shown to modulate the activity of PG hydrolases (Emirian et al., 2009).

3.2.4. Discussion

In this chapter, we report the construction and screening of transposon libraries to identify mutants with reduced or abolished AtlA surface activity on agar plates. Unlike the mutagenesis described in chapter 3.1., the parental strain used here had a wild-type AtlA activity. Several mutants distinct from the ones previously described were identified.

pZXL5 as a transposon mutagenesis system in *E. faecalis*

The transposon mutagenesis system we used was originally described in *E. faecium* (Zhang et al., 2012a). This work showed that it also works in *E. faecalis*. However, our preliminary attempts using JH2-2 as a recipient strain suggested that the transposition efficiency in this strain is relatively low since a large proportion of gentamycin resistant clones (>30%) was also resistant to chloramphenicol, indicating that the whole plasmid was integrated on the chromosome. As we finished our first mutagenesis attempt in JH2-2, we had some feedback from colleagues who also tried unsuccessfully to construct a library in the same genetic background (A. Benachour, personal communication).

We therefore decided to use *E. faecalis* OG1RF instead. To limit the isolation of identical mutants resulting from clonal expansion, we built three independent libraries that were successively screened to identify AtlA-deficient mutants numbered from 1 to 106. The *admA* transposon mutant was largely overrepresented and isolated more than 40 times (across all three libraries). Given the multitude and variety of mutations isolated in *atlA*, it is tempting to think that finding the same mutant over and over was more reflecting its key role in the control of AtlA activity rather than a low quality library. It could also indicate a better fitness.

AtlA is essential for *M. luteus* hydrolysis

Most of the mutants (14 out of 22) had insertions in the gene encoding *atlA*. This probably reflects the fact that abolishing the production of AtlA gives a complete lack of halo around colonies, which is easier to detect on the plates. In agreement with this hypothesis, virtually all the *atlA* insertion mutants are located in the first half of the gene where a gene interruption is likely to completely abolish the enzymatic activity. Although insertion of the transposon towards the end of the gene (after the second LysM module) could potentially reduce the activity of AtlA, none of these events were identified. The gene encoding AtlA is also relatively large (2.3 kbp), hence increasing the probability of transposon insertions in it.

AtlA-deficient mutants harbouring a transposon insertion in *admA* (*EF_0773* in V583) were identified. This confirmed our previous results from the screen of spontaneous mutants that led to the isolation of an *admA* mutant forming longer chains than the parental strain (table 6).

Transcriptional control of carbohydrate metabolism modulate AtlA activity

Three genes required for AtlA activity were related to sugar metabolism indicating that carbohydrate metabolism modulates AtlA activity or expression. Two genes (*EF_0018* and *EF_0954*) are transcriptional regulators whilst the third (*EF_0020*) encodes a sugar transporter. *EF_0018* is a σ^{54}-interacting transcription factor that was shown to control the expression of EF_0020 in *E. faecalis* (Hechard et al., 2001). Mutations in *E. faecalis*, σ^{54} were isolated in a screen to identify mutants with enhanced biofilm formation (Iyer and Hancock, 2012) and were associated with an altered biofilm composition. In particular, biofilms in σ^{54} mutants had a reduced content of extracellular DNA resulting from AtlA-mediated autolysis, clearly linking this transcriptional regulation network to AtlA activity (**Fig. 56**). The contribution of σ^{54} to the activity of EF_0954 is unknown.

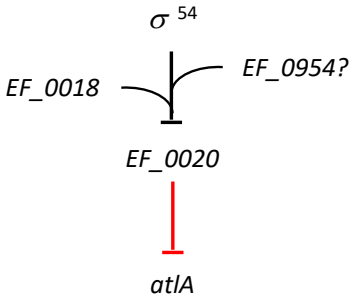

Figure 56. Proposed regulatory network modulating the activity of AtlA. *E. faecalis* σ^{54} is a master regulator of sugar metabolism. It negatively controls AtlA-mediated autolysis via *EF_0018*, which controls *EF_0020* expression (Hechard et al., 2001). The direct contribution of EF_0954 to EF_0020 transcriptional control is hypothetical. Black lines indicate transcriptional control, red lines post-transcriptional control.

Previous work indicated that in *Lactobacillus plantarum*, the σ^{54}-controlled mannose PTS system homologous to EF_0020 was capable of transporting glucose (Stevens et al., 2010). In *E. faecalis*, two surface polysaccharides, the capsule and Epa contain glucose and sugars derived from glucose (Hancock and Gilmore, 2002). Since OG1RF does not produce any capsule (Thurlow et al., 2009). One can assume that Epa composition is modulating AtlA activity. Further analyses are required to formally confirm this hypothesis. The identification of genes involved in sugar metabolism is in agreement with previous studies indicating that surface carbohydrates inhibit the enzymatic activity of AtlA *in vitro* (Emirian et al., 2009). The mechanism by which Epa inhibits AtlA activity is unknown, but by analogy with the work published in *S. aureus*, it is tempting to assume that steric hindrance prevents the binding of AtlA to its substrate (Schlag et al., 2010) at this stage, we do not know if the mutations identified have an impact on Epa structure, composition or abundance. Further experiments are also required to test if they alter AtlA binding to PG or AtlA enzymatic activity (or both).

<u>Two genes encoding an oligoendopeptidase and a transcriptional regulator potentially regulate AtlA activity</u>

Without further experiments, it is difficult to explain how the transposon insertions in the genes encoding an oligoendopeptidase and a transcriptional regulator from the Gntr family negatively control AtlA activity. Both genes are not part of operons so it is unlikely that the transposon insertion is causing any polar effect. It is possible that the peptidase plays a role in the cleavage of peptide stems in muropeptides to facilitate their recycling. The target of the Gntr regulator remains to be identified.

3.3. Functional analysis of the genes potentially modulating septum cleavage

3.3.1. In-frame deletion of the genes identified by transposon mutagenesis

To confirm that the genes identified are responsible for the chain forming phenotype observed, we chose a selection of genes to build in-frame deletion mutants. An *admA* mutant had already been built by S. Kulakauskas (INRA, Jouy en Josas, France) and was shown to have the same long-chain forming phenotype.

We focused on 3 other genes with a potential role in polysaccharide biosynthesis: *EF0018* and *EF0954*, identified in our screen and *EF0782* (*rpoN*) encoding σ^{54} and potentially required for the activity of EF_0018 and EF_0954. *EF0782* has been shown to have a role in the expression of a phosphotransferase system (PTS) involved in sugar transport. Although a *rpoN* mutant was not isolated during our screen, deletion of *EF0782* has been reported to lead to an increased resistance to autolysis (Iyer and Hancock, 2012). How RpoN affects AtlA activity remains unexplained.

The strategy was the same for all genes (**Fig. 57**). Two homology regions (named H1 and H2, 600 to 700 nucleotides each) were PCR amplified and fused together by PCR to create a deletion in the middle part of the candidate gene (**Fig. 57**). All PCR fragments corresponding to individual homology regions were successfully amplified (**Fig. 57A**) and fused (**Fig. 57B**). Several attempts were performed to clone these fragments in the thermosensitive plasmid pGhost9 either by Gibson assembly or conventional restriction cloning, but no positive clones were isolated (**Fig. 57C**).

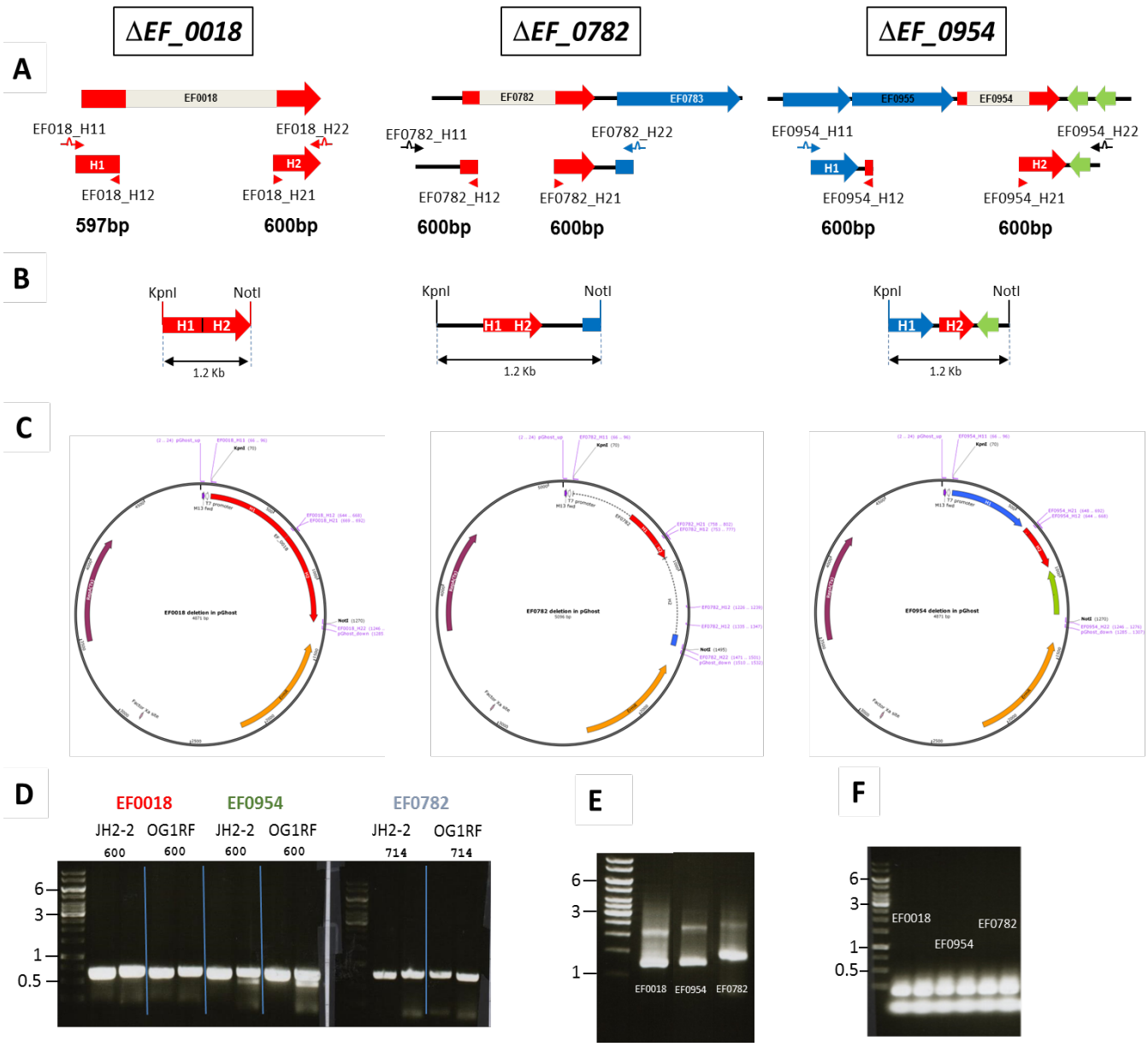

Figure 57. Summary of the construction strategy of in-frame deletion (**A),** PCR strategy to amplify and fuse of homology regions. **(B),** Schematic representation of the fused homology regions (*ca.* 600 nucleotides each). (**C),** Recombinant plasmids for gene replacement. (**D),** PCR products corresponding to homology regions H1 and H2. (**E**), PCR products corresponding to the fusion of H1 and H2 regions. (**F**), PCR screening of recombinant plasmids. Molecular weights in kbp are indicated on the left side of the gel.

3.3.2. Complementation experiments

To confirm that the transposon insertion is responsible for the phenotype observed in the mutants isolated, we undertook complementation experiments to restore the phenotype of the parental strains.

3.3.2.1. Construction of the complementation vectors for *EF_0018*, *EF_0954* and *EF_0782*

We first attempted to use plasmid pJEH11 (**Fig. 58A**), a shuttle expression vector that can replicate in both *E. coli* and *E. faecalis* (Bellais et al., 2006).

pJEH11 contains a constitutive promoter and ribosome binding site and allows the expression of open reading frames (ORF) cloned as NcoI-BamHI fragments. It contains both spectinomycin ($Spec^{R}$) and kanamycin (Km^{R}) resistance markers that are used for the selection of the plasmid. We focused on the genes that we tried to delete (*EF_0018, EF_0954* and (*EF_0782*) *rpoN* the gene encoding σ^{54}).

Bsal and BamHI restriction sites were introduced into the 5' and 3' ends of *EF0018* and NcoI and BamHI were introduced into the 5' and 3' ends of *EF0954 and EF0782* by PCR (**Fig. 58B**). PCR fragment (**Fig. 58C**) were purified and digested by NcoI and BamHI and cloned into pJEH11 similarly digested. Following transformation of *E. coli* with the ligation products, putative clones were screened by PCR but no positive clones could be identified could be (**Fig. 58D**).

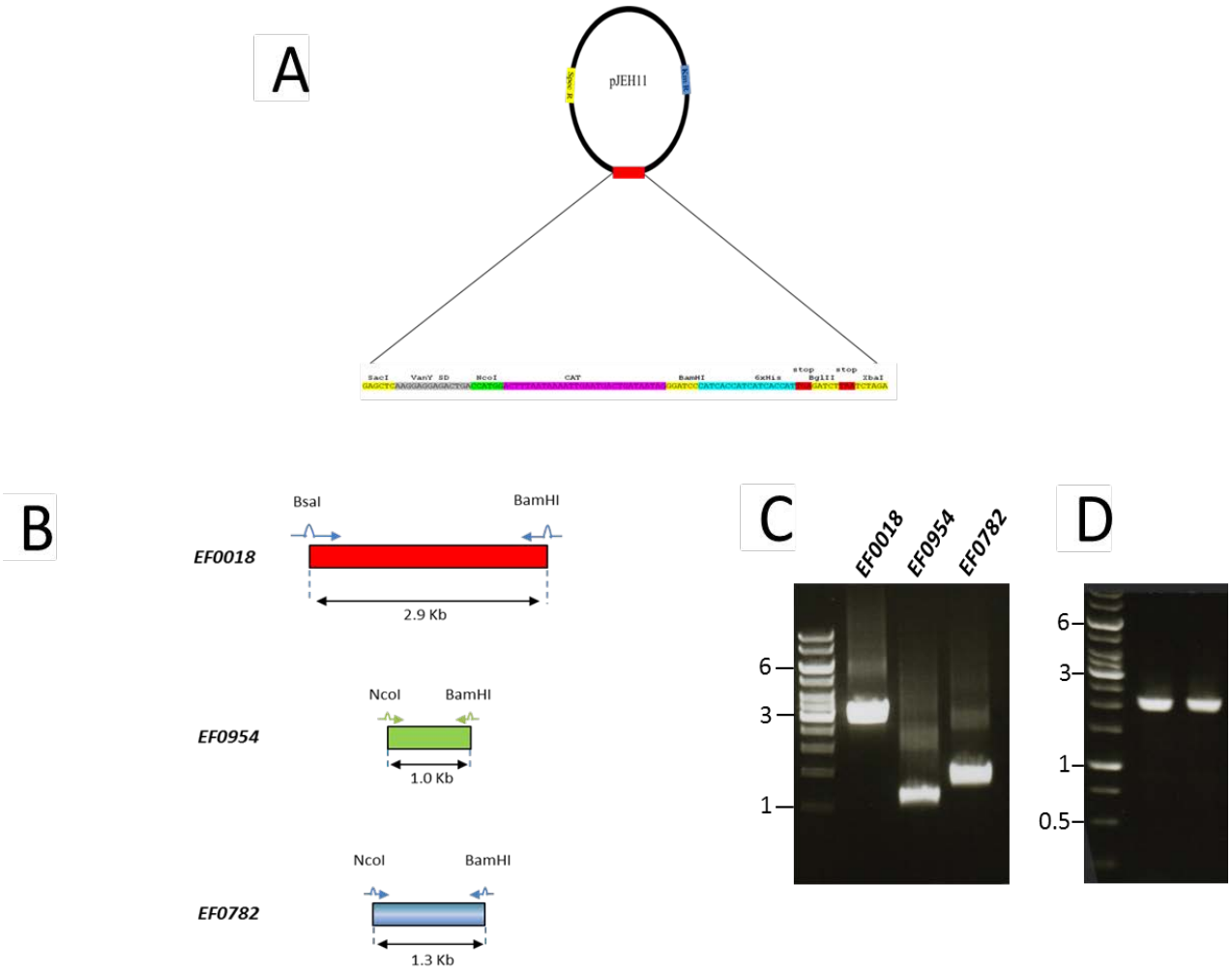

Figure 58. Strategy for complementation expressing using pJETH. (A): Map of the plasmid used for complementation pJEH11. **(B):** Description of PCR strategy used to introduce restriction sites followed by amplification ORF**. (C):** PCR products corresponding to ORF**. (D):** PCR screening of putative recombinant pJEH11 clones using plasmid specific oligos Molecular weights in kbp are indicated on the left side of the gel.

3.3.2.2. Construction of the complementation vectors for *secA*, *secY* and *atlA* mutants

While we tried to complement the mutations from the transposon screen, we also attempted to complement the spontaneous mutants identified in (chapter 3.1.) using an alternative strategy. This time, we used the shuttle plasmid pTetH recently constructed in the laboratory. This replicative plasmid is a pAT18 derivative (**Fig. 59**). It contains:

- A pAMβ1 origin of replication functional in *E. faecalis*;
- An oriR origin of replication functional in *E. coli*;
- A gene conferring resistance to Erythromycin in both *E. coli* and *E. faecalis;*

- A gene encoding the TetR repressor;
- A promoter containing two operator sequences recognised by the TetR repressor and induced in the presence of anhydrotetracycline;
- Two cloning sites (NcoI and BamHI) to clone an open reading frame fused to a 8-Histidine C-terminal tag.

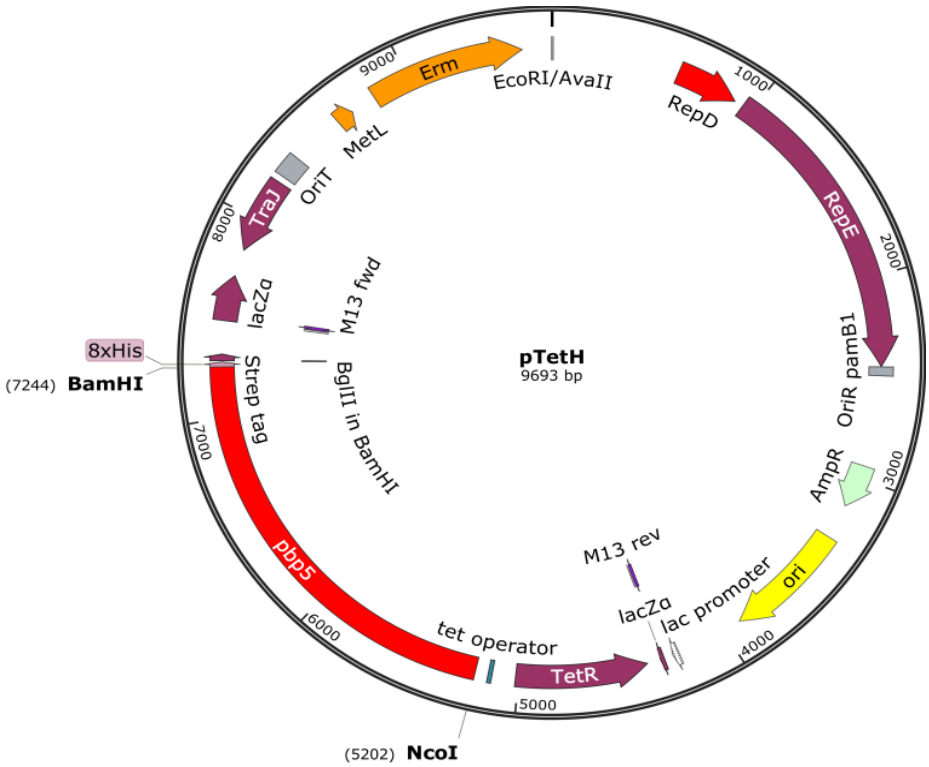

Figure 59. Map of plasmid pTetH used as an inducible system for complementation experiments. The genes of interest for complementation experiments are cloned between the NcoI and BamHI sites to replace the open reading frame encoding *E. faecalis* Pbp5.

The same cloning strategy (Gibson assembly) was applied for all target genes except for LysM, which is difficult to amplify by PCR due to the similarity of the binding modules. pTetH doubly digested by BamHI and NcoI (**Fig. 60A**) was used to clone the genes to complement. *atlA*, *secA* and *secY* alleles were amplified using oligonucleotides AtlA_G_Rev and AtlA_G_Fw, SecA_G_Fw and SecA_G_Rev, SecY_G_Fw and SecY_G_Rev, respectively (**Fig. 60B**). Gibson assembly products were transformed into *E. coli*. Colonies resistant to erythromycin were chosen to extract DNA plasmids that were analysed by restriction using two enzymes on either side of the insert (EcoRI + SphI). All pTetH recombinant could be obtained except the one encoding the *secA* R70H allele (**Fig. 60C**).

	Template	Allele(s) to complement[a]	Expected phenotype
secA			
WT	JH2-2	R70H / ΔE377 / R548H	Longer chains
R70H	98, 11	WT	Shorter chains
ΔE377	2, 18, 23, 25	WT	Shorter chains
R548H	4	WT	Shorter chains
secY			
WT	JH2-2	L337S	Longer chains
L337S	0	*atlA*_E212Q	Shorter chains
atlA			
WT	JH2-2	Δ*atlA*	Shorter chains
E212Q	*atlA*_E_{212}Q	WT / Δ*atlA*	Longer chains
LysM	JH2-2	WT / Δ*atlA*	Longer chains

Table 7. Summary of the complementation experiments.

[a] All point mutations to complement are in a JH2-2 *atlA*$_{E212Q}$-*gfp* background

The different steps of plasmid constructions are summarised in (**Fig. 60**). All pTetH derivatives had the expected sequence and could therefore be used to transform *E. faecalis*.

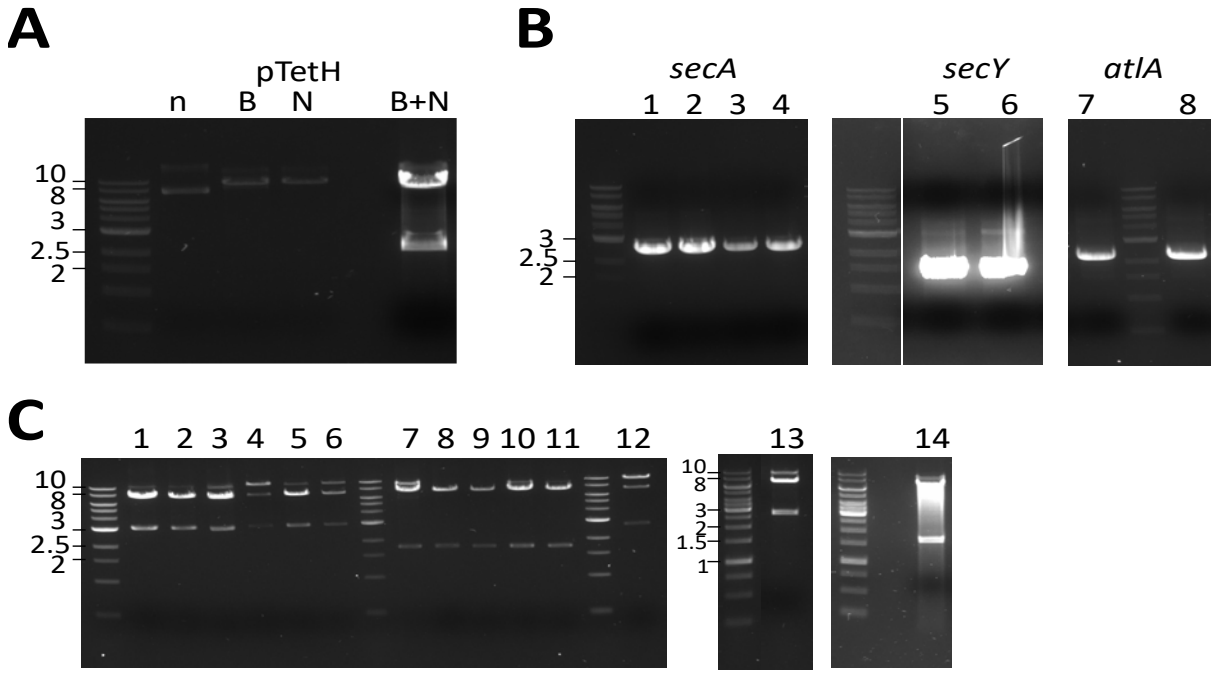

Figure 60. Construction of pTetH derivatives to complement the *atlA*, *secA* and *secY* mutants. (**A**), digestion of pTetH (n, native plasmid; B, BamHI; N, NcoI; B+N, BamHI + NcoI). (**B**), PCR amplification of *secA*, *secY* and *atlA* alleles used for Gibson assembly into pTetH digested by BamHI+NcoI: (1, *secA*_WT; 2, *secA*_R70H; 3, *secA*_ΔE377; 4, *secA*_R548H; 5, wild-type *secY*; 6, *secY*_L337S; 7, *atlA*_WT; 8, *atlA*_E212Q). (**C**), Restriction analysis of putative recombinant pTetH plasmids (1 and 2, pSecA_WT; 3 and 4, pSecA_ΔE377; 5 and 6, pSecA_R548H; 7, 8 and 9, pSecY_WT; 10 and 11, pSecY_L337S; 12, pAtlA_WT; 13, pAtlA_E212Q; 14, pAtlA_LysM). The *secA*_R70H allele could not be cloned. Molecular weights in kbp are indicated on the left side of the gel.

3.3.3. Analysis of the AdmA protein

To gain insights into the function of AdmA, we overexpressed the protein and purified it to determine its three dimensional structure using X-ray crystallography. The similarity to structures of proteins with known functions could suggest a function for AdmA.

3.3.3.1. Expression of the recombinant AdmA protein

The protein corresponding to residues 26 to 172 of AdmA was expressed as an N-terminally His-tagged protein in *E. coli*. A PCR product was amplified from chromosomal DNA using oligos introducing NcoI and BamHI sites at the 3' and 5' end of the fragment, respectively (**Fig. 61A**). The PCR product was digested by the two restriction enzymes and cloned into plasmid pET2817 similarly digested. After transformation of *E. coli*, most colonies screened by PCR with oligos on either side of the cloning site were positive (**Fig. 61B**). One of the colonies was chosen to extract the plasmid. Sequencing confirmed the absence of mutation.

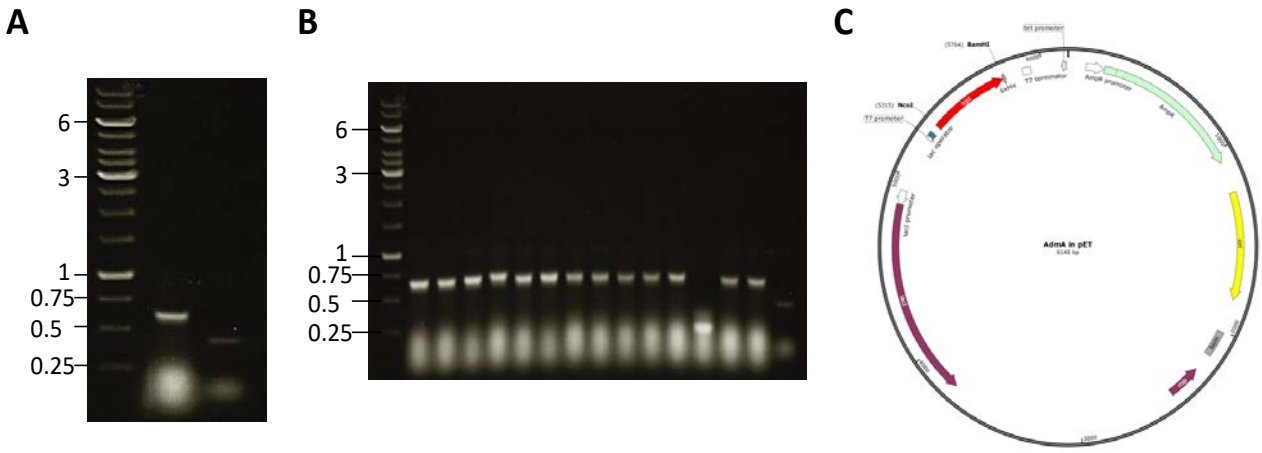

Figure 61. Construction of the pET2817 derivative for recombinant AdmA expression. (A) PCR product of the fragment encoding residues 26-172. **(B)**, PCR screening of putative recombinant pET2817 plasmsids using pET specific primers (pET_up and pET_dn). **(C)**, Map of the pET-2817 expressing AdmA. Molecular weights in kbp are indicated on the left side of the gel.

3.3.3.2. IMAC purification of the recombinant AdmA

AdmA overexpression was induced from a 1 L culture and expression of the protein was checked as described in sections 2.9.1 and 2.9.2. The soluble fraction was purified using 2 mL of Ni-Nta resin and the purification analysed by SDS-PAGE (**Fig. 62**).

Approximately 10 mL of protein at 3.2 mg/mL was recovered from this first purification step.

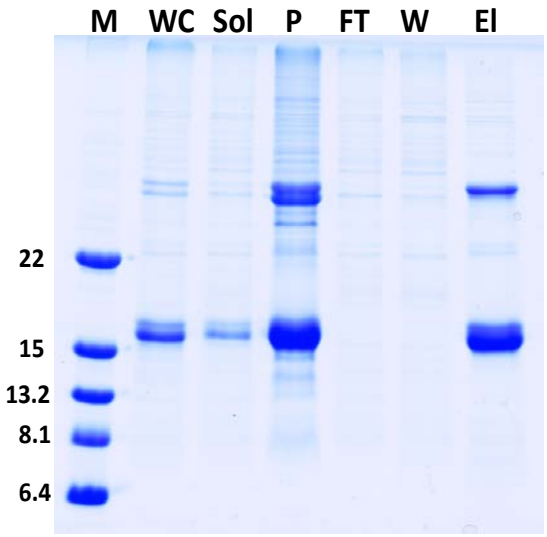

Figure 62. Overexpression of recombinant AdmA in *E. coli* and IMAC purification. The SDS-PAGE shows a comparison of crude extract (WC), soluble (Sol) and insoluble (P) fractions. After IMAC purification, the flow through (FT), wash (W) and eluted fractions (El) were loaded on a 15% SDS-PAGE. Molecular weights corresponding to the ladder are indicated in kDa on the left side The expected size of AdmA is around 17kDa. Molecular weights in kDa are indicated on the left side of the gel.

3.3.3.3. Size-exclusion purification of AdmA

The eluted fractions from IMAC were filtered, loaded onto a Superdex 75 26/60 colunm pre-equilibrated with buffer A (see 2.9.2) and eluted with an isocratic gradient at 3 mL/min (**Fig. 63**). Six fractions 3 mL each corresponding to 14.5mg of protein were pooled and concentrated to 6 mg/mL on a 10kDa Amicon unit (Fisher Scientific). The concentrated protein was sent to Dr Avinash Punekar (Warwick University) for crystallogenesis.

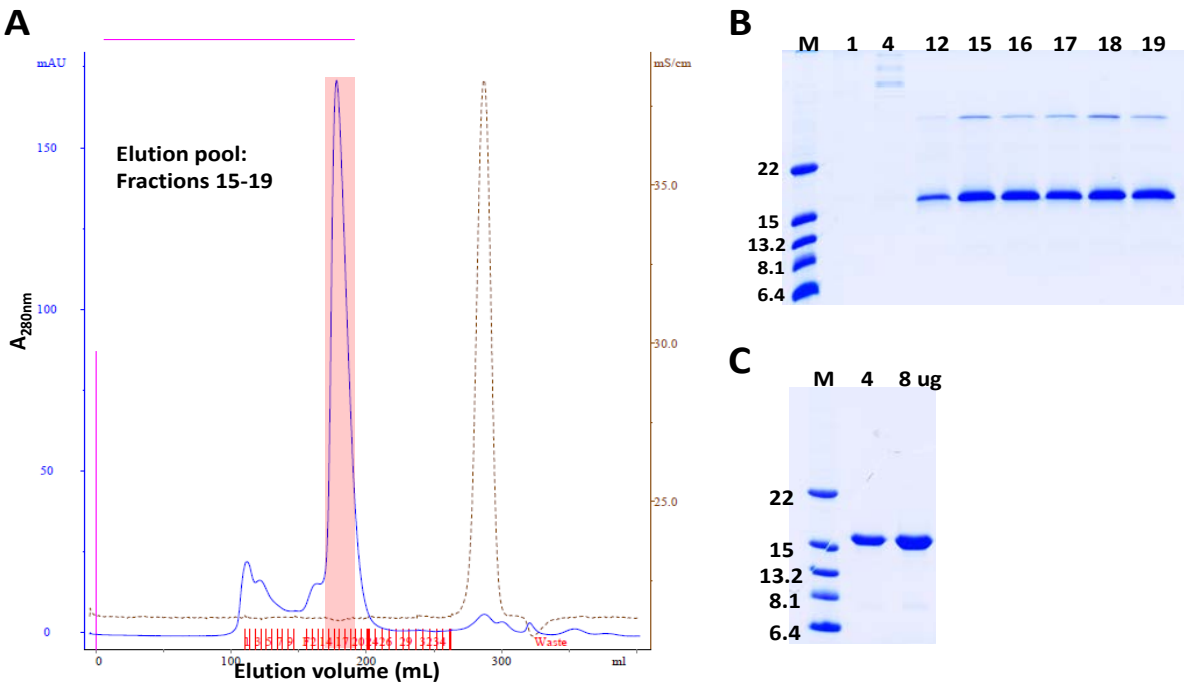

Figure 63. Size-exclusion purification of AdmA. (**A**), chromatogram of size-exclusion chromatography Fractions 15 to 19 (in red) were pooled. (**B**), an aliquot of each individual fraction were resuspended in loading buffer without reducing agent and 5 µg were loaded on a 15% SDS-PAGE . Fractions 15 to 19 revealed the presence of two band of 17 and 35 kDa. (**C**), an aliquot of the pool corresponding to fractions 15 to 19 was resuspended in loading buffer containing 50 mM of DTT and 4 µg and 8 µg were loaded on a 15% SDS-PAGE. In reducing conditions, the higher molecular weight band disappeared, suggesting that it corresponds to an AdmA dimer. Molecular weights in kDa are indicated on the left side of the gel.

4. General discussion and future work

Bioinformatic analyses suggest that the *E. faecalis* genome encodes at least 2**1** putative PG hydrolases. Only one of them (AtlA) has autolytic properties (Qin et al., 1998). AtlA plays a key role during cell division as it is dedicated to septum cleavage to allow the separation of daughter cells (Mesnage et al., 2008). Recent work in the laboratory has shown that although AtlA activity is not essential, it is necessary for *E. faecalis* pathogenesis in the zebrafish model of infection (B. Salamaga and S. Mesnage, unpublished). Formation of long chains increases uptake by phagocytes which severely impairs the virulence of *E. faecalis*. Given the key role of AtlA during growth and division, its potential suicidal activity and its contribution to pathogenesis, we sought to explore the mechanisms controlling AtlA activity.

4.1. Two complementary strategies provide distinct insights into the mechanisms underpinning AtlA activity

We used two approaches to isolate either spontaneous or transposon mutants with altered AtlA activity. In both cases, mutants with septum cleavage defects had mutations in the *atlA* gene itself. Only one gene required for optimal septum cleavage (*admA*) was found using both methods. Unlike transposon mutagenesis, which allows the identification of loss-of-function mutations, spontaneous mutants mostly had single nucleotide polymorphism generating missense or nonsense mutations (amino acid substitutions and premature stop codons).

One mutation corresponded to a single amino acid deletion. Apart from *admA*, distinct sets of genes were identified using the two mutagenesis strategies. This result indicated that combining two types of screens expands the range of mutations identified and allowed identifying the contribution of essential genes such as *secY* and *secA* to the septum cleavage mechanism.

4.2. The control of AtlA activity involves a multitude of mechanisms, allowing both spatial and temporal control of activity

4.2.1. AtlA post-translational modifications modulate enzymatic activity

Recent data from the host laboratory indicate that the N-terminal domain of AtlA is the target of post-translational modifications: glycosylation and proteolytic cleavage by extracellular proteases (A. Jareño and S. Mesnage, unpublished).

The glycosylation occurring on the N-terminal region of AtlA exacerbates the inhibitory role of this domain, most likely by steric hindrance, preventing the catalytic site of the enzyme to access its substrate. Two major proteases are secreted by *E. faecalis*: the metalloprotease GelE and the serine protease SprE. In the absence of GelE, cells form longer cell chains (Waters et al., 2003), suggesting that this enzyme is capable of cleaving AtlA. GelE-mediated cleavage, likely to result in the truncation of the N-terminal domain, would ensure that the enzyme is only fully active once translocated at the cell surface where it will be able to cleave its substrate, peptidoglycan. Although mutations in GelE are expected to reduce the activity of AtlA, we did not identify any *gelE* mutant in our screens. It is also worth mentioning that several *E. faecalis* strains do not produce GelE (such JH2-2 that we used to isolate spontaneous mutants). It is tempting to assume that other proteases can cleave the N-terminal domains during growth. Whether the gene we identified annotated as an endopeptidase (see table 6) is involved in this process remain to be established.

4.2.2. AtlA targeting to the division site prevents septum cleavage by other PGHs

Most mutations suppressing the long chain phenotype of the strain expressing a catalytically inactive AtlA ($AtlA_{E212Q}$-GFP) are predicted to abolish AtlA production or PG binding. This result indicated that other PGHs are able to access the septum and to cleave it in the absence of AtlA. This has already been proposed for AtlB and AtlC, which have a weak septum cleavage activity that can only be detected in the absence of AtlA (Mesnage et al., 2008).

The reason why AtlA is so efficient at cleaving the septum awaits further analysis. Several possibilities (non-mutually exclusive) have to be considered: (i) AtlA could be produced in larger amounts; (ii) AtlA could bind peptidoglycan with a higher affinity than other PGHs; it is worth pointing out that the AtlA LysM domain has 6 imperfect repeats, whereas all other 11 *E. faecalis* LysM proteins have only one or two LysM repeats; (iii) AtlA is preferentially targeted to the septum; (iv) the structure of PG at the septum is preferentially recognised and cleaved by AtlA. In this case, both the PG binding activity of AtlA and its catalytic activity could be involved. Recent work suggests that in *E. coli*, the PG at the septum is enriched in denuded glycan chains generated by an amidase activity (Yahashiri et al., 2015). Interestingly, LysM domains bind to chitooligosaccharides ($GlcNAc_{5-6}$) more rapidly than they bind to PG fragments (Mesnage et al., 2014).

If *E. faecalis* PG is also enriched in denuded glycan chains, it is t possible that AtlA LysM domain will preferentially bind to this site. Whether glycan chains without a peptide stem are better substrates for the catalytic domain is currently being investigated in the laboratory.

4.2.3. *admA* is a novel gene required for the septum cleavage activity of AtlA

The host laboratory has shown that AtlA localisation is restricted to the septum (B. Salamaga and S. Mesnage, unpublished). Some of the results presented in this work provide some information on the mechanism underpinning this localisation, but also raise several questions. a*dmA* was identified independently in our two screens, strongly suggesting that this gene is a key player for AtlA optimal activity. A mutation in *admA* does not abolish the activity of AtlA but decreases the proportion of enzyme exposed at the cell surface. Zymogram analyses suggest a defect in translocation as indicated by an increased amount of pre-protein in crude extracts (**Fig. 44**).

Fluorescence microscopy confirmed that in the *admA* mutant, AtlA is sequestered inside the cell, either associated with the membrane or in the cytoplasm. How AdmA contributes to AtlA surface display is puzzling. A tempting hypothesis is that AdmA interacts directly with AtlA to recruit it at the septum where it is secreted. If this is the case, the septal localisation of AdmA itself at the septum remains to be elucidated. Another possibility is an indirect role of AdmA in AtlA subcellular localisation. Topological and structural predictions suggest that AdmA is a membrane-anchored cytoplasmic protein with polysaccharide *N*-deacetylase activity. In this case, two possible substrates can be proposed: AtlA itself, which is very likely to be modified by GlcNAc residues (Rolain et al., 2013) or the rhamnopolysaccharide Epa cytoplasmic precursors (not peptidoglycan, which does not contain any deacetylated sugars in *E. faecalis*). The first hypothesis implies that the de-acetylation of AtlA glycosyl residues is required for optimal secretion.

An expected consequence is that the lack of glycosylation should suppress the long chain phenotype of the *admA* mutant. The construction of the double *gtfAB admA* mutant could test this hypothesis. The second hypothesis (AdmA deacetylates Epa precursors) is difficult to connect to a mis-localisation of AtlA unless we imagine that LysM domains are recruited by GlcNAc residues from Epa precursors. In this case, one has to imagine that the synthesis of Epa, occurring at the septum is a key step to bring AtlA in the vicinity of the secretion apparatus, also preferentially located at the septum.

This model is plausible but very speculative. Several experiments to gain insights into the localisation of SecY, SecA or the Epa biosynthetic machinery would be required to further test this hypothesis.

4.2.4. Secretion of AtlA as a mechanism controlling its activity

Our phenotypic screen led to the identification of mutations in *secA* and *secY* associated with the formation of shorter cell chains. These mutations, clustering around the SecY channel entrance are reminiscent of the *prl* mutations described in *E coli secY*. *prl* mutations have been proposed to destabilise the closed state of the secretion channel or stabilize the open form, thus allowing secretion of proteins without prior binding to the signal peptide as a triggering event (Smith et al., 2005).

By analogy, it is tempting to assume that the mutants we isolated allow an increased secretion of surface proteins including some that contribute to cleave the septum. The identification of the proteins affected by the mutations identified remains to be identified. Another question that awaits further investigations is the mechanism of AtlA secretion. Unlike the *N*-acetylmuramidase AtlB which has a 21 residues-long signal peptide, AtlA secretion signal is unusually long (53 residues). Interestingly, such extended signal peptides (ESP) have only been reported in Gram-negative bacteria so far (Desvaux et al., 2007). It has been proposed that ESPs mediate post-translational translocation across the cytoplasmic membrane. Their presence severely delays inner membrane translocation, but the mechanism responsible for this delay is unclear. It has been proposed that they could adopt a particular conformation or mediate interactions with a cytoplasmic or inner membrane co-factor, prior to inner membrane translocation (Peterson et al., 2006). Slowing down the surface translocation of AtlA could create a temporal control of AtlA activity as this enzyme has to cleave the septum towards the end of cell division, once the septum is fully formed.

4.2.5. Impact of carbohydrate metabolism on AtlA activity

Several genes identified in our transposon mutant screen were involved in carbohydrate metabolism, suggesting that cell surface polymers have an impact on the activity of AtlA. The modification of PG associated-polysaccharides is expected to modulate AtlA activity by several potential mechanisms:

(i) steric hindrance that could prevent binding and/or catalytic activity; (ii) modification of the cell wall charge that could impair binding of the AtlA LysM domain or (iii) an indirect impact on AtlA resulting from inhibition/alterations in PG synthesis. It is tempting to assume that the regulatory network controlling carbohydrate metabolism is under the control of the master regulator σ^{54} (RpoN).

E. faecalis has been linked to the transcriptional control of PTS systems including *EF_0020* that we identified in our screen, via *EF_0018*. The link between RpoN and autolysis and the release of extracellular DNA has been clearly established (Iyer and Hancock, 2012). Surprisingly, although *rpoN* deletion inhibits autolysis, this mutation has no impact on AtlA activity detected by zymogram using *M. luteus* as a substrate (Iyer and Hancock, 2012). One possibility is that rpoN mutation has no impact on AtlA itself, but instead leads to modification of the cell wall properties . Zymogram experiments should be carried out using *rpoN* cells as a substrate to test this hypothesis.

4.3. Future experiments and perspectives

This study represents the first step towards understanding the regulation of AtlA-mediated septum cleavage. Due to time constraints, several key experiments could not be completed to confirm the impact of the mutations identified on AtlA activity. The priority will be to carry out complementation experiments using the plasmids already constructed towards the end of this work in the pTetH vector (for *atlA*, *secA* and *secY*); as for *admA*, a complementation vector has been provided by S. Kulakauskas (INRA, Jouy-en-Josas). pTetH derivatives also need to be constructed to confirm that the transposon insertions are responsible for the chain forming phenotypes observed. Once the complementation experiments have been carried out, we will have to answer the following questions:

- **How do surface carbohydrates modulate AtlA activity?**

A simple experiment will be to measure the activity of recombinant AtlA on mutant cell walls and PG. To do this, the specific activity of AtlA could be measured using a turbidity assay *in vitro*. A more relevant assay will be the septum cleavage assay that specifically measures the cleavage of septal PG by AtlA. The next step will be to establish the role of the genes identified in carbohydrate biosynthesis: do they alter the amount of surface polysaccharides produced by *E. faecalis* and/or their composition? This will involve the extraction of surface polysaccharides from WT and mutant strains and their analysis using NMR or gas chromatography.

- **How does AdmA contribute to the septal localization of AtlA?**

Recent experiments in the lab revealed that AtlA is no longer localised at the septum in the *admA* mutant, but instead found in the cytoplasm. As a first step, we need to test a direct interaction between AtlA and AdmA, which could directly recruit this autolysin to the septum. The access to purified enzyme (see paragraph 3.3.3.) will allow testing this hypothesis using biophysical methods such as microscale thermophoresis or isothermal calorimetry available in the department. If these results do not show any interaction between recombinant proteins, we will have to consider an indirect role of AdmA in AtlA localisation and we will therefore need to explore other possibilities. For example, we could try to identify AdmA partners that in turn could recruit AtlA directly. This could be achieved using co-purification experiments. Finally, based on the topology and structure predictions, we could also explore the contribution of AdmA in the production of surface polymers using the strategies mentioned above. Crystallisation trails are currently in process. Determining the structure of AdmA may provide insights into the role of this protein.

- **Does AtlA secretion contribute to the functional specialisation of this enzyme?**

We identified several *sec* mutations associated with a modification of the chain forming phenotype. At this stage, we do not know if these mutations alter the secretion of AtlA only, all secreted proteins except AtlA or all secreted proteins. To answer this question, we need to carry out proteomics experiments to compare the proteins secreted by the WT and mutant strains. We could compare surface proteins (using 8M urea to recover all non-covalently bound surface proteins) and secreted proteins in supernatants. Alternatively, we could use the pTetH derivative expressing a His-tagged AtlA to follow its secretion rate in WT and *sec* mutant genetic backgrounds. The outcome of these experiments may provide information concerning the specific recognition of signal peptides from secreted proteins by the Sec machinery, a process poorly understood.

References

ABEE, T., KROCKEL, L. & HILL, C. 1995. Bacteriocins: modes of action and potentials in food preservation and control of food poisoning. *Int J Food Microbiol,* 28**,** 169-85.

ADLERBERTH, I. & WOLD, A. E. 2009. Establishment of the gut microbiota in Western infants. *Acta Paediatr,* 98**,** 229-38.

ARBELOA, A., SEGAL, H., HUGONNET, J. E., JOSSEAUME, N., DUBOST, L., BROUARD, J. P., GUTMANN, L., MENGIN-LECREULX, D. & ARTHUR, M. 2004. Role of class A penicillin-binding proteins in PBP5-mediated beta-lactam resistance in *Enterococcus faecalis*. *J Bacteriol,* 186**,** 1221-8.

ARSENE, S. & LECLERCQ, R. 2007. Role of a qnr-like gene in the intrinsic resistance of *Enterococcus faecalis* to fluoroquinolones. *Antimicrob Agents Chemother,* 51**,** 3254-8.

ATRIH, A., BACHER, G., ALLMAIER, G., WILLIAMSON, M. P. & FOSTER, S. J. 1999. Analysis of peptidoglycan structure from vegetative cells of *Bacillus subtilis* 168 and role of PBP 5 in peptidoglycan maturation. *J Bacteriol,* 181**,** 3956-66.

ATRIH, A., ZOLLNER, P., ALLMAIER, G. & FOSTER, S. J. 1996. Structural analysis of *Bacillus subtilis* 168 endospore peptidoglycan and its role during differentiation. *J Bacteriol,* 178**,** 6173-83.

BABA, T. & SCHNEEWIND, O. 1996. Target cell specificity of a bacteriocin molecule: a C-terminal signal directs lysostaphin to the cell wall of *Staphylococcus aureus*. *EMBO J,* 15**,** 4789-97.

BARRETEAU, H., KOVAC, A., BONIFACE, A., SOVA, M., GOBEC, S. & BLANOT, D. 2008. Cytoplasmic steps of peptidoglycan biosynthesis. *FEMS Microbiol Rev,* 32**,** 168-207.

BARTHE, P., MUKAMOLOVA, G. V., ROUMESTAND, C. & COHEN-GONSAUD, M. 2010. The structure of PknB extracellular PASTA domain from *mycobacterium tuberculosis* suggests a ligand-dependent kinase activation. *Structure,* 18**,** 606-15.

BATEMAN, A. & BYCROFT, M. 2000. The structure of a LysM domain from *E. coli* membrane-bound lytic murein transglycosylase D (MltD). *J Mol Biol,* 299**,** 1113-9.

BEEBY, M., GUMBART, J. C., ROUX, B. & JENSEN, G. J. 2013. Architecture and assembly of the Gram-positive cell wall. *Mol Microbiol,* 88**,** 664-72.

BELLAIS, S., ARTHUR, M., DUBOST, L., HUGONNET, J. E., GUTMANN, L., VAN HEIJENOORT, J., LEGRAND, R., BROUARD, J. P., RICE, L. & MAINARDI, J. L. 2006. Aslfm, the D-aspartate ligase responsible for the addition of D-aspartic acid onto the peptidoglycan precursor of *Enterococcus faecium*. *J Biol Chem,* 281**,** 11586-94.

BENACHOUR, A., LADJOUZI, R., LE JEUNE, A., HEBERT, L., THORPE, S., COURTIN, P., CHAPOT-CHARTIER, M. P., PRAJSNAR, T. K., FOSTER, S. J. & MESNAGE, S. 2012. The lysozyme-induced peptidoglycan *N*-acetylglucosamine deacetylase PgdA (EF1843) is required for *Enterococcus faecalis* virulence. *J Bacteriol,* 194**,** 6066-73.

BENACHOUR, A., MULLER, C., DABROWSKI-COTON, M., LE BRETON, Y., GIARD, J. C., RINCE, A., AUFFRAY, Y. & HARTKE, A. 2005. The *Enterococcus faecalis* sigV protein is an extracytoplasmic function sigma factor contributing to survival following heat, acid, and ethanol treatments. *J Bacteriol,* 187**,** 1022-35.

BERA, A., HERBERT, S., JAKOB, A., VOLLMER, W. & GOTZ, F. 2005. Why are pathogenic staphylococci so lysozyme resistant? The peptidoglycan *O*-acetyltransferase OatA is the major determinant for lysozyme resistance of *Staphylococcus aureus*. *Mol Microbiol,* 55**,** 778-87.

BIERNE, H. & DRAMSI, S. 2012. Spatial positioning of cell wall-anchored virulence factors in Gram-positive bacteria. *Curr Opin Microbiol,* 15**,** 715-23.

BONAFEDE, M. E., CARIAS, L. L. & RICE, L. B. 1997. Enterococcal transposon Tn5384: evolution of a composite transposon through cointegration of enterococcal and staphylococcal plasmids. *Antimicrob Agents Chemother,* 41**,** 1854-8.

BONECA, I. G., DUSSURGET, O., CABANES, D., NAHORI, M. A., SOUSA, S., LECUIT, M., PSYLINAKIS, E., BOURIOTIS, V., HUGOT, J. P., GIOVANNINI, M., COYLE, A., BERTIN, J., NAMANE, A., ROUSSELLE, J. C., CAYET, N., PREVOST, M. C., BALLOY, V., CHIGNARD, M., PHILPOTT, D. J., COSSART, P. & GIRARDIN, S. E. 2007. A critical role for peptidoglycan *N*-deacetylation in Listeria evasion from the host innate immune system. *Proc Natl Acad Sci U S A,* 104**,** 997-1002.

BOSLEY, G. S., FACKLAM, R. R. & GROSSMAN, D. 1983. Rapid identification of *enterococci*. *J Clin Microbiol,* 18**,** 1275-7.

BOUHSS, A., JOSSEAUME, N., SEVERIN, A., TABEI, K., HUGONNET, J. E., SHLAES, D., MENGIN-LECREULX, D., VAN HEIJENOORT, J. & ARTHUR, M. 2002. Synthesis of the L-alanyl-L-alanine cross-bridge of *Enterococcus faecalis* peptidoglycan. *J Biol Chem,* 277**,** 45935-41.

BRINSTER, S., FURLAN, S. & SERROR, P. 2007a. C-terminal WxL domain mediates cell wall binding in *Enterococcus faecalis* and other gram-positive bacteria. *Journal of Bacteriology,* 189**,** 1244-1253.

BRINSTER, S., POSTERARO, B., BIERNE, H., ALBERTI, A., MAKHZAMI, S., SANGUINETTI, M. & SERROR, P. 2007b. Enterococcal leucine-rich repeat-containing protein involved in virulence and host inflammatory response. *Infect Immun,* 75**,** 4463-71.

BUGG, T. D. & WALSH, C. T. 1992. Intracellular steps of bacterial cell wall peptidoglycan biosynthesis: enzymology, antibiotics, and antibiotic resistance. *Nat Prod Rep,* 9**,** 199-215.

BUIST, G., KOK, J., LEENHOUTS, K. J., DABROWSKA, M., VENEMA, G. & HAANDRIKMAN, A. J. 1995. Molecular cloning and nucleotide sequence of the gene encoding the major peptidoglycan hydrolase of *Lactococcus lactis*, a muramidase needed for cell separation. *J Bacteriol,* 177**,** 1554-63.

BUIST, G., STEEN, A., KOK, J. & KUIPERS, O. P. 2008. LysM, a widely distributed protein motif for binding to (peptido)glycans. *Mol Microbiol,* 68**,** 838-47.

BYAPPANAHALLI, M. N., NEVERS, M. B., KORAJKIC, A., STALEY, Z. R. & HARWOOD, V. J. 2012. *Enterococci* in the environment. *Microbiol Mol Biol Rev,* 76**,** 685-706.

CALIOT, E., DRAMSI, S., CHAPOT-CHARTIER, M. P., COURTIN, P., KULAKAUSKAS, S., PECHOUX, C., TRIEU-CUOT, P. & MISTOU, M. Y. 2012. Role of the Group B antigen of *Streptococcus agalactiae*: a peptidoglycan-anchored polysaccharide involved in cell wall biogenesis. *PLoS Pathog,* 8**,** e1002756.

CANDELA, T. & FOUET, A. 2005. Bacillus anthracis CapD, belonging to the gamma-glutamyltranspeptidase family, is required for the covalent anchoring of capsule to peptidoglycan. *Mol Microbiol,* 57**,** 717-26.

CARBALLIDO-LOPEZ, R., FORMSTONE, A., LI, Y., EHRLICH, S. D., NOIROT, P. & ERRINGTON, J. 2006. Actin homolog MreBH governs cell morphogenesis by localization of the cell wall hydrolase LytE. *Dev Cell,* 11**,** 399-409.

CHAPOT-CHARTIER, M. P. & KULAKAUSKAS, S. 2014. Cell wall structure and function in lactic acid bacteria. *Microb Cell Fact,* 13 Suppl 1**,** S9.

CHUANG, O. N., SCHLIEVERT, P. M., WELLS, C. L., MANIAS, D. A., TRIPP, T. J. & DUNNY, G. M. 2009. Multiple functional domains of *Enterococcus faecalis* aggregation substance Asc10 contribute to endocarditis virulence. *Infect Immun,* 77**,** 539-48.

COBURN, P. S. & GILMORE, M. S. 2003. The *Enterococcus faecalis* cytolysin: a novel toxin active against eukaryotic and prokaryotic cells. *Cell Microbiol,* 5**,** 661-9.

COLEY, J., TARELLI, E., ARCHIBALD, A. R. & BADDILEY, J. 1978. The linkage between teichoic acid and peptidoglycan in bacterial cell walls. *FEBS Lett,* 88**,** 1-9.

COURVALIN, P. 2006. Vancomycin resistance in gram-positive cocci. *Clin Infect Dis,* 42 Suppl 1**,** S25-34.

DE LAS RIVAS, B., J. L. GARCı´A, R. LO´PEZ, AND P. GARCı´A. 2002. Purification and polar localization of pneumococcal LytB, a putative endo-*N*-acetylglucosaminidase: the chain-dispersing murein hydrolase. *J. Bacteriol,* 5000**,** 4988–5000.

DEN BLAAUWEN, T., DE PEDRO, M. A., NGUYEN-DISTECHE, M. & AYALA, J. A. 2008. Morphogenesis of rod-shaped sacculi. *FEMS Microbiol Rev,* 32**,** 321-44.

DENG, L., KASPER, D. L., KRICK, T. P. & WESSELS, M. R. 2000. Characterization of the linkage between the type III capsular polysaccharide and the bacterial cell wall of group B *Streptococcus*. *J Biol Chem,* 275**,** 7497-504.

DESVAUX, M., SCOTT-TUCKER, A., TURNER, S. M., COOPER, L. M., HUBER, D., NATARO, J. P. & HENDERSON, I. R. 2007. A conserved extended signal peptide region directs posttranslational protein translocation via a novel mechanism. *Microbiology,* 153**,** 59-70.

DORAN, T. I. & MATTINGLY, S. J. 1982. Association of type- and group-specific antigens with the cell wall of serotype III group B *streptococcus*. *Infect Immun,* 36**,** 1115-22.

DUBE, L., CAILLON, J., JACQUELINE, C., BUGNON, D., POTEL, G. & ASSERAY, N. 2012. The optimal aminoglycoside and its dosage for the treatment of severe *Enterococcus faecalis* infection. An experimental study in the rabbit endocarditis model. *Eur J Clin Microbiol Infect Dis,* 31**,** 2545-7.

DUEZ, C., ZORZI, W., SAPUNARIC, F., AMOROSO, A., THAMM, I. & COYETTE, J. 2001. The penicillin resistance of *Enterococcus faecalis* JH2-2r results from an overproduction of the low-affinity penicillin-binding protein PBP4 and does not involve a psr-like gene. *Microbiology,* 147**,** 2561-9.

DUNNY, G. M., BROWN, B. L. & CLEWELL, D. B. 1978. Induced cell aggregation and mating in *Streptococcus faecalis*: evidence for a bacterial sex pheromone. *Proc Natl Acad Sci U S A,* 75**,** 3479-83.

ECKERT, C., LECERF, M., DUBOST, L., ARTHUR, M. & MESNAGE, S. 2006. Functional analysis of AtlA, the major *N*-acetylglucosaminidase of *Enterococcus faecalis*. *J Bacteriol,* 188**,** 8513-9.

EMIRIAN, A., FROMENTIN, S., ECKERT, C., CHAU, F., DUBOST, L., DELEPIERRE, M., GUTMANN, L., ARTHUR, M. & MESNAGE, S. 2009. Impact of peptidoglycan O-acetylation on autolytic activities of the *Enterococcus faecalis N*-acetylglucosaminidase AtlA and *N*-acetylmuramidase AtlB. *FEBS Lett,* 583**,** 3033-8.

FACKLAM, R. R. 1973. Comparison of several laboratory media for presumptive identification of *enterococci* and group D *streptococci*. *Appl Microbiol,* 26**,** 138-45.

FACKLAM, R. R. & COLLINS, M. D. 1989. Identification of *Enterococcus* species isolated from human infections by a conventional test scheme. *J Clin Microbiol,* 27**,** 731-4.

FERTALLY, S. S. & FACKLAM, R. 1987. Comparison of physiologic tests used to identify non-beta-hemolytic aerococci, *enterococc*i, and *streptococci*. *J Clin Microbiol,* 25**,** 1845-50.

FRANKENBERG, L., BRUGNA, M. & HEDERSTEDT, L. 2002. *Enterococcus faecalis* Heme-Dependent Catalase. *Journal of Bacteriology,* 184**,** 6351-6356.

GALLOWAY-PENA, J. R., LIANG, X., SINGH, K. V., YADAV, P., CHANG, C., LA ROSA, S. L., SHELBURNE, S., TON-THAT, H., HOOK, M. & MURRAY, B. E. 2015. The identification and functional characterization of WxL proteins from *Enterococcus faecium* reveal surface proteins involved in extracellular matrix interactions. *J Bacteriol,* 197**,** 882-92.

GARCIA, E., LLULL, D., MUNOZ, R., MOLLERACH, M. & LOPEZ, R. 2000. Current trends in capsular polysaccharide biosynthesis of *Streptococcus pneumoniae*. *Res Microbiol,* 151**,** 429-35.

GARNIER, F., TAOURIT, S., GLASER, P., COURVALIN, P. & GALIMAND, M. 2000. Characterization of transposon Tn1549, conferring VanB-type resistance in *Enterococcus* spp. *Microbiology,* 146 (Pt 6)**,** 1481-9.

GEISS-LIEBISCH, S., ROOIJAKKERS, S. H., BECZALA, A., SANCHEZ-CARBALLO, P., KRUSZYNSKA, K., REPP, C., SAKINC, T., VINOGRADOV, E., HOLST, O., HUEBNER, J. & THEILACKER, C. 2012. Secondary cell wall polymers of *Enterococcus faecalis* are critical for resistance to complement activation via mannose-binding lectin. *J Biol Chem,* 287**,** 37769-77.

GORDON, E., MOUZ, N., DUEE, E. & DIDEBERG, O. 2000. The crystal structure of the penicillin-binding protein 2x from *Streptococcus pneumoniae* and its acyl-enzyme form: implication in drug resistance. *J Mol Biol,* 299**,** 477-85.

GORDON, M. H. 1905. A READY METHOD OF DIFFERENTIATING STREPTOCOCCI AND SOME RESULTS ALREADY OBTAINED BY ITS APPLICATION. *The Lancet,* 166**,** 1400-1403.

GUIRAL, S., MITCHELL, T. J., MARTIN, B. & CLAVERYS, J. P. 2005. Competence-programmed predation of noncompetent cells in the human pathogen *Streptococcus pneumoniae*: genetic requirements. *Proc Natl Acad Sci U S A,* 102**,** 8710-5.

GUTIERREZ, J., SMITH, R. & POGLIANO, K. 2010. SpoIID-mediated peptidoglycan degradation is required throughout engulfment during *Bacillus subtilis* sporulation. *J Bacteriol,* 192**,** 3174-86.

HALLER, C., BERTHOLD, M., WOBSER, D., KROPEC, A., LAURIOLA, M., SCHLENSAK, C. & HUEBNER, J. 2014. Cell-wall glycolipid mutations and their effects on virulence of *E. faecalis* in a rat model of infective endocarditis. *PLoS One,* 9**,** e91863.

HALLGREN, A., ABEDNAZARI, H., EKDAHL, C., HANBERGER, H., NILSSON, M., SAMUELSSON, A., SVENSSON, E. & NILSSON, L. E. 2001. Antimicrobial susceptibility patterns of *enterococci* in intensive care units in Sweden evaluated by different MIC breakpoint systems. *J Antimicrob Chemother,* 48**,** 53-62.

HANAHAN, D. 1983. Studies on transformation of *Escherichia coli* with plasmids. *J Mol Biol,* 166**,** 557-80.

HANCOCK, L. & PEREGO, M. 2002. Two-component signal transduction in *Enterococcus faecalis*. *J Bacteriol,* 184**,** 5819-25.

HANCOCK, L. E. & GILMORE, M. S. 2002. The capsular polysaccharide of *Enterococcus faecalis* and its relationship to other polysaccharides in the cell wall. *Proc Natl Acad Sci U S A,* 99**,** 1574-9.

HANCOCK, L. E., SHEPARD, B. D. & GILMORE, M. S. 2003. Molecular analysis of the *Enterococcus faecalis* serotype 2 polysaccharide determinant. *J Bacteriol,* 185**,** 4393-401.

HARDIE, J. M. & WHILEY, R. A. 1997. Classification and overview of the genera *Streptococcus* and *Enterococcus*. *Soc Appl Bacteriol Symp Ser,* 26**,** 1S-11S.

HARZ, H., BURGDORF, K. & HOLTJE, J. V. 1990. Isolation and separation of the glycan strands from murein of *Escherichia coli* by reversed-phase high-performance liquid chromatography. *Anal Biochem,* 190**,** 120-8.

HAYHURST, E. J., KAILAS, L., HOBBS, J. K. & FOSTER, S. J. 2008. Cell wall peptidoglycan architecture in *Bacillus subtilis*. *Proc Natl Acad Sci U S A,* 105**,** 14603-8.

HEBERT, L., COURTIN, P., TORELLI, R., SANGUINETTI, M., CHAPOT-CHARTIER, M. P., AUFFRAY, Y. & BENACHOUR, A. 2007. *Enterococcus faecalis* constitutes an unusual bacterial model in lysozyme resistance. *Infect Immun,* 75**,** 5390-8.

HECHARD, Y., PELLETIER, C., CENATIEMPO, Y. & FRERE, J. 2001. Analysis of sigma(54)-dependent genes in *Enterococcus faecalis*: a mannose PTS permease (EII(Man)) is involved in sensitivity to a bacteriocin, mesentericin Y105. *Microbiology,* 147**,** 1575-80.

HENDRICKX, A. P., WILLEMS, R. J., BONTEN, M. J. & VAN SCHAIK, W. 2009. LPxTG surface proteins of *enterococci*. *Trends Microbiol,* 17**,** 423-30.

HORSBURGH, G. J., ATRIH, A. & FOSTER, S. J. 2003. Characterization of LytH, a differentiation-associated peptidoglycan hydrolase of *Bacillus subtilis* involved in endospore cortex maturation. *J Bacteriol,* 185**,** 3813-20.

IYER, V. S. & HANCOCK, L. E. 2012. Deletion of sigma(54) (rpoN) alters the rate of autolysis and biofilm formation in *Enterococcus faecalis*. *J Bacteriol,* 194**,** 368-75.

IZUMI, E., DOMINGUES PIRES, P., BITTENCOURT DE MARQUES, E. & SUZART, S. 2005. Hemagglutinating and hemolytic activities of *Enterococcus faecalis* strains isolated from different human clinical sources. *Res Microbiol,* 156**,** 583-7.

JACOB, A. E. & HOBBS, S. J. 1974. Conjugal transfer of plasmid-borne multiple antibiotic resistance in *Streptococcus faecalis* var. *zymogenes*. *J Bacteriol,* 117**,** 360-72.

JOHNSON, J. W., FISHER, J. F. & MOBASHERY, S. 2013. Bacterial cell-wall recycling. *Ann N Y Acad Sci,* 1277**,** 54-75.

KAJIMURA, J., FUJIWARA, T., YAMADA, S., SUZAWA, Y., NISHIDA, T., OYAMADA, Y., HAYASHI, I., YAMAGISHI, J., KOMATSUZAWA, H. & SUGAI, M. 2005. Identification and molecular characterization of an *N*-acetylmuramyl-L-alanine amidase Sle1 involved in cell separation of *Staphylococcus aureus*. *Mol Microbiol,* 58**,** 1087-101.

KEEP, N. H., WARD, J. M., COHEN-GONSAUD, M. & HENDERSON, B. 2006. Wake up! Peptidoglycan lysis and bacterial non-growth states. *Trends Microbiol,* 14**,** 271-6.

KEMP, K. D., SINGH, K. V., NALLAPAREDDY, S. R. & MURRAY, B. E. 2007. Relative contributions of *Enterococcus faecalis* OG1RF sortase-encoding genes, srtA and bps (srtC), to biofilm formation and a murine model of urinary tract infection. *Infect Immun,* 75**,** 5399-404.

KLEIN, G. 2003. Taxonomy, ecology and antibiotic resistance of *enterococci* from food and the gastro-intestinal tract. *Int J Food Microbiol,* 88**,** 123-31.

KLINE, K. A., KAU, A. L., CHEN, S. L., LIM, A., PINKNER, J. S., ROSCH, J., NALLAPAREDDY, S. R., MURRAY, B. E., HENRIQUES-NORMARK, B., BEATTY, W., CAPARON, M. G. & HULTGREN, S. J. 2009. Mechanism for sortase localization and the role of sortase localization in efficient pilus assembly in *Enterococcus faecalis*. *J Bacteriol,* 191**,** 3237-47.

KRISTICH, C. J., NGUYEN, V. T., LE, T., BARNES, A. M., GRINDLE, S. & DUNNY, G. M. 2008. Development and use of an efficient system for random mariner transposon mutagenesis to identify novel genetic determinants of biofilm formation in the core *Enterococcus faecalis* genome. *Appl Environ Microbiol,* 74**,** 3377-86.

LANCEFIELD, R. C. 1933. A Serological Differentiation of Human and Other Groups of Hemolytic *Streptococci*. *J Exp Med,* 57**,** 571-95.

LAYEC, S., GERARD, J., LEGUE, V., CHAPOT-CHARTIER, M. P., COURTIN, P., BORGES, F., DECARIS, B. & LEBLOND-BOURGET, N. 2009. The CHAP domain of Cse functions as an endopeptidase that acts at mature septa to promote *Streptococcus thermophilus* cell separation. *Mol Microbiol,* 71**,** 1205-17.

LE BRETON, Y., PICHEREAU, V., SAUVAGEOT, N., AUFFRAY, Y. & RINCE, A. 2005. Maltose utilization in *Enterococcus faecalis*. *J Appl Microbiol,* 98**,** 806-13.

LEAVIS, H. L., BONTEN, M. J. & WILLEMS, R. J. 2006. Identification of high-risk *enterococca*l clonal complexes: global dispersion and antibiotic resistance. *Curr Opin Microbiol,* 9**,** 454-60.

LEBRETON, F., WILLEMS, R. J. L. & GILMORE, M. S. 2014. *Enterococcus* Diversity, Origins in Nature, and Gut Colonization.

LENZ, L. L., MOHAMMADI, S., GEISSLER, A. & PORTNOY, D. A. 2003. SecA2-dependent secretion of autolytic enzymes promotes *Listeria monocytogenes* pathogenesis. *Proc Natl Acad Sci U S A,* 100**,** 12432-7.

LEPAGE, E., BRINSTER, S., CARON, C., DUCROIX-CREPY, C., RIGOTTIER-GOIS, L., DUNNY, G., HENNEQUET-ANTIER, C. & SERROR, P. 2006. Comparative genomic hybridization analysis of *Enterococcus faecalis*: identification of genes absent from food strains. *J Bacteriol,* 188**,** 6858-68.

LI, H. 2013. Aligning sequence reads, clone sequences and assembly contigs with BWA-MEM. *arXiv preprint arXiv:1303.3997*.

LIPSKI, A., HERVE, M., LOMBARD, V., NURIZZO, D., MENGIN-LECREULX, D., BOURNE, Y. & VINCENT, F. 2015. Structural and biochemical characterization of the beta-*N*-acetylglucosaminidase from Thermotoga maritima: toward rationalization of mechanistic knowledge in the GH73 family. *Glycobiology,* 25**,** 319-30.

LOPEZ, R., GARCIA, E. & RONDA, C. 1981. Bacteriophages of *Streptococcus pneumoniae*. *Rev Infect Dis,* 3**,** 212-23.

LU, J. Z., FUJIWARA, T., KOMATSUZAWA, H., SUGAI, M. & SAKON, J. 2006. Cell wall-targeting domain of glycylglycine endopeptidase distinguishes among peptidoglycan cross-bridges. *J Biol Chem,* 281**,** 549-58.

MAEKAWA, S., YOSHIOKA, M. & KUMAMOTO, Y. 1992. Proposal of a new scheme for the serological typing of *Enterococcus faecalis* strains. *Microbiology and immunology*, 36**,** 671-681.

MARTIN, M. 2011. Cutadapt removes adapter sequences from high-throughput sequencing reads. *EMBnet. journal,* 17**,** pp. 10-12.

MATOS, R. C., LAPAQUE, N., RIGOTTIER-GOIS, L., DEBARBIEUX, L., MEYLHEUC, T., GONZALEZ-ZORN, B., REPOILA, F., LOPES MDE, F. & SERROR, P. 2013. *Enterococcus faecalis* prophage dynamics and contributions to pathogenic traits. *PLoS Genet,* 9**,** e1003539.

MCBRIDE, S. M., FISCHETTI, V. A., LEBLANC, D. J., MOELLERING, R. C., JR. & GILMORE, M. S. 2007. Genetic diversity among *Enterococcus faecalis*. *PLoS One,* 2**,** e582.

MEESKE, A. J., SHAM, L. T., KIMSEY, H., KOO, B. M., GROSS, C. A., BERNHARDT, T. G. & RUDNER, D. Z. 2015. MurJ and a novel lipid II flippase are required for cell wall biogenesis in *Bacillus subtilis*. *Proc Natl Acad Sci U S A,* 112**,** 6437-42.

MERCIER, C., DURRIEU, C., BRIANDET, R., DOMAKOVA, E., TREMBLAY, J., BUIST, G. & KULAKAUSKAS, S. 2002. Positive role of peptidoglycan breaks in *lactococcal* biofilm formation. *Mol Microbiol,* 46**,** 235-43.

MESNAGE, S., CHAU, F., DUBOST, L. & ARTHUR, M. 2008. Role of *N*-acetylglucosaminidase and *N*-acetylmuramidase activities in *Enterococcus faecalis* peptidoglycan metabolism. *J Biol Chem,* 283**,** 19845-53.

MESNAGE, S., DELLAROLE, M., BAXTER, N. J., ROUGET, J. B., DIMITROV, J. D., WANG, N., FUJIMOTO, Y., HOUNSLOW, A. M., LACROIX-DESMAZES, S., FUKASE, K., FOSTER, S. J. & WILLIAMSON, M. P. 2014. Molecular basis for bacterial peptidoglycan recognition by LysM domains. *Nat Commun,* 5**,** 4269.

MESNAGE, S., FONTAINE, T., MIGNOT, T., DELEPIERRE, M., MOCK, M. & FOUET, A. 2000. Bacterial SLH domain proteins are non-covalently anchored to the cell surface via a conserved mechanism involving wall polysaccharide pyruvylation. *EMBO J,* 19**,** 4473-84.

MIERAU, I. & KLEEREBEZEM, M. 2005. 10 years of the nisin-controlled gene expression system (NICE) in *Lactococcus lactis*. *Appl Microbiol Biotechnol,* 68**,** 705-17.

MIR, M., ASONG, J., LI, X., CARDOT, J., BOONS, G.-J. & HUSSON, R. N. 2011. The Extracytoplasmic Domain of the *Mycobacterium tuberculosis* Ser/Thr Kinase PknB Binds Specific Muropeptides and Is Required for PknB Localization. *PLoS Pathogens,* 7**,** e1002182.

MISTOU, M. Y., SUTCLIFFE, I. C. & VAN SORGE, N. M. 2016. Bacterial glycobiology: rhamnose-containing cell wall polysaccharides in Gram-positive bacteria. *FEMS Microbiol Rev,* 40**,** 464-79.

MOHAMMADI, T., VAN DAM, V., SIJBRANDI, R., VERNET, T., ZAPUN, A., BOUHSS, A., DIEPEVEEN-DE BRUIN, M., NGUYEN-DISTECHE, M., DE KRUIJFF, B. & BREUKINK, E. 2011. Identification of FtsW as a transporter of lipid-linked cell wall precursors across the membrane. *EMBO J,* 30**,** 1425-32.

MOIR, A. 2006. How do spores germinate? *J Appl Microbiol,* 101**,** 526-30.

MORLOT, C., NOIRCLERC-SAVOYE, M., ZAPUN, A., DIDEBERG, O. & VERNET, T. 2004. The D,D-carboxypeptidase PBP3 organizes the division process of *Streptococcus pneumoniae*. *Mol Microbiol,* 51**,** 1641-8.

MUKAMOLOVA, G. V., KAPRELYANTS, A. S., YOUNG, D. I., YOUNG, M. & KELL, D. B. 1998. A bacterial cytokine. *Proc Natl Acad Sci U S A,* 95**,** 8916-21.

MUNOZ-LOPEZ, M. & GARCIA-PEREZ, J. L. 2010. DNA transposons: nature and applications in genomics. *Curr Genomics,* 11**,** 115-28.

MURRAY, B. E. 1990. The life and times of the *Enterococcus*. *Clin Microbiol Rev,* 3**,** 46-65.

MURRAY, B. E. & MEDERSKI-SAMAROJ, B. 1983. Transferable beta-lactamase. A new mechanism for in vitro penicillin resistance in *Streptococcus faecalis*. *J Clin Invest,* 72**,** 1168-71.

MURRAY, B. E., SINGH, K. V., ROSS, R. P., HEATH, J. D., DUNNY, G. M. & WEINSTOCK, G. M. 1993. Generation of restriction map of *Enterococcus faecalis* OG1 and investigation of growth requirements and regions encoding biosynthetic function, *J Bacteriol*. 1993 Aug;175(16):5216-23.

NALLAPAREDDY, S. R., SINGH, K. V., SILLANPAA, J., GARSIN, D. A., HOOK, M., ERLANDSEN, S. L. & MURRAY, B. E. 2006. Endocarditis and biofilm-associated pili of *Enterococcus faecalis*. *J Clin Invest,* 116**,** 2799-807.

NARDI, M., RENAULT, P. & MONNET, V. 1997. Duplication of the pepF gene and shuffling of DNA fragments on the lactose plasmid of *Lactococcus lactis*. *J Bacteriol,* 179**,** 4164-71.

NEUHAUS, F. C. & BADDILEY, J. 2003. A continuum of anionic charge: structures and functions of D-alanyl-teichoic acids in gram-positive bacteria. *Microbiol Mol Biol Rev,* 67**,** 686-723.

NIVEN, C. F. & SHERMAN, J. M. 1944. Nutrition of the *Enterococci*. *J Bacteriol,* 47**,** 335-42.

OHNUMA, T., ONAGA, S., MURATA, K., TAIRA, T. & KATOH, E. 2008. LysM domains from Pteris ryukyuensis chitinase-A: a stability study and characterization of the chitin-binding site. *J Biol Chem,* 283**,** 5178-87.

PALMER, K. L., GODFREY, P., GRIGGS, A., KOS, V. N., ZUCKER, J., DESJARDINS, C., CERQUEIRA, G., GEVERS, D., WALKER, S., WORTMAN, J., FELDGARDEN, M., HAAS, B., BIRREN, B. & GILMORE, M. S. 2012. Comparative genomics of enterococci: variation in *Enterococcus faecalis*, clade structure in *E. faecium*, and defining characteristics of *E. gallinarum* and *E. casseliflavus*. *MBio,* 3**,** e00318-11.

PARACUELLOS, P., BALLANDRAS, A., ROBERT, X., KAHN, R., HERVE, M., MENGIN-LECREULX, D., COZZONE, A. J., DUCLOS, B. & GOUET, P. 2010. The extended conformation of the 2.9-A crystal structure of the three-PASTA domain of a Ser/Thr kinase from the human pathogen *Staphylococcus aureus*. *J Mol Biol,* 404**,** 847-58.

PAULSEN, I. T., BANERJEI, L., MYERS, G. S., NELSON, K. E., SESHADRI, R., READ, T. D., FOUTS, D. E., EISEN, J. A., GILL, S. R., HEIDELBERG, J. F., TETTELIN, H., DODSON, R. J., UMAYAM, L., BRINKAC, L., BEANAN, M., DAUGHERTY, S., DEBOY, R. T., DURKIN, S., KOLONAY, J., MADUPU, R., NELSON, W., VAMATHEVAN, J., TRAN, B., UPTON, J., HANSEN, T., SHETTY, J., KHOURI, H., UTTERBACK, T., RADUNE, D., KETCHUM, K. A., DOUGHERTY, B. A. & FRASER, C. M. 2003. Role of mobile DNA in the evolution of vancomycin-resistant *Enterococcus faecalis*. *Science,* 299**,** 2071-4.

PAWSON, T. 1995. Protein modules and signalling networks. *Nature,* 373**,** 573-80.

PETERSON, J. H., SZABADY, R. L. & BERNSTEIN, H. D. 2006. An unusual signal peptide extension inhibits the binding of bacterial presecretory proteins to the signal recognition particle, trigger factor, and the SecYEG complex. *J Biol Chem,* 281**,** 9038-48.

POYART, C., LAMBERT, T., MORAND, P., ABASSADE, P., QUESNE, G., BAUDOUY, Y. & TRIEU-CUOT, P. 2002. Native valve endocarditis due to *Enterococcus hirae*. *J Clin Microbiol,* 40**,** 2689-90.

PRAJSNAR, T. K., RENSHAW, S. A., OGRYZKO, N. V., FOSTER, S. J., SERROR, P. & MESNAGE, S. 2013. Zebrafish as a novel vertebrate model to dissect *enterococcal* pathogenesis. *Infect Immun,* 81**,** 4271-9.

QIN, X., SINGH, K. V., XU, Y., WEINSTOCK, G. M. & MURRAY, B. E. 1998. Effect of disruption of a gene encoding an autolysin of *Enterococcus faecalis* OG1RF. *Antimicrob Agents Chemother,* 42**,** 2883-8.

RAMIREZ, M. S. & TOLMASKY, M. E. 2010. Aminoglycoside modifying enzymes. *Drug Resist Updat,* 13**,** 151-71.

RAU, A., HOGG, T., MARQUARDT, R. & HILGENFELD, R. 2001. A new lysozyme fold. Crystal structure of the muramidase from Streptomyces coelicolor at 1.65 A resolution. *J Biol Chem,* 276**,** 31994-9.

RAYMOND, J. B., MAHAPATRA, S., CRICK, D. C. & PAVELKA, M. S., JR. 2005. Identification of the namH gene, encoding the hydroxylase responsible for the *N*-glycolylation of the mycobacterial peptidoglycan. *J Biol Chem,* 280**,** 326-33.

RESTE DE ROCA, F. R., DUCHE, C., DONG, S., RINCE, A., DUBOST, L., PRITCHARD, D. G., BAKER, J. R., ARTHUR, M. & MESNAGE, S. 2010. Cleavage specificity of *Enterococcus faecalis* EnpA (EF1473), a peptidoglycan endopeptidase related to the LytM/lysostaphin family of metallopeptidases. *J Mol Biol,* 398**,** 507-17.

REUTER, G. 1992. Culture media for *enterococci* and group D-*streptococci*. *Int J Food Microbiol,* 17**,** 101-11.

RICH, R. L., KREIKEMEYER, B., OWENS, R. T., LABRENZ, S., NARAYANA, S. V., WEINSTOCK, G. M., MURRAY, B. E. & HOOK, M. 1999. Ace is a collagen-binding MSCRAMM from *Enterococcus faecalis*. *J Biol Chem,* 274**,** 26939-45.

RINCE, A., FLAHAUT, S. & AUFFRAY, Y. 2000. Identification of general stress genes in *Enterococcus faecalis*. *Int J Food Microbiol,* 55**,** 87-91.

ROLAIN, T., BERNARD, E., BEAUSSART, A., DEGAND, H., COURTIN, P., EGGE-JACOBSEN, W., BRON, P. A., MORSOMME, P., KLEEREBEZEM, M., CHAPOT-CHARTIER, M. P., DUFRENE, Y. F. & HOLS, P. 2013. *O*-glycosylation as a novel control mechanism of peptidoglycan hydrolase activity. *J Biol Chem,* 288**,** 22233-47.

RUGGIERO, A., SQUEGLIA, F., MARASCO, D., MARCHETTI, R., MOLINARO, A. & BERISIO, R. 2011a. X-ray structural studies of the entire extracellular region of the serine/threonine kinase PrkC from *Staphylococcus aureu*s. *Biochem J,* 435**,** 33-41.

RUIZ-GARBAJOSA, P., BONTEN, M. J., ROBINSON, D. A., TOP, J., NALLAPAREDDY, S. R., TORRES, C., COQUE, T. M., CANTON, R., BAQUERO, F., MURRAY, B. E., DEL CAMPO, R. & WILLEMS, R. J. 2006. Multilocus sequence typing scheme for *Enterococcus faecalis* reveals hospital-adapted genetic complexes in a background of high rates of recombination. *J Clin Microbiol,* 44**,** 2220-8.

SAMBROOK & MANIATIS, A. T. 1989. Molecular cloning: a laboratory manual. *Cold Spring Harbor.*

SÁNCHEZ-VALLET, A., SALEEM-BATCHA, R., KOMBRINK, A., HANSEN, G., VALKENBURG, D.-J., THOMMA, B. P. & MESTERS, J. R. 2013. Fungal effector Ecp6 outcompetes host immune receptor for chitin binding through intrachain LysM dimerization. *Elife,* 2**,** e00790.

SCHANDA, P., TRIBOULET, S., LAGURI, C., BOUGAULT, C. M., AYALA, I., CALLON, M., ARTHUR, M. & SIMORRE, J. P. 2014. Atomic model of a cell-wall cross-linking enzyme in complex with an intact bacterial peptidoglycan. *J Am Chem Soc,* 136**,** 17852-60.

SCHEFFERS, D. J. & PINHO, M. G. 2005. Bacterial cell wall synthesis: new insights from localization studies. *Microbiol Mol Biol Rev,* 69**,** 585-607.

SCHINDLER, M., MIRELMAN, D. & SCHWARZ, U. 1976. Quantitative determination of *N*-acetylglucosamine residues at the non-reducing ends of peptidoglycan chains by enzymic attachment of [14C]-D-galactose. *Eur J Biochem,* 71**,** 131-4.

SCHLAG, M., BISWAS, R., KRISMER, B., KOHLER, T., ZOLL, S., YU, W., SCHWARZ, H., PESCHEL, A. & GOTZ, F. 2010. Role of staphylococcal wall teichoic acid in targeting the major autolysin Atl. *Mol Microbiol,* 75**,** 864-73.

SCHLEIFER, K. H. & KANDLER, O. 1972. Peptidoglycan types of bacterial cell walls and their taxonomic implications. *Bacteriol Rev,* 36**,** 407-77.

SCHLEIFER, K. H. & KILPPER-BÄLZ, R. 1984. Transfer of *Streptococcus faecalis* and *Streptococcus faecium* to the Genus *Enterococcus* nom. rev. as *Enterococcus faecalis* comb. nov. and *Enterococcus faecium* comb. nov. *International Journal of Systematic and Evolutionary Microbiology,* 34**,** 31-34.

SCHLUTER, S., FRANZ, C. M., GESELLCHEN, F., BERTINETTI, O., HERBERG, F. W. & SCHMIDT, F. R. 2009. The high biofilm-encoding Bee locus: a second pilus gene cluster in *Enterococcus faecalis*? *Curr Microbiol,* 59**,** 206-11.

SCHNEEWIND, O., MODEL, P. & FISCHETTI, V. A. 1992. Sorting of protein A to the staphylococcal cell wall. *Cell,* 70**,** 267-81.

SHAM, L. T., BUTLER, E. K., LEBAR, M. D., KAHNE, D., BERNHARDT, T. G. & RUIZ, N. 2014. Bacterial cell wall. MurJ is the flippase of lipid-linked precursors for peptidoglycan biogenesis. *Science,* 345**,** 220-2.

SHANKAR, N., BAGHDAYAN, A. S. & GILMORE, M. S. 2002. Modulation of virulence within a pathogenicity island in vancomycin-resistant *Enterococcus faecalis. Nature,* 417**,** 746-50.

SHANKAR, N., LOCKATELL, C. V., BAGHDAYAN, A. S., DRACHENBERG, C., GILMORE, M. S. & JOHNSON, D. E. 2001. Role of *Enterococcus faecalis* surface protein Esp in the pathogenesis of ascending urinary tract infection. *Infect Immun,* 69**,** 4366-72.

SHERMAN, J. M. 1937. The Streptococci. *Bacteriol Rev,* 1**,** 3-97.

SHOCKMAN, G. & HÖLTJE, J. 1994. Microbial peptidoglycan (murein) hydrolases. *New comprehensive biochemistry,* 27**,** 131-131.

SIEVERT, D. M., RICKS, P., EDWARDS, J. R., SCHNEIDER, A., PATEL, J., SRINIVASAN, A., KALLEN, A., LIMBAGO, B. & FRIDKIN, S. 2013. Antimicrobial-resistant pathogens associated with healthcare-associated infections: summary of data reported to the National Healthcare Safety Network at the Centers for Disease Control and Prevention, 2009-2010. *Infect Control Hosp Epidemiol,* 34**,** 1-14.

SILHAVY, T. J., KAHNE, D. & WALKER, S. 2010. The bacterial cell envelope. *Cold Spring Harb Perspect Biol,* 2**,** a000414.

SINGH, K. V., LEWIS, R. J. & MURRAY, B. E. 2009. Importance of the epa locus of *Enterococcus faecalis* OG1RF in a mouse model of ascending urinary tract infection. *J Infect Dis,* 200**,** 417-20.

SINGH, K. V., WEINSTOCK, G. M. & MURRAY, B. E. 2002. An *Enterococcus faecalis* ABC homologue (Lsa) is required for the resistance of this species to clindamycin and quinupristin-dalfopristin. *Antimicrob Agents Chemother,* 46**,** 1845-50.

SMITH, M. A., CLEMONS, W. M., JR., DEMARS, C. J. & FLOWER, A. M. 2005. Modeling the effects of prl mutations on the *Escherichia coli* SecY complex. *J Bacteriol,* 187**,** 6454-65.

SQUEGLIA, F., MARCHETTI, R., RUGGIERO, A., LANZETTA, R., MARASCO, D., DWORKIN, J., PETOUKHOV, M., MOLINARO, A., BERISIO, R. & SILIPO, A. 2011. Chemical basis of peptidoglycan discrimination by PrkC, a key kinase involved in bacterial resuscitation from dormancy. *J Am Chem Soc,* 133**,** 20676-9.

STEEN, A., BUIST, G., LEENHOUTS, K. J., EL KHATTABI, M., GRIJPSTRA, F., ZOMER, A. L., VENEMA, G., KUIPERS, O. P. & KOK, J. 2003. Cell wall attachment of a widely distributed peptidoglycan binding domain is hindered by cell wall constituents. *J Biol Chem,* 278**,** 23874-81.

STEVENS, M. J., MOLENAAR, D., DE JONG, A., DE VOS, W. M. & KLEEREBEZEM, M. 2010. sigma54-Mediated control of the mannose phosphotransferase sytem in *Lactobacillus plantarum* impacts on carbohydrate metabolism. *Microbiology,* 156**,** 695-707.

TENDOLKAR, P. M., BAGHDAYAN, A. S. & SHANKAR, N. 2005. The N-terminal domain of enterococcal surface protein, Esp, is sufficient for Esp-mediated biofilm enhancement in *Enterococcus faecalis*. *J Bacteriol,* 187**,** 6213-22.

TENG, F., JACQUES-PALAZ, K. D., WEINSTOCK, G. M. & MURRAY, B. E. 2002. Evidence that the enterococcal polysaccharide antigen gene (epa) cluster is widespread in *Enterococcus faecalis* and influences resistance to phagocytic killing of *E. faecalis*. *Infect Immun,* 70**,** 2010-5.

TENG, F., SINGH, K. V., BOURGOGNE, A., ZENG, J. & MURRAY, B. E. 2009. Further characterization of the epa gene cluster and Epa polysaccharides of *Enterococcus faecalis*. *Infect Immun,* 77**,** 3759-67.

THIERCELIN, M. 1899. Morphologie et modes de reproduction de l'enterocoque. *Seances Soc Biol Fil,* 11**,** 551–553.

THUMM, G. & GOTZ, F. 1997. Studies on prolysostaphin processing and characterization of the lysostaphin immunity factor (Lif) of *Staphylococcus simulans* biovar staphylolyticus. *Mol Microbiol,* 23**,** 1251-65.

THURLOW, L. R., THOMAS, V. C. & HANCOCK, L. E. 2009. Capsular polysaccharide production in *Enterococcus faecalis* and contribution of CpsF to capsule serospecificity. *J Bacteriol,* 191**,** 6203-10.

THURLOW, L. R., THOMAS, V. C., NARAYANAN, S., OLSON, S., FLEMING, S. D. & HANCOCK, L. E. 2010. Gelatinase contributes to the pathogenesis of endocarditis caused by *Enterococcus faecalis*. *Infect Immun,* 78**,** 4936-43.

TON-THAT, H., MARRAFFINI, L. A. & SCHNEEWIND, O. 2004. Protein sorting to the cell wall envelope of Gram-positive bacteria. *Biochim Biophys Acta,* 1694**,** 269-78.

VAN HEIJENOORT, J. 2001. Recent advances in the formation of the bacterial peptidoglycan monomer unit. *Nat Prod Rep,* 18**,** 503-19.

VAN HEIJENOORT, J. 2007. Lipid intermediates in the biosynthesis of bacterial peptidoglycan. *Microbiol Mol Biol Rev,* 71**,** 620-35.

VOLLMER, W. 2008. Structural variation in the glycan strands of bacterial peptidoglycan. *FEMS Microbiol Rev,* 32**,** 287-306.

VOLLMER, W. & BERTSCHE, U. 2008. Murein (peptidoglycan) structure, architecture and biosynthesis in *Escherichia coli*. *Biochim Biophys Acta,* 1778**,** 1714-34.

VOLLMER, W., JORIS, B., CHARLIER, P. & FOSTER, S. 2008. Bacterial peptidoglycan (murein) hydrolases. *FEMS Microbiol Rev,* 32**,** 259-86.

VOLLMER, W. & TOMASZ, A. 2000. The pgdA gene encodes for a peptidoglycan *N*-acetylglucosamine deacetylase in *Streptococcus pneumoniae*. *J Biol Chem,* 275**,** 20496-501.

WANG, Y., HUEBNER, J., TZIANABOS, A. O., MARTIROSIAN, G., KASPER, D. L. & PIER, G. B. 1999. Structure of an antigenic teichoic acid shared by clinical isolates of *Enterococcus faecalis* and vancomycin-resistant *Enterococcus faecium*. *Carbohydr Res,* 316**,** 155-60.

WATERS, C. M., ANTIPORTA, M. H., MURRAY, B. E. & DUNNY, G. M. 2003. Role of the *Enterococcus faecalis* GelE protease in determination of cellular chain length, supernatant pheromone levels, and degradation of fibrin and misfolded surface proteins. *J Bacteriol,* 185**,** 3613-23.

WATERS, C. M., HIRT, H., MCCORMICK, J. K., SCHLIEVERT, P. M., WELLS, C. L. & DUNNY, G. M. 2004. An amino-terminal domain of *Enterococcus faecalis* aggregation substance is required for aggregation, bacterial internalization by epithelial cells and binding to lipoteichoic acid. *Mol Microbiol,* 52**,** 1159-71.

WEIDENMAIER, C., KOKAI-KUN, J. F., KRISTIAN, S. A., CHANTURIYA, T., KALBACHER, H., GROSS, M., NICHOLSON, G., NEUMEISTER, B., MOND, J. J. & PESCHEL, A. 2004. Role of teichoic acids in *Staphylococcus aureus* nasal colonization, a major risk factor in nosocomial infections. *Nat Med,* 10**,** 243-5.

WEIDENMAIER, C. & PESCHEL, A. 2008. Teichoic acids and related cell-wall glycopolymers in Gram-positive physiology and host interactions. *Nat Rev Microbiol,* 6**,** 276-87.

WEISBLUM, B. 1995. Erythromycin resistance by ribosome modification. *Antimicrob Agents Chemother,* 39**,** 577-85.

WHEELER, R., MESNAGE, S., BONECA, I. G., HOBBS, J. K. & FOSTER, S. J. 2011. Super-resolution microscopy reveals cell wall dynamics and peptidoglycan architecture in ovococcal bacteria. *Mol Microbiol,* 82**,** 1096-109.

WITTE, W. 2003. The *Enterococci*: Pathogenesis, Molecular Biology, and Antimicrobial Resistance. *International Journal of Medical Microbiology,* 292**,** 462.

WRIGHT, G. D. 2011. Molecular mechanisms of antibiotic resistance. *Chem Commun (Camb),* 47**,** 4055-61.

XU, Y., JIANG, L., MURRAY, B. E. & WEINSTOCK, G. M. 1997. *Enterococcus faecalis* antigens in human infections. *Infect Immun,* 65**,** 4207-15.

XU, Y., SINGH, K. V., QIN, X., MURRAY, B. E. & WEINSTOCK, G. M. 2000. Analysis of a gene cluster of *Enterococcus faecalis* involved in polysaccharide biosynthesis. *Infect Immun,* 68**,** 815-23.

YAHASHIRI, A., JORGENSON, M. A. & WEISS, D. S. 2015. Bacterial SPOR domains are recruited to septal peptidoglycan by binding to glycan strands that lack stem peptides. *Proc Natl Acad Sci U S A,* 112**,** 11347-52.

YAMADA, S., SUGAI, M., KOMATSUZAWA, H., NAKASHIMA, S., OSHIDA, T., MATSUMOTO, A. & SUGINAKA, H. 1996. An autolysin ring associated with cell separation of *Staphylococcus aureus*. *J Bacteriol,* 178**,** 1565-71.

YEATS, C., FINN, R. D. & BATEMAN, A. 2002. The PASTA domain: a beta-lactam-binding domain. *Trends Biochem Sci,* 27**,** 438.

YOUNG, R. 1992. Bacteriophage lysis: mechanism and regulation. *Microbiol Rev,* 56**,** 430-81.

YUEN, G. J. & AUSUBEL, F. M. 2014. *Enterococcus* infection biology: lessons from invertebrate host models. *J Microbiol,* 52**,** 200-10.

ZHANG, X., PAGANELLI, F. L., BIERSCHENK, D., KUIPERS, A., BONTEN, M. J., WILLEMS, R. J. & VAN SCHAIK, W. 2012a. Genome-wide identification of ampicillin resistance determinants in *Enterococcus faecium*. *PLoS Genet,* 8**,** e1002804.

ZIMMERMANN, R. A., MOELLERING, R. C., JR. & WEINBERG, A. N. 1971. Mechanism of resistance to antibiotic synergism in *enterococci*. *J Bacteriol,* 105**,** 873-9.